WATER SCIENCE SERIES

Quantifying Aquifer-Stream Exchanges Along Bertrand Creek, British Columbia and Washington State, Using a Numerical Groundwater Flow Model

Alexandre H. Nott and Diana M. Allen

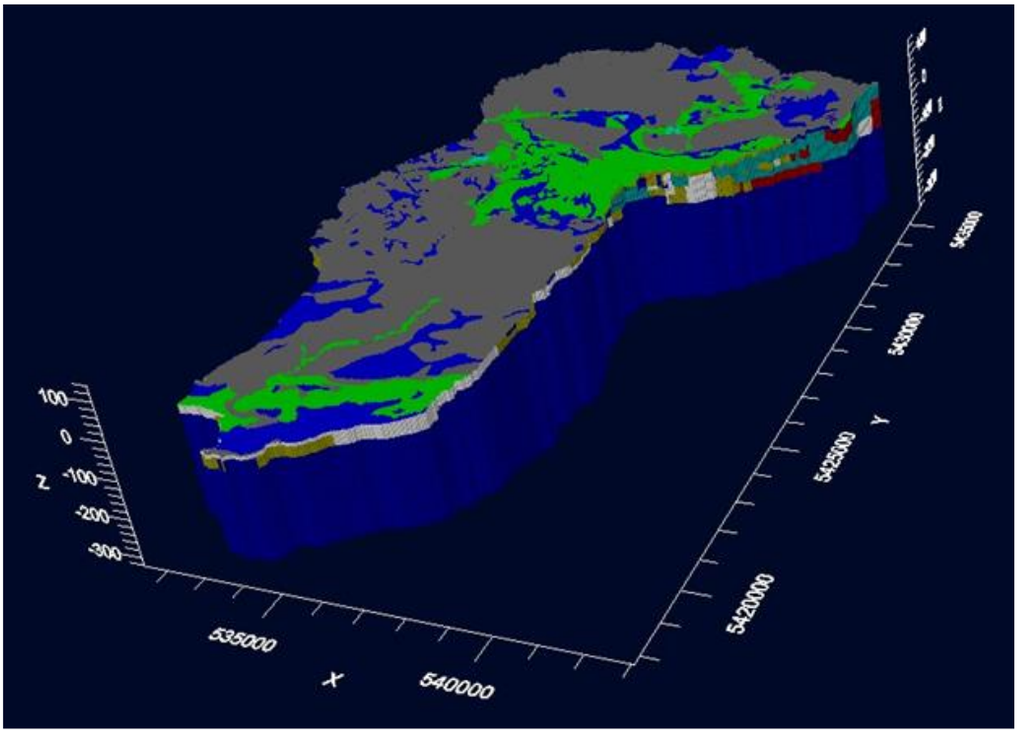

December 2020

BRITISH COLUMBIA

SFU SIMON FRASER UNIVERSITY
THINKING OF THE WORLD

No. 2020-06

The **Water Science Series** are scientific technical reports relating to the understanding and management of B.C.'s water resources. The series communicates scientific knowledge gained through water science programs across B.C. government, as well as scientific partners working in collaboration with provincial staff. For additional information visit: http://www2.gov.bc.ca/gov/content/environment/air-land-water/water/water-science-data/water-science-series.

ISBN: 978-0-7726-7980-2

Citation:

Nott, A.H. and D.M. Allen, 2020. Quantifying Aquifer-Stream Exchanges Along Bertrand Creek, British Columbia and Washington State, Using a Numerical Groundwater Flow Model. Water Science Series WSS2020-06, Province of British Columbia, Victoria.

Author's Affiliation:

Alexandre H Nott, Undergraduate student
Department of Earth Sciences
Simon Fraser University

Diana M Allen, Professor, P.Geo.
Department of Earth Sciences
Simon Fraser University

Cover Photographs: 3D numerical groundwater flow model of the Bertrand Creek Watershed

Acknowledgements

The authors gratefully acknowledge the Township of Langley for providing the LiDAR data used in the model. We also sincerely thank Klaus Rathfelder and Amy Sloma for their helpful suggestions for improving this report.

EXECUTIVE SUMMARY

This study focuses on Bertrand Creek Watershed, a transboundary watershed in the Central Fraser Lowlands between British Columbia and Washington State. Ongoing groundwater research in Bertrand Creek Watershed has involved a multi-year field investigation on aquifer-stream hydraulic connectivity, specifically streamflow depletion due to groundwater pumping. This study was motivated by observations at the field site, Otter Park, notably in 2018/2019, of Bertrand Creek experiencing substantial streamflow and stage decline during the summer, with certain stream segments running dry. Bertrand Creek provides critical habitat and spawning grounds for several species of fish including Coho salmon, the Nooksack Dace and the Salish Sucker, of which the latter two are endangered. During the summer months when monthly precipitation rates are at their lowest, groundwater discharge sustains the streamflow.

The purpose of this study was to quantify aquifer-stream exchanges along Bertrand Creek, in order to identify reaches where streamflow drought may occur. A steady-state three-dimensional numerical groundwater flow model of the watershed was developed by refining a pre-existing regional groundwater flow model that encompassed the Abbotsford-Sumas aquifer (Scibek and Allen, 2005). The output from this new model is used to quantify vertical fluxes and volumetric exchanges between streams and the groundwater system under natural (non-pumping) conditions and pumping conditions.

The Bertrand Creek Watershed is a transboundary watershed, located partly in the Township of Langley and Abbotsford, BC, and partly in Whatcom County, Washington State, US. The watershed is approximately 110 km^2 in area and features a main perennial stream, Bertrand Creek, which has several smaller ephemeral tributaries. The Abbotsford-Sumas aquifer and the Hopington aquifer are the two unconfined surficial aquifers in the watershed.

The conceptual hydrogeological model was built by first considering the top and bottom bounding surfaces of the model. Light detection and ranging (LiDAR) point cloud data, provided by the Township of Langley, were used to create a 0.5 m LiDAR-derived bare-earth digital elevation model (DEM) of the Canadian portion of the watershed. Portions of the watershed not covered by the LiDAR-derived DEM were combined with a 25 m provincial DEM and a 0.3 m LiDAR-derived DEM available for the US. These were mosaicked and resampled to create a 0.5 m surface DEM. To create a lower bounding surface of the model, bedrock elevation data from Scibek and Allen (2005) were clipped and resampled to 0.5 m.

Many of the major lithostratigraphic units are time-transgressive, and many occur in highly heterogenous and nested discontinuous patches with many unconformities bounding these sequences of sedimentary deposits. Therefore, determining the depth to specific lithostratigraphic units is extremely difficult, if not impossible. Even using relative unit thicknesses may be problematic due to pinch-outs and lenses. Consequently, hydrostratigraphic units were defined directly within the numerical groundwater model using Leapfrog Geo v5.1 (Seequent Limited) as a visualization tool for the assignment of hydraulic property zones. Lithology logs used to develop the original regional model were supplemented with more recent lithology logs (since 2005) from the BC GWELLS database, digitized well logs from the Washington Department of Ecology well database, and digitized well logs from the LENS study (Cox and Kahle, 1994). In total, 613 new well lithology logs were added to the existing database. The well log lithologies were then standardized using a similar approach to Scibek and Allen (2005). Thus, the Bertrand Creek Watershed study area has 1178 wells with standardized borehole lithologies.

The headwater source of the Bertrand Creek is located north of Aldergrove, BC, with the creek discharging into the Nooksack River in Washington. Smaller ephemeral streams are also mapped. Recharge to the Bertrand Creek Watershed occurs primarily as precipitation that percolates through the

soil column and into the unconfined aquifers. Based on spatially-distributed recharge estimated by Scibek and Allen (2006), the watershed receives an annual spatially-averaged recharge of approximately 1016 mm/yr.

Visual MODFLOW Flex v6.1 (Waterloo Hydrogeologic Inc., 2019) was used to construct the model. The model was discretized into 25 m x 25 m cells with 17 computational layers of variable thicknesses. The Bertrand Creek Watershed boundary was used to define the domain, based on minimal cross-catchment flow (into and out of the watershed from adjacent watersheds) as verified in the regional model. The hydrostratigraphic units, represented by hydraulic property zones, were delineated using the same distributions as in the original regional model, but were subsequently refined into higher detail zones by referencing the lithology logs in Leapfrog Geo. Most internal boundary conditions used to represent the Nooksack River (constant head boundary condition), streams (river boundary condition) and ephemeral streams (drain boundary conditions) were conserved from the original regional model. Exceptions included: 1) modifications to the river and drain conductance values made by Pruneda (2007) who had modified the original model to incorporate measured conductance values on the US side; 2) modifications of the conductance values on the Canadian side to align with streambed hydraulic conductivity measurements at Otter Park; and 3) adjustments to drain and river elevations using the new surface DEM produced in this study.

For the pumping simulation, 989 pumping wells were added to the model. Existing pumping wells from Scibek and Allen (2005) were used, in addition to new wells (2020) from GWELLS. Pumping rates were assigned based on the well use, of which four were identified: private domestic, commercial and industrial, irrigation, and water supply systems. Pumping rates were estimated based on values in the municipality of Abbotsford derived from Forstner et al. (2018) and the Abbotsford-Sumas aquifer factsheet (Aquifer 15 GWELLS). The approximated rates are as follows: private domestic (910 wells) at 2.86 m^3/day, commercial and industrial (22 wells) at 27.4 m^3/day, irrigation (48 wells) at 61.64 m^3/day, and water supply systems (9 wells) at 152.79 m^3/day. A total of 1025 observation wells were used in the model; 603 of these were obtained directly from the regional model and 422 were newly added. Finally, 11 zone budgets were assigned only to Bertrand Creek using segments of the stream. These segmentations are based on where distinct changes to the hydrostratigraphy occur in the uppermost surficial geology layer along stretches of Bertrand Creek.

While a 1 m thick soil zone was included in the conceptual hydrogeological model, a numerical model including this soil zone would not converge. Too many dry cells were causing the solution to oscillate leading to non-convergence with cell re-wetting activated. Model calibration was achieved by removing the 1 m soil layer and adjusting the surficial geology layer to 10 m rather than 9 m. Additionally, final calibration involved slightly adjusting hydrostratigraphic unit distributions in local areas based on more detailed examination of well log lithologies in Leapfrog. A normalized root mean squared error (NRMSE) of 11.17% was achieved with a correlation coefficient of 0.9. The three uppermost layers show the best calibration while layers 4, 5, 6 and 7 show the poorest calibration, similar to the original regional model.

Under non-pumping conditions, segments of Bertrand Creek upstream of Otter Park are dominantly losing reaches. At Otter Park, Bertrand Creek transitions from being dominantly losing to receiving a larger contribution of groundwater, resulting in partial losing conditions. Otter Park is located at a sharp meander of Bertrand Creek, where streamflow transitions from East-West to North-South and aligns with the regional groundwater flow direction. At the transition zone, the water table contours intersect the surface DEM contour marking the point at which Bertrand Creek experiences a greater contribution of groundwater flux into the stream. All stream segments downstream of Otter Park have the water table intersecting the surface contours within the riverbed. In segments upstream of Otter Park, the

water table is well below any surface contours, causing the stream to seep water into the groundwater system.

Under pumping conditions, all stream segments of Bertrand Creek experience increased negative vertical fluxes. This suggests that the entirety of Bertrand Creek is hydraulically connected to surficial aquifers. Because of the nature of this hydraulic connectivity, all of Bertrand Creek is sensitive to groundwater abstraction. Increases in river leakage into the groundwater system range from approximately +0.1 to +5.3 % while decreases in river leakage into certain stream segments range from approximately -1.1 to -13.7 %. River leakage into Bertrand Creek (stream recharge) only begins to occur significantly, downstream of Otter Park. In total, for a total pumping rate of 20,003 m^3/day across the watershed, approximately 3,460 m^3/day of additional water seeps into the groundwater system under pumping conditions and approximately 1,298 m^3/day less water seeps into Bertrand Creek. More stream water is redirected into the aquifers to accommodate pumping resulting in less groundwater being able to recharge the stream.

Based on the modelling results, streamflow drought is likely to occur in reaches of Bertrand Creek upstream of Otter Park as a result of the water table being deeper than the ground surface, coupled with the losing nature of the stream in these upstream segments. Groundwater abstraction is likely to exacerbate the losing nature of the stream, due to the sensitivity of the stream to the influence of pumping, increasing the likelihood of drought in Bertrand Creek.

The following recommendations would allow more accurate insight into the dynamics of streamflow drought within the Bertrand Creek Watershed: 1) Extend the use of the steady-state model by using it to map areas where pumping might lead to more or less impact on streamflow; 2) Develop a transient groundwater flow model or an integrated land surface – subsurface flow model to examine seasonal impacts on streamflow; 3) Integrate climate change projections into the model; and 4) Acquire accurate groundwater use and other hydrologic/hydrogeologic data. The first three recommendations are an obvious next step and could be acted upon in the short term. Acting on the fourth recommendation is more ambitious, but steps can be taken now to begin acquiring these critical datasets.

CONTENTS

1. INTRODUCTION

1.1 Background and Purpose

Groundwater is an essential component to aquatic habitats and ecosystems in freshwater streams, sustaining stream baseflow during periods of low flow (Hayashi and Rosenberry, 2002), modulating hyporheic water temperatures at groundwater-surface water exchange sites (Alexander and Caissie, 2003) and providing nutrients to aquatic organisms (Hayashi and Rosenberry, 2002; Malcolm et al., 2004). Globally, many groundwater systems are being severely stressed by over-abstraction (de Graaf et al., 2019), degrading water quality due to contamination (Burri et al., 2019), and by climate change induced drought (Bloomfield et al., 2019), among many other factors. Negative impacts to streamflow are also linked to stressed groundwater systems, particularly where aquifers are being over-abstracted. Over-abstraction can cause a reduction in groundwater discharge into streams, effectively lowering the baseflow and severely impacting aquatic ecosystems (de Graaf et al., 2019). Increased rates of abstraction, including current rates, are potentially exacerbating declines in the water table as well as reducing groundwater storage in aquifers (Green et al., 2011).

Bertrand Creek, located in the Central Fraser Lowlands of British Columbia, Canada and Washington State, U.S.A. provides critical habitat and spawning grounds for several species of fish including Coho salmon, the Nooksack Dace, and the Salish Sucker, of which the latter two are endangered (Pearson, 2004). During the summer months when monthly precipitation rates are at their lowest, groundwater discharge sustains the streamflow (Berg and Allen, 2007). Recharge to the surficial aquifers that underlie Bertrand Creek is primarily from precipitation (Scibek and Allen, 2005). Therefore, spatial and temporal variations in recharge, coupled with groundwater abstraction, will influence the magnitude of baseflow, and potentially cause severe consequences to ecological habitats.

In late summer 2018, a portion of the stream running through Otter Park in the Township of Langley went dry (Figure 1). Otter Park (see Figure 2 for location) is a field site for research on aquifer-stream connectivity (Allen et al., 2020). In recent years, staff from the British Columbia (BC) Ministry of Forests, Lands, Natural Resources Operations and Rural Development (FLNRORD) noted substantial streamflow and stage decline in the Bertrand Creek, with certain segments running completely dry during the summer months. These observations motivated this study and prompted the questions. Why do certain segments of Bertrand Creek run dry? Is this because of some spatial variation in the groundwater discharge to the stream? What might cause this spatial variation – the surficial geology?

The purpose of this study was to determine the nature of the hydraulic connectivity between Bertrand Creek and the underlying surficial aquifers to quantify and assess the spatial variability of groundwater-stream exchanges, e.g. gaining and losing reaches of Bertrand Creek. Specifically, the goal was to identify segments of Bertrand Creek that have a lower groundwater flux and thus may be more sensitive to streamflow drought. This study involved developing a steady-state three-dimensional groundwater flow model for Bertrand Creek Watershed based on a pre-existing regional model that encompassed the Abbotsford-Sumas aquifer (Scibek and Allen, 2005). As a steady-state model, the transient nature of the hydraulic connectivity is not addressed. Rather, the spatial variation under average annual groundwater conditions is investigated.

The specific objectives included:

1) Reviewing the report by Scibek and Allen (2005) and gathering necessary spatial data from the original datasets and other sources;
2) Contextualizing the geologic setting and retrieving borehole lithology logs within the watershed, standardizing these intervals and grouping them by material type;

3) Creating a high resolution (0.5 m) surface digital elevation model (DEM) using Light detection and ranging (LiDAR) point data provided by the Township of Langley;
4) Building a new conceptual hydrogeological model of the watershed using the new surface DEM and standardized borehole lithology groupings;
5) Constructing a refined steady-state 3D numerical groundwater model of the Bertrand Creek Watershed;
6) Determining the spatial variability in groundwater fluxes and quantifying stream exchanges with the groundwater system along segments of Bertrand Creek; and
7) Analyzing the effects of pumping on groundwater-stream interactions in the watershed.

Figure 1: Bertrand Creek at Otter Park in the Bertrand Creek Watershed. Photograph taken August 8, 2018 when the stream was almost dry. Shown in the foreground are nested instream piezometers (steel tubes), along with a white section of pipe used to shield two Onset Tidbit temperature loggers placed at two depths in the streambed.

1.2 Bertrand Creek Watershed

The Bertrand Creek Watershed is a transboundary watershed that spans the Township of Langley and Abbotsford, BC, and Whatcom County, Washington State, US (Figure 2). The watershed is approximately 110 km^2 in area and features multiple small streams such as Bori, Cave and Howes creeks, which are tributaries to Bertrand Creek, the main perennial stream in the watershed. Several smaller ephemeral tributaries also flow into the Bertrand Creek among drainage ditches and other surficial water features.

Several watershed delineations exist for Bertrand Creek (sources: Canadian Freshwater Atlas (FWA), Environment and Climate Change Canada (ECCC) and the Washington Water Resources Inventory Area (WRIA)). These watershed polygons differ in terms of which water courses they encompass. Ultimately, the WRIA polygon was chosen for this study as it is the only delineation that includes Cave Creek and Perry Homestead Brook both of which flow into Bertrand Creek. Moreover, it covers both sides of the Canada-US border (Figure 2).

1.3 Aquifers

Many interconnected confined and unconfined aquifers underlie the Bertrand Creek Watershed (Figure 3). These consist of coarse-grained drift deposits originating from the last glaciation. Ten aquifers have been mapped and identified (Table 1), with spatial data available in the BC Data Catalogue and the BC GWELLS database.

Table 1: Mapped aquifers that underlie Bertrand Creek Watershed. Data retrieved from the BC Data Catalogue.

Aquifer Name	Aquifer ID	Aquifer Material	Aquifer Sub-Type	Quaternary Lithostratigraphic Unit	Area (km^2)
Abbotsford-Sumas	15	Sand and Gravel	Unconfined - glacial outwash	Sumas Drift	94.87
Aldergrove AB	27	Sand and Gravel	Confined - glaciomarine	Fort Langley Formation	46.68
Unnamed	32	Sand and Gravel	Confined - glaciomarine	Early Fort Langley or late Vashon	50.00
West of Aldergrove	33	Sand and Gravel	Confined - glacial	Early Fort Langley or Vashon	73.05
Hopington AB	35	Sand and Gravel	Unconfined - glacial outwash	Sumas Drift	23.87
South of Hopington	50	Sand and Gravel	Confined - glacial	Fort Langley Formation	19.67
Langley Upland	52	Sand and Gravel	Confined - glacial	Fort Langley Formation	49.75
Hopington C	1144	Sand and Gravel	Confined - glaciomarine	Fort Langley Formation	16.47
Aldergrove Quadra	1193	Sand and Gravel	Confined - glacial	Quadra Sands	41.29
O Avenue Aquifer	1228	Sand and Gravel	Confined - glacial	Fort Langley or Vashon	1.70
South of Aldergrove	1233	Sand and Gravel	Confined - glacial	Fort Langley Formation	11.50

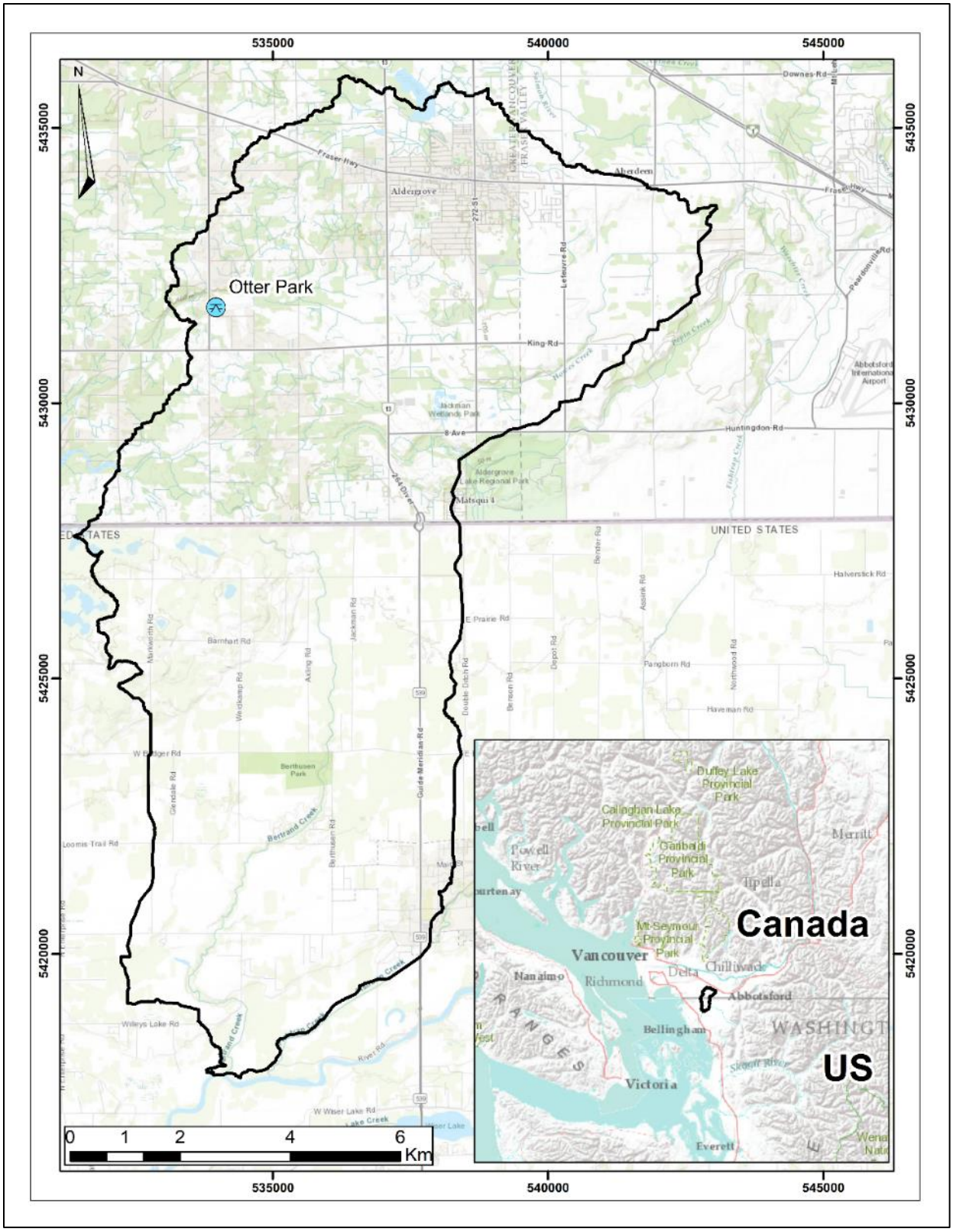

Figure 2: Bertrand Creek transboundary watershed in the Central Fraser Lowlands between British Columbia and Washington State. Also shown is the Otter Park field site where detailed site investigations of aquifer-stream connectivity are ongoing.

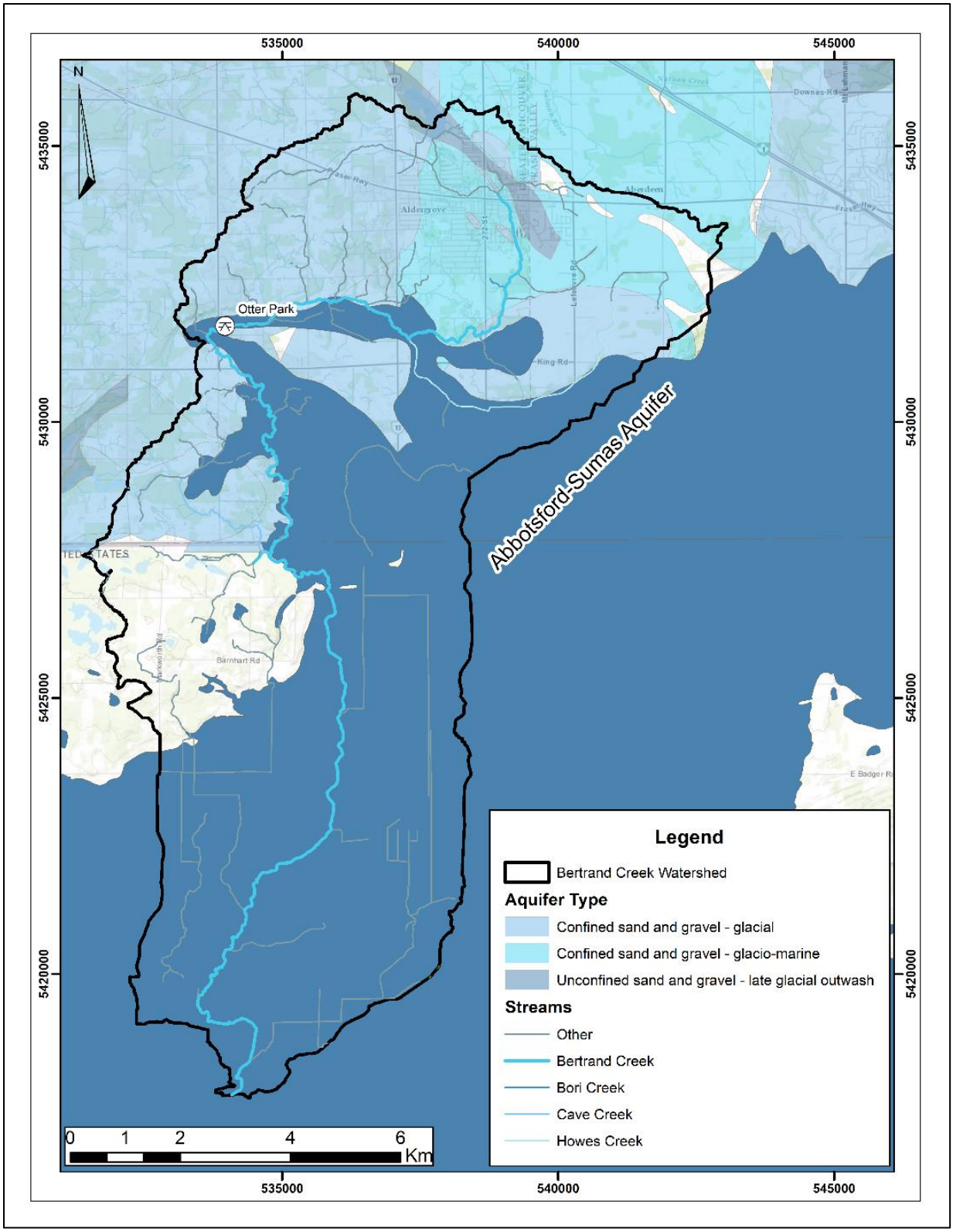

Figure 3: Mapped aquifers in the Bertrand Creek Watershed. Data retrieved from the BC Data Catalogue and Scibek and Allen (2005) for the Washington portion of the watershed. The Abbotsford-Sumas aquifer is in dark blue.

The Abbotsford-Sumas aquifer and the Hopington aquifer are the two unconfined surficial aquifers that underlie the watershed. The Abbotsford-Sumas transboundary aquifer is also the largest surficial aquifer within and adjacent to the watershed, and it spans across the border into Washington State. Bertrand Creek primarily flows through the Abbotsford-Sumas aquifer, but it crosscuts into confining material that lies above the confined aquifers in its northern reaches near Aldergrove.

1.4 Abbotsford-Sumas Model

This study is primarily based on a pre-existing numerical regional groundwater flow model of the Abbotsford-Sumas developed by Scibek and Allen (2005). A large majority of the spatial data and data used to construct the original numerical model were utilized in this study.

The original model by Scibek and Allen (2005) was developed as a regional base model to investigate various stressors to the aquifer, including the impact of climate change on groundwater (Scibek and Allen, 2006) and the transport of nitrate (Chesnaux and Allen, 2006, 2007). Scibek and Allen (2005) reported that the model predicted regional flow quite well but struggled to resolve local scale flow systems.

Therefore, for the purposes of this study, the model was refined. This refinement involved extracting a portion of the model specific to Bertrand Creek Watershed and creating a higher resolution representation of the surface topography and subsurface hydrostratigraphy. This required a more in-depth examination of the geology and the hydrostratigraphy, as described in the following section.

2. OVERVIEW OF GEOLOGIC SETTING

A proper detailed understanding of the geological context of an area is important for developing a geological model. Understanding aspects such as the tectonic setting, the regional geology and the geologic history provided the necessary framework for building the three-dimensional geologic model in this study.

2.1 Regional Geology

The Bertrand Creek Watershed is located in southwestern British Columbia and extends southward into Washington State in what is known as the Fraser Lowlands (Clague and Luternauer, 1983). The Fraser Lowlands are characterized by low relief topography and flat gently rolling hills bounded by the Coast Mountains to the east-northeast and by the Cascade Range to the south-southeast. Many valleys feed outward from the mountain ranges into the Fraser Lowlands, such as the Fraser Valley that terminates at the Fraser Delta, which progrades into the Strait of Georgia (Clague and Luternauer, 1983).

The Fraser Lowlands occur within the ancient Georgia Basin, a Cretaceous-aged sedimentary forearc basin overlying the current subduction zone at the forefront of the North American Plate and the subducting Juan de Fuca Plate (England and Bustin, 1998). The Georgia Basin extends from the Strait of Georgia in the north, and down into the Puget Sound to the south, and is underlain by three basements including the Coast and Cascade Ranges forming the plutonic basements, and Wrangellian terrane to the west, forming the metamorphic basement, part of Vancouver Island (Monger, 1990) (Figure 4). Tectonic activity in the Late Cretaceous post-dates the formation of both mountain ranges (Coast and Cascade) but was the main contributor to the development of the Georgia Basin itself due to cycles of subsidence and episodes of uplift and erosion (England and Bustin, 1998).

Lithification and consolidation of sediments accumulating in the Georgia Basin during the late Cretaceous (Nanaimo Group) and late Eocene (Huntingdon and Chuckanut formations) resulted in sandstones, mudstones, shales, conglomerates and coal, which have formed complex stratigraphic sequences of marine and non-marine sedimentary units within the Georgia Basin (Mustard and Rouse, 1994).

Quaternary glaciations beginning in the late Pliocene to early Pleistocene resulted in the deposition of approximately 300 m of alternating glacial and non-glacial sediments within the Fraser Lowlands (Clague and Luternauer, 1983; Clague, 1994). These Quaternary deposits overlie the Georgia Basin sedimentary bedrock succession. Present day (Holocene) geomorphological processes continue to shape the landforms observed around the Fraser Lowlands, including deltaic, fluvial, floodplain, bog and mass wasting events.

2.2 Bedrock Surface

The Cretaceous-Paleogene-Neogene successions of the Georgia Basin are cross-cut by a profound unconformity on which the Quaternary sediments have been deposited. This unconformity, or the bedrock surface itself, is a high-relief erosional surface, that outcrops above sea level and reaches depths of 700 m below sea level (Hamilton and Ricketts, 1994). The digitized bedrock surface DEM produced by Scibek and Allen (2005), based on the contour map by Hamilton and Ricketts (1994), is discussed in Section 3.2. Bedrock contours digitized by Scibek and Allen (2005) are shown in Figure 5.

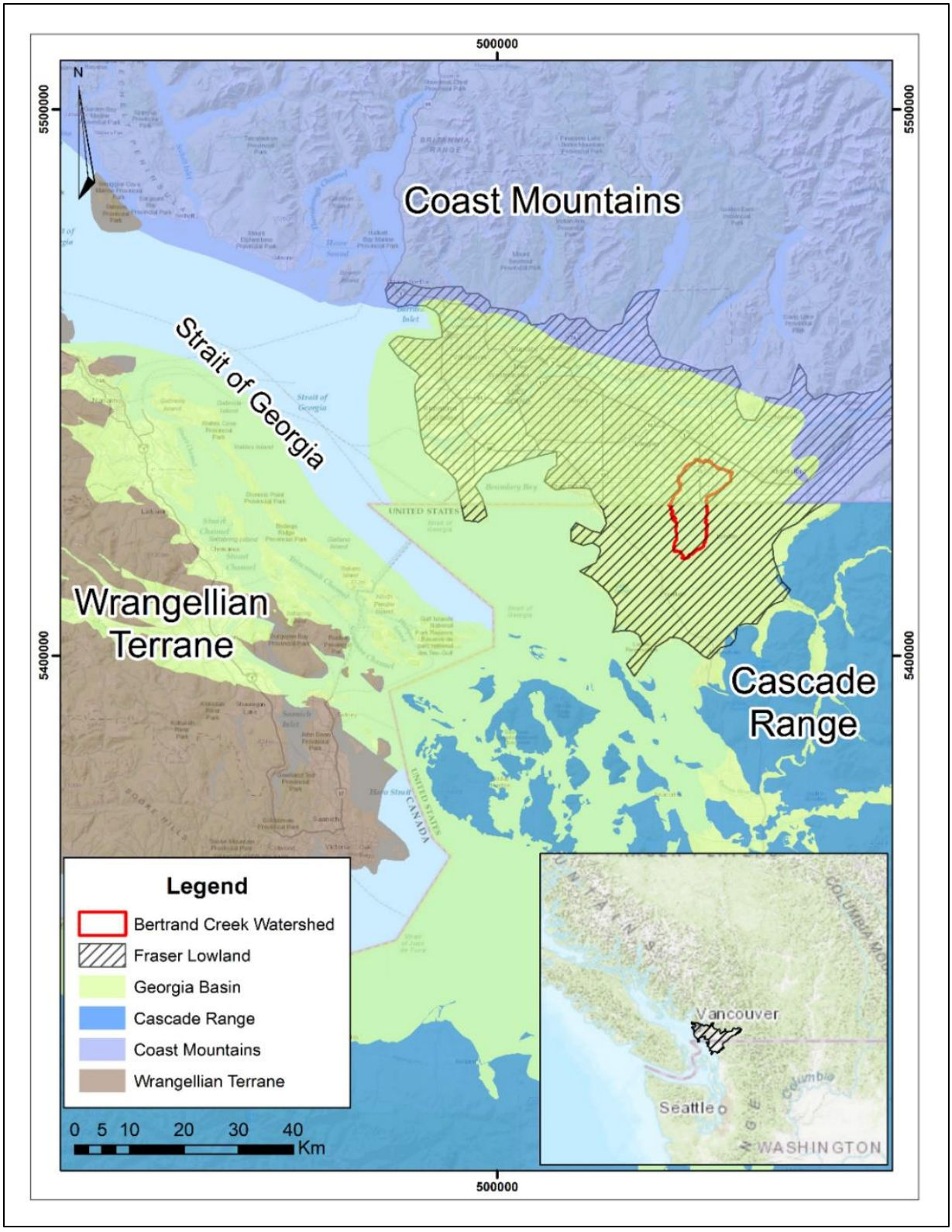

Figure 4: Geologic map of the Georgia Basin and the surrounding geologic units. The red outline shows Bertrand Creek Watershed within the Fraser Lowland (hatched area). Source: BC Data Catalogue.

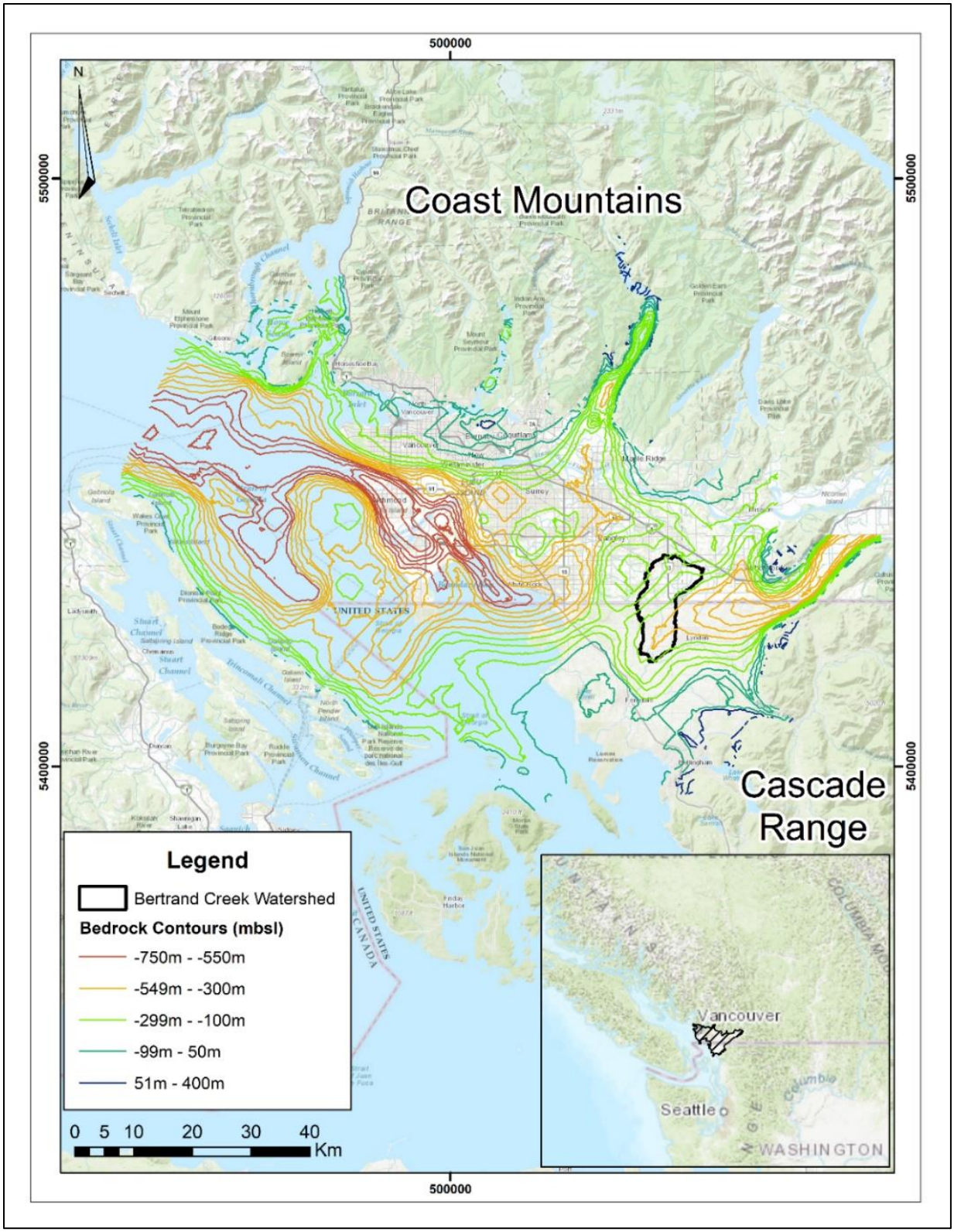

Figure 5: Map showing the bedrock contour elevations (mbsl) within the Georgia Basin (Source: Scibek and Allen, 2005).

2.3 Quaternary Geology

The Fraser Lowlands have been subject to several glaciations with intervening interglacial periods during the last 800,000 years of the Pleistocene (Clague, 2000). In southwestern B.C., stratigraphic records span back to pre-Wisconsinan, more than 100,000 years before present day (Armstrong, 1984). During the Early Wisconsinan, two glaciations are recorded: the Westlynn Glaciation which precedes the Semiahmoo Glaciation. These glaciations are separated by the Highbury non-glacial interval. The Middle Wisconsinan consisted of the Olympia non-glacial interval, during which the Fraser Lowlands and adjacent landscapes were free of glacial ice (Armstrong, 1984). The most recent glaciation, the Fraser Glaciation, during the Late Wisconsinan, represents the basis for most of the knowledge regarding the stratigraphy and sedimentary sequences left by the Cordilleran ice sheet in southwestern British Columbia (Armstrong, 1984; Clague and Ward, 2011). Early Pleistocene glaciations are poorly preserved in the Quaternary stratigraphic record as they were eroded away during the most recent Fraser Glaciation in B.C. (Clague and Ward, 2011). Much of southwestern B.C. was ice-free, preceding the rapid advance of the Cordilleran ice sheet during the Fraser Glaciation, approximately 26,000 years before present day (Clague et al., 1980). This ice sheet reached its maximum extent approximately 15,000 years before present day and rapidly receded into the mountains, forming the remnants of the Cordilleran ice sheet, represented by present day ice cover of the Coast Mountains of B.C. (Clague et al., 1997; Clague and James, 2002).

Beginning approximately 26,000 years before present day, the Georgia Basin and surrounding areas were quickly encroached by the Cordilleran ice sheet, marking the beginning of the Fraser Glaciation. This ice sheet was composed of valley and piedmont glaciers sourced from the Coast Mountain Range (Clague et al., 1996). Throughout the Fraser Glaciation, the Cordilleran ice sheet underwent many cycles of growth and decay (Clague, 2000). The Fraser Glaciation reached its climax approximately 15,000 years before present day, during the Vashon Stade, and is characterized by the Vashon Drift (Clague et al., 1980; Armstrong, 1981). The Cordilleran ice sheet began deglaciation shortly after reaching its glacial maxima, when the climate began to warm. At approximately 13,000 years before present day, calving events lasting almost 1,000 years led to the Fraser Lowlands being free of ice (Clague et al., 1997). By this time, many of the ice lobes had been confined to valleys and fjords. A small re-advance into the Fraser Lowlands 12,000 years before present day, during the Sumas Stade characterized by the Sumas Drift deposits, marked the final extent of Cordilleran ice sheet. The Fraser Lowlands were free of ice by 11,000 years before present and shortly after, the Fraser Glaciation came to an end (Armstrong, 1981; Clague and Luternauer, 1983).

At its maximum extent, the ice sheet was over 1.5 km thick in the Fraser Lowlands (Clague et al., 1997). Variations in ice sheet thickness, and therefore overall ice sheet mass, resulted in profound effects to the underlying crust as a result of isostatic equilibrium adjustments due to lithospheric flexure. Local minimum isostatic depression of the crust was approximately 300 m (Armstrong, 1981; Clague and James, 2002). Isostatic uplifts and depressions varied cyclically due to differences in ice sheet decay and growth rates, with deglaciation rates overcoming growth rates (Clague and James, 2002). These cycles of glacio-isostatic adjustments caused vertical fluctuations in the marine shoreline limit, varying spatially across southern B.C. (Clague and Luternauer, 1983). These cycles of glacial intervals caused local changes in relative sea level, up to 200 m, with periods of regression and transgression of the shoreline with respect to land (Armstrong, 1981). Global continental ice sheet growth during this time would have caused eustatic sea level changes, approximately 121 m during glacial maxima, exposing much of B.C.'s continental shelf to a non-marine environment (Fairbanks, 1989; Clague and Ward, 2011). Therefore, there would have been a combined and overlapping effect from eustatic sea level changes on the relative sea level changes within the Georgia Basin. Generally, the highest marine limit was approximately 200 m higher than present day sea level in the Fraser Lowlands (Clague and Luternauer,

1983; Clague and James, 2002; Fedje et al., 2018). Lowlands that are now above sea level, but previously below sea level due to glacio-isostatic depression, allowed the sea to come into contact with the retreating ice sheet in a glaciomarine depositional environment (Clague and Luternauer, 1983).

Quaternary deposits occur in complex diachronous successions of alternating marine, glacial and non-glacial sequences, as a result of glacio-isostatic adjustments causing relative sea level changes; eustatic sea level changes from mass balance redistribution caused by the accumulation of land ice; and tectonic adjustments stemming from the underlying, and on-going, subduction of the Juan de Fuca Plate (Armstrong, 1981; Clague and Luternauer, 1983).

2.4 Quaternary Deposits

Over 300 m of Quaternary deposits occur in Fraser Lowlands (Armstrong, 1981). These comprise primarily Fraser Glaciation deposits and postglacial Holocene deposits that include present day sedimentation (Armstrong, 1984). These sedimentary deposits consist of thick drift intervals bounded by glacial unconformities, non-glacial unconformities, and non-glacial deposits (Clague, 2000; Clague and Luternauer, 1983). Older surficial deposits of the Olympia non-glacial interval occur at depth or are confined to interior valleys and some coastal outcrops due to having been eroded (Clague and Luternauer, 1983; Armstrong, 1984). Unconformities and many thin and patchy non-glacial sediments bound the larger glacial deposit sequences (Clague, 1986).

Armstrong (1984) outlines the following Quaternary stratigraphic sequence of the Fraser Glaciation:

1) The Middle Wisconsinan Olympia non-glacial interval deposits consist of the Cowichan Head Formation.
2) The Late Wisconsinan Fraser Glaciation deposits consist of the Quadra Sands and Coquitlam Drift; the Vashon Drift; the Capilano sediments, the Sumas Drift; and the Fort Langley Formation.
3) The overlying, present-day, Holocene post glacial sediments consist of the Salish and Fraser River sediments.

Clague and Luternauer (1983) discussed these stratigraphic units by chronological ordering based on the ice sheet phase: 1) Advance phase at the beginning of the Late Wisconsinan, approximately 25,000 years before present day; 2) Climax phase, approximately 15,000 years before present during the Vashon Stade; and 3) Recessional phase, immediately succeeding the climax until the beginning of the Holocene. These are summarized as follows:

Advance Phase

Approximately 26,000 years before present, the deposition of the Quadra Sands, a sandy outwash deposit approximately 100 m thick occurring as isolated bodies, was laid onto older Pleistocene deposits. This unit was deposited pro-glacially, in front and along the margins of the advancing glacier. Simultaneously, the Coquitlam Drift was deposited within the Coquitlam Valley consisting of glaciofluvial and glaciolacustrine sediments.

Climax

During the Vashon Stade, beginning 18,000 years before present day, the Vashon Drift was deposited atop an extensive glacial unconformity that incised into the Quadra Sands. Armstrong (1984) remarks that fluvial dissection of the Quadra Sands had occurred before the deposition of the Vashon Drift, a thick glacial package of till, glaciofluvial and glaciolacustrine sediments. Climax was achieved at approximately 15,000 years before present day.

Recessional Phase

Retreat of the ice sheet resulted in the formation of proglacial lakes and the relative sea level rise further advancing the shoreline inland. This caused the coeval deposition of the Capilano sediments in the western Fraser Lowlands, and the Fort Langley Formation in the eastern Fraser Lowlands. The Sumas Drift directly overlies the Fort Langley Formation. Both the Capilano sediments and Fort Langley Formation consist of thick stratified stony muds and clays including shell fragments. Sumas Drift deposits are not overlain by marine sediments, suggesting deposition on land. Fort Langley Formation deposits are overlain by marine sediments.

2.5 Quaternary Lithostratigraphy of the Bertrand Creek Watershed

2.5.1 Lithostratigraphic Units

Figure 6 shows the mapped surficial geology units in the study area. The original surficial geology polygons developed for the Abbotsford groundwater model by Scibek and Allen (2005) were created by digitizing surficial geology units from Armstrong (1984) to construct the Canadian side of the watershed, and surficial geology units from the Washington State Department of Ecology for the US side of the watershed. In this study, unit names and polygons were updated using digitized surficial geology units retrieved from the Canadian GEOSCAN database to construct the Canadian side of the watershed and surficial geology units from the Washington State Department of Natural Resources for the US side of the watershed. It is important to note that these units were originally mapped at the surface; almost all are Vashon Stade in age or younger (Armstrong, 1984). Mapped surficial units within the Bertrand Watershed include Sumas Drift, Salish sediments and Fort Langley Formation.

The following lithostratigraphic unit descriptions are directly from Armstrong's (1984, 1981) detailed reports on the surficial geology of the Fraser Lowlands. Table 2 shows the stratigraphic sequence of these units and their chronological order considering their time-transgressive nature, adapted from Armstrong (1984).

Table 2: Generalized stratigraphic sequence within the Fraser Lowlands. Adapted from Armstrong (1984).

<table>
<tr><th>Geologic Time Unit</th><th>Geoclimatic Unit</th><th colspan="2">Lithostratigraphic Unit</th></tr>
<tr><td>Holocene</td><td>Present-day Non-glacial Interval</td><td colspan="2">Salish Sediments and Fraser River Sediments</td></tr>
<tr><td rowspan="5">Late Wisconsinan</td><td>Post-Glacial</td><td colspan="2">Salish Sediments</td></tr>
<tr><td rowspan="4">Fraser Glaciation</td><td rowspan="2">Capilano Sediments</td><td>Sumas Drift</td></tr>
<tr><td>Fort Langley Formation</td></tr>
<tr><td colspan="2">Vashon Drift</td></tr>
<tr><td>Quadra Sand</td><td>Coquitlam Drift</td></tr>
<tr><td>Middle Wisconsinan</td><td>Olympia Non-glacial Interval</td><td colspan="2">Cowichan Head Formation</td></tr>
<tr><td rowspan="3">Early Wisconsinan</td><td>Semiahmoo Glaciation</td><td colspan="2">Semiahmoo Drift</td></tr>
<tr><td>Highbury non-glacial Interval</td><td colspan="2">Highbury Sediments</td></tr>
<tr><td>Westlynn Glaciation</td><td colspan="2">Westlynn Drift</td></tr>
</table>

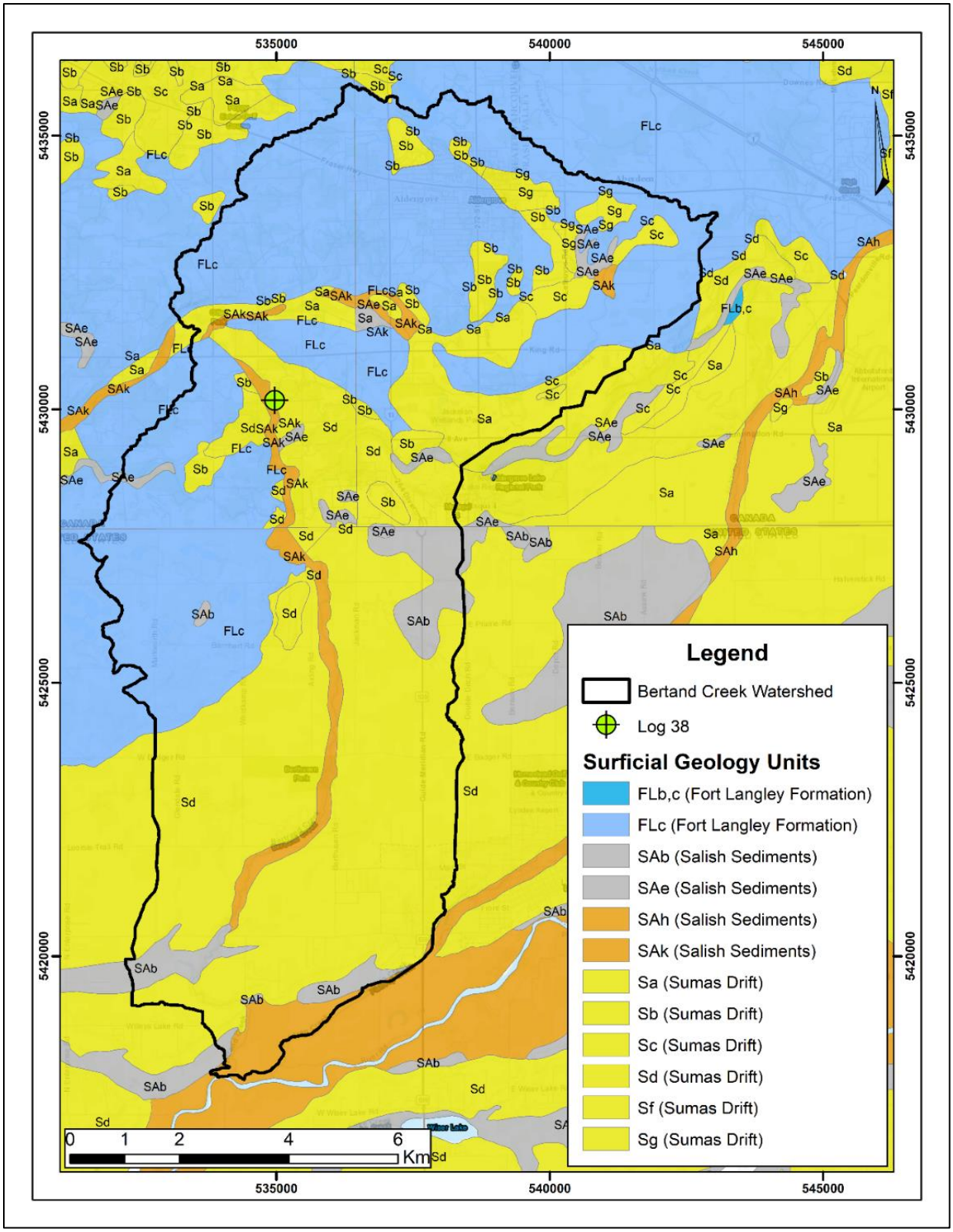

Figure 6: Surficial geology map of the Bertrand Creek Watershed study area. Retrieved from: Canadian GEOSCAN database and Washington Department of Natural Resources. The lithology for Log 38 is shown in Table 3.

Early Wisconsinan Units

For the purposes of this study, the following lithostratigraphic units have been grouped as Early Wisconsinan units: Westlynn Drift glacial deposits, non-glacial Highbury Sediments, Semiahmoo Drift glacial deposits. The Westlynn Drift deposits consist of till diamictons and glacio-fluvial/marine/lacustrine sediments. The glaciomarine sediments contain fossil shells. The Highbury Sediments consist of fluvial, organic-rich silts and peat, and fine-grained marine sediments. The Semiahmoo Drift consists of till diamictons and glacio-fluvial/marine/lacustrine sediments.

Cowichan Head Formation

The Cowichan Head Formation is the lithostratigraphic unit that characterizes the Olympia non-glacial interval, which directly pre-dates the Fraser Glaciation. This unit consists of organic-rich colluvium and bog and swamp deposits with interbedded floodplain sediments. These all overlie marine sediments, which include silt, sand and gravel containing marine shells. Fluvial sediments consist of silt, sand and gravel with organic interbeds. At the top of this unit, there is a large glacial unconformity at the Cowichan Head-Quadra Sand interface demarcating the beginning of the Fraser Glaciation and its associated depositional units.

Quadra Sand

The Quadra Sand represents the proglacial advance sediments that are in part coeval, younger and older than the Coquitlam Drift unit (Armstrong, 1981). However, the Coquitlam Drift is confined to the Coquitlam Valley area (Armstrong, 1981) and does not extend into the Bertrand Creek Watershed area. The Quadra Sand consists of glaciofluvial floodplain sands and gravels with some organic-rich layers as well as sand and gravel deltaic deposits.

Vashon Drift

The Vashon Drift represents the climax of the Fraser Glaciation during the Vashon Stade (Clague et al., 1980). It unconformably overlies the Quadra Sand unit but not the Coquitlam Drift. It is composed of three till diamictons (lodgement, outwash and flow) and glaciofluvial sand and gravel sediments with minor pro-glacial deposits. Lodgement tills can be interbedded with glaciofluvial silt, sand, and gravel or can be interbedded with the outwash or flow tills. Most of the tills contain 1 to 5 m thick lenses of silt, sand or gravel. Glaciolacustrine silt, fine sand, silty clay, and stony clays also occur in some areas.

Fort Langley Formation

The Fort Langley Formation represents a series of ice sheet advances characterized by thick successions of interbedded marine and glaciomarine sediments, as well as 1 to 3 m thick lodgment till interbeds (Armstrong, 1981). This formation occurs widely in the central Fraser Lowlands and was deposited in a predominantly glaciomarine environment (Clague et al., 1997). These sediments were deposited directly after the climax of the Fraser Glaciation and represent deglaciation deposits (Armstrong 1981).

Sumas Drift

The Sumas Drift directly overlies the Fort Langley Formation deposits but does not overlie the Capilano Sediments, which were deposited synchronously with both the Sumas Drift and Fort Langley Formation deposits (Armstrong, 1981). The Capilano Sediments were deposited in the western Fraser Lowlands during a period of transgression, with sea levels approximately 15 m higher than present day levels (Armstrong, 1981). Because of the relation between these three units, the Capilano Sediments will not be encountered in the subsurface in the Bertrand Creek Watershed study area. The Sumas Drift consists of lodgement and flow tills, glaciofluvial sands and gravels, and glaciolacustrine clayey silt, silty clay and fine sand. This unit represents the last deposits laid down during the Fraser Glaciation.

Salish Sediments

The Salish Sediments represent a post-glacial depositional setting including present day sedimentation processes. This unit consists of near-shore marine gravel and sand, deltaic and floodplain gravel and sand, lacustrine fine-grained sediments, eolian fine sand, colluvial talus sediments, and organic-rich bog and swamp deposits.

2.5.2 Lithostratigraphic Unit Thicknesses

Determining the sequence below what is mapped at the surface is challenging and relies on detailed borehole lithology logs. Nevertheless, it is expected that older units of the early Pleistocene and pre-glaciation from the Early and Middle Wisconsinan will be encountered at depth and overlie bedrock. Many of the major lithostratigraphic units are time-transgressive due to diachronous glacier growth (Armstrong, 1981, 1984; Clague, 1986). Additionally, many of these units occur in highly heterogenous and nested discontinuous patches with many unconformities bounding these sequences of sedimentary deposits (Clague, 1986). Therefore, determining the depth to specific lithostratigraphic units is extremely difficult, if not impossible. Even using relative unit thicknesses may be problematic due to pinch-outs and lenses. Lastly, as Armstrong (1984) points out, correlating units in a sequential order based solely on age ignores the Quaternary geologic history. Diachronous and positional location matter just as much as unit age. Table 3 shows approximate maximum unit thicknesses for each lithostratigraphic unit compiled from Armstrong (1984) depending on environment of deposition.

Table 3: Compilation of maximum unit thicknesses, adapted from Armstrong (1984) from oldest to youngest. "Other" includes eolian, colluvial and organic deposits.

Litho-stratigraphic Unit	Till (m)	Glacio-fluvial (m)	Glacio-lacustrine (m)	Glacio-marine (m)	Marine (m)	Fluvial (m)	Lacustrine (m)	Other (m)
Early Wisconsinan	27	40	45	20	75	20	-	5
Cowichan Head Formation	-	-	-	-	20	25	-	20
Quadra Sand	85	-	-	-	-	-	-	-
Vashon Drift	25	60	80	-	-	-	-	-
Fort Langley Formation	5	50	-	60	30	-	-	-
Sumas Drift	6	45	75	-	-	-	-	-
Salish Sediments	-	-	-	-	8	20	20	20

Additionally, Armstrong (1984) provides a multitude of correlated borehole lithology logs that have been lithostratigraphically interpreted. For example, Log 38, located 2 km southeast of Otter Park (Figure 6), can be used to gauge stratigraphic position and unit thickness in the surrounding area. Table 4 outlines approximate encountered unit thicknesses from this borehole lithology log.

Table 4: Borehole lithology log of log 38 (Armstrong, 1984). Units identified below the Vashon Drift are uncertain. Elevation is in metres above sea level (masl). The location of this lithology log is shown on Figure 3.

Lithostratigraphic Unit	Dominant Lithology	Top of Unit Elevation (masl)	Thickness (m)
Sumas Drift	Glaciofluvial sand and gravel	65	20
Sumas Drift	Lodgement till	45	5
Sumas Drift	Glaciofluvial sand and gravel	40	5
Fort Langley Formation	Glaciomarine stony silt and clay	35	20
Vashon Drift	Sandy lodgement till and glaciofluvial gravel and sand	15	25
Cowichan Head Formation	Marine silt, clay and sand with gravel lenses	-10	43
Semiahmoo Drift	Sandy lodgement till, glaciomarine stony silt and clay, and glaciofluvial gravel and sand	-53	25
Highbury Sediments	Marine fine sand	-78	5
Westlynn Drift and Older Sediments	Silty lodgement till and glaciomarine stony silty clay	-83	59
Bedrock	Neogene-Paleogene bedrock	-142	-

2.6 Recognizing Order

Stratigraphic relationships between these heterogeneously distributed marine, glacial and non-glacial sequences of sedimentary units may seem impossible to recognize. Clague (1986) outlines a strategy for recognizing order in these chaotic sequences of sediments. There were several key take-aways including the following:

1) During ice sheet growth, thick proglacial fluvial and lacustrine units were deposited in coastal lowlands.
2) Advance of glaciers over proglacial deposits created erosional surfaces, or glacial unconformities, on which drift sediments were deposited.
3) Retreating glaciers proglacially deposited thick glaciolacustrine, glaciomarine and glaciofluvial sediments which form the uppermost facies of a glacial sequence.
4) Sediment supply decreased shortly after the glaciers had retreated causing persistent erosion throughout interglacial periods. The splintered stratigraphic record is due to this erosion.
5) Deposits exist as discrete packages bounded by unconformities or thin interglacial deposits.

2.7 Soils Data

Because the Fraser Lowlands have geologically only recently been free of ice (approximately 11,000 years), the soils that have been in development are relatively young and underdeveloped compared to non-glaciated regions in Canada. The Quaternary surficial geology units make up the soil parent material, often referred to as the C-horizon. Resting above the C-horizon is the soil column commonly composed of the B- and A-horizons, in a typical soil pedon (a cross-section that shows all horizons). Oftentimes these horizons are capped with an O-horizon, an organic rich horizon. Therefore, directly underlying these soils are the surficial geological units, and in some cases, the surficial units are directly exposed at the surface.

Scibek and Allen (2006) acquired soil data for B.C. from the B.C. Ministry of Agriculture and Food, and from the National SSURGO Data, US Dept of Agriculture, Natural Resources Conservation Service for Watcom County, and classified the soils according to their drainage properties, assigning a soil drainage code to each soil (Figure 7). These soil data were used solely for recharge modelling (Scibek and Allen,

2006), with the resulting gridded recharge being applied to the groundwater model. The groundwater flow model only comprised the surficial sediments. In this study, soils data were used for the top layer of the preliminary model (see Section 4.3.2).

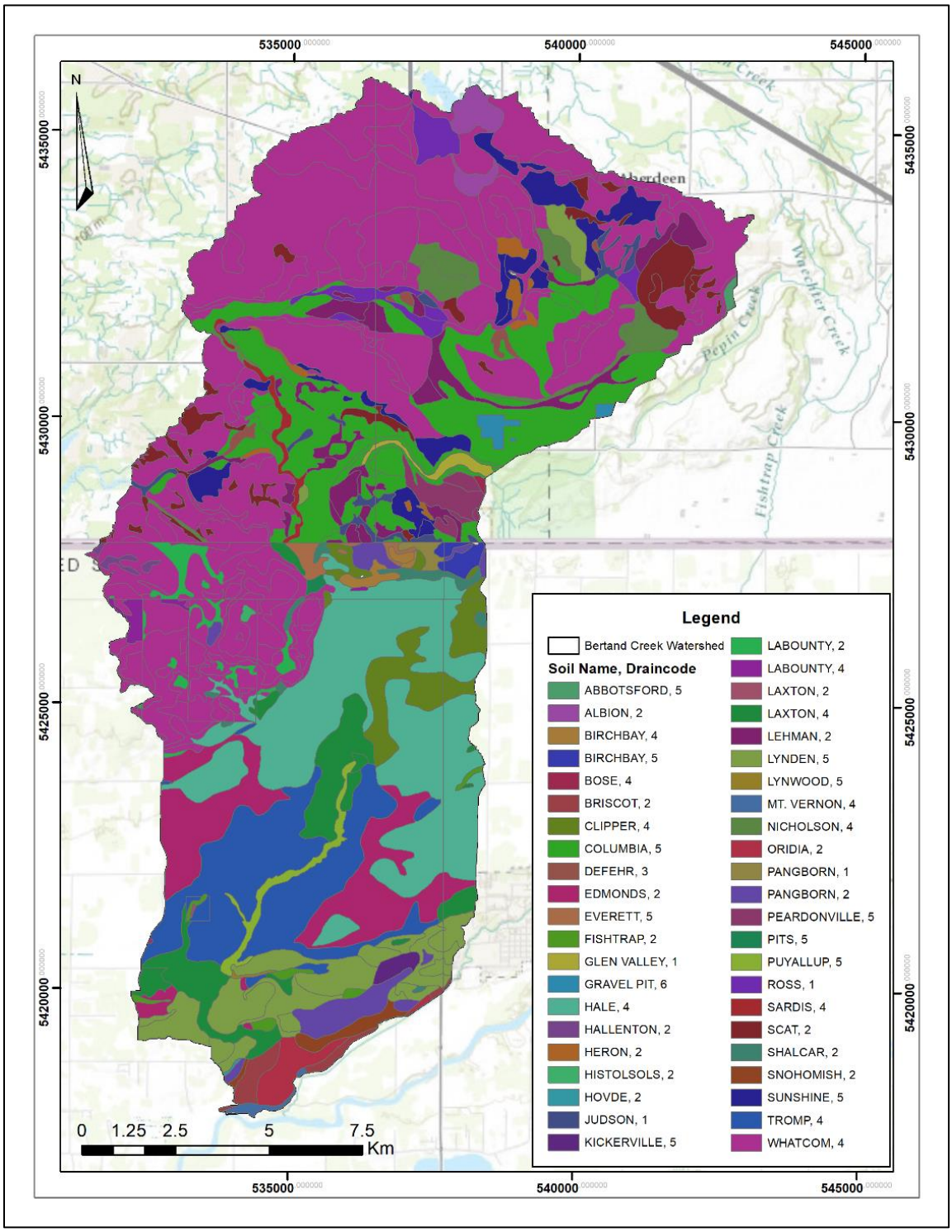

Figure 7: Soil map of the Bertrand Creek Watershed study area showing soil name and drainage code assigned by Scibek and Allen (2006) for recharge modelling. Map adapted from Scibek and Allen (2006).

3. CONCEPTUAL HYDROGEOLOGICAL MODEL

3.1 Surface Digital Elevation Model (DEM)

Digital elevation models, or DEMs, are bare-earth representations of ground surface and can be derived using various methods such as through surveyed topographic maps, photogrammetry, GPS points and remotely sensed satellite imagery and data (Yang et al., 2014). Light detection and ranging (LiDAR)-derived DEMs offer high resolution results for elevation mapping as return points capture highly accurate horizontal and vertical measurements. As noted in several studies (Wang and Hiu, 2006; Thomas et al., 2017; Petresova et al., 2017), LiDAR-derived DEMs, particularly at sub-metre resolutions, allow for the observation of microtopographic features such as stream channels, pits, ponds and small water features. It is important to note that traditional near-infrared (NIR) LiDAR does not easily penetrate through water due to turbidity and random scatter and is best suited for topographical mapping (Pratomo et al., 2019). Therefore, point cloud representation of any water body basin or stream channel is limited by the returns detected by the instrument and generally yields lower point densities.

3.1.1 Data Source and Software

Raw three-dimensional (3D) LiDAR point cloud data, tiled into 1 km^2 sections, were provided by the Township of Langley in the form of LAS (v1.4) formatted point data. This LiDAR dataset encompasses a large, but incomplete, portion of the Bertrand Creek Watershed. Therefore, the LiDAR dataset was combined with the lower resolution provincial DEM and the high-resolution DEM available for the US. A detailed description of the various steps in creating the DEM including mosaicking and resampling, validation of positional accuracy and bias correction are described in Appendix A.

LiDAR data processing and analysis as well as DEM map-making for this study were performed in ArcMap v10.6 (ESRI, 2018), specifically using the 3D Analyst extension, which allows for manipulation and processing of raw 3D point cloud information in the LAS file format.

The final surface DEM is shown in Figure 8.

3.2 Bedrock DEM

The bedrock surface is located beneath several hundred metres of Quaternary sediment and is not exposed at surface. The easiest way to determine bedrock elevation at depth is using borehole log data. Using the depth-to-bedrock from multiple boreholes, a point cloud of bedrock elevation can be generated and then interpolated to create a surface. However, very few wells in this study region extend down to bedrock. Therefore, Scibek and Allen (2005) produced a bedrock DEM for the Fraser Valley region using all available deep borehole data, bedrock contour maps (Hamilton and Rickets, 1994), valley profiles and cross-sections (see Figure 5 for the original contour map of the bedrock surface).

The bedrock DEM is quite coarse in resolution at 200 m. Thus, a point grid for this study was derived from this DEM and a new surface was interpolated using a bilinear interpolation technique to a pixel size of 0.5 m, in order to match the surface DEM. No additional data were added beyond data used by Scibek and Allen (2005). While this new interpolation does not improve the resolution of the bedrock surface, the pixel size is consistent with the ground surface DEM. Figure 9 shows the final bedrock DEM.

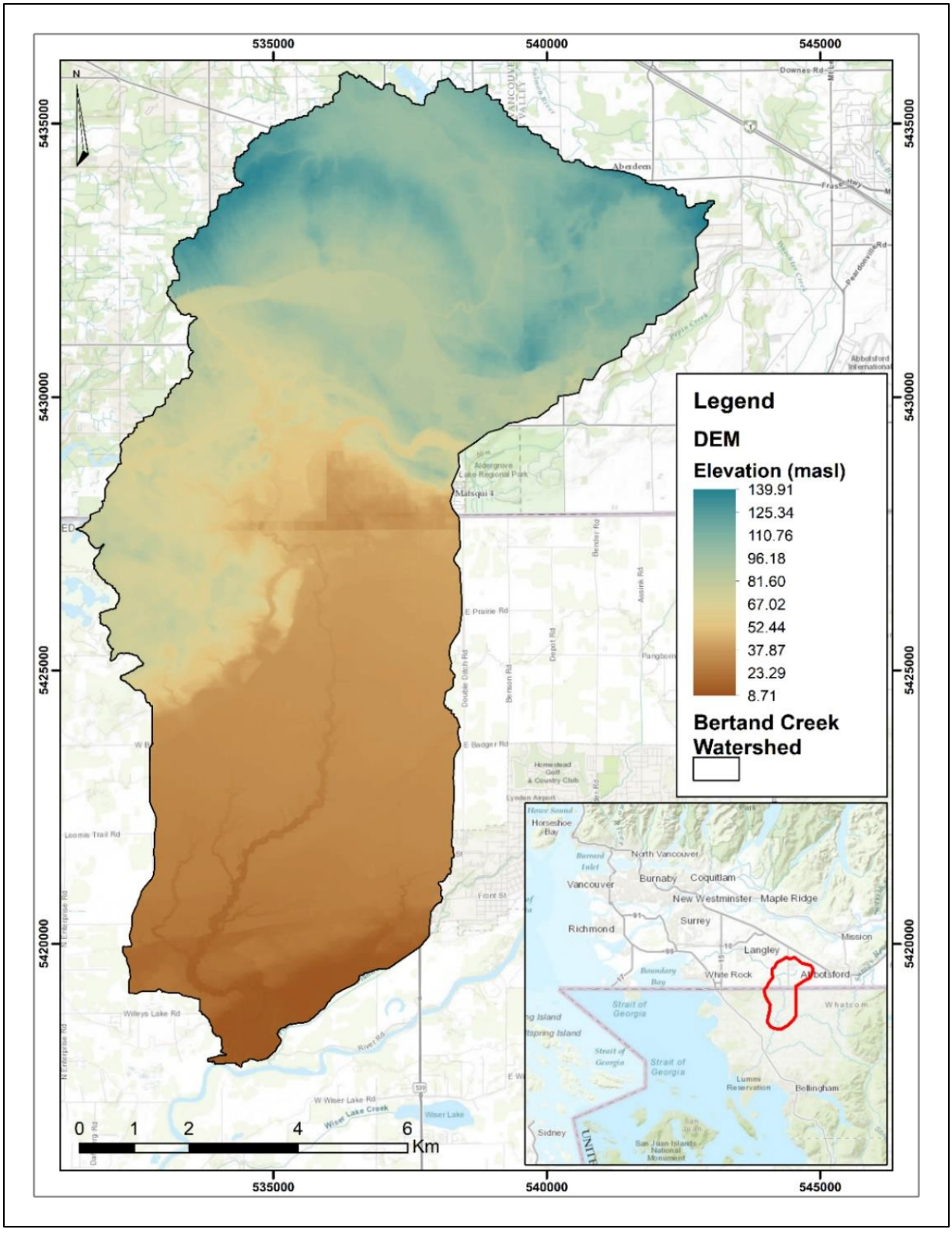

Figure 8: Surface DEM with elevation in metres above mean sea level (masl).

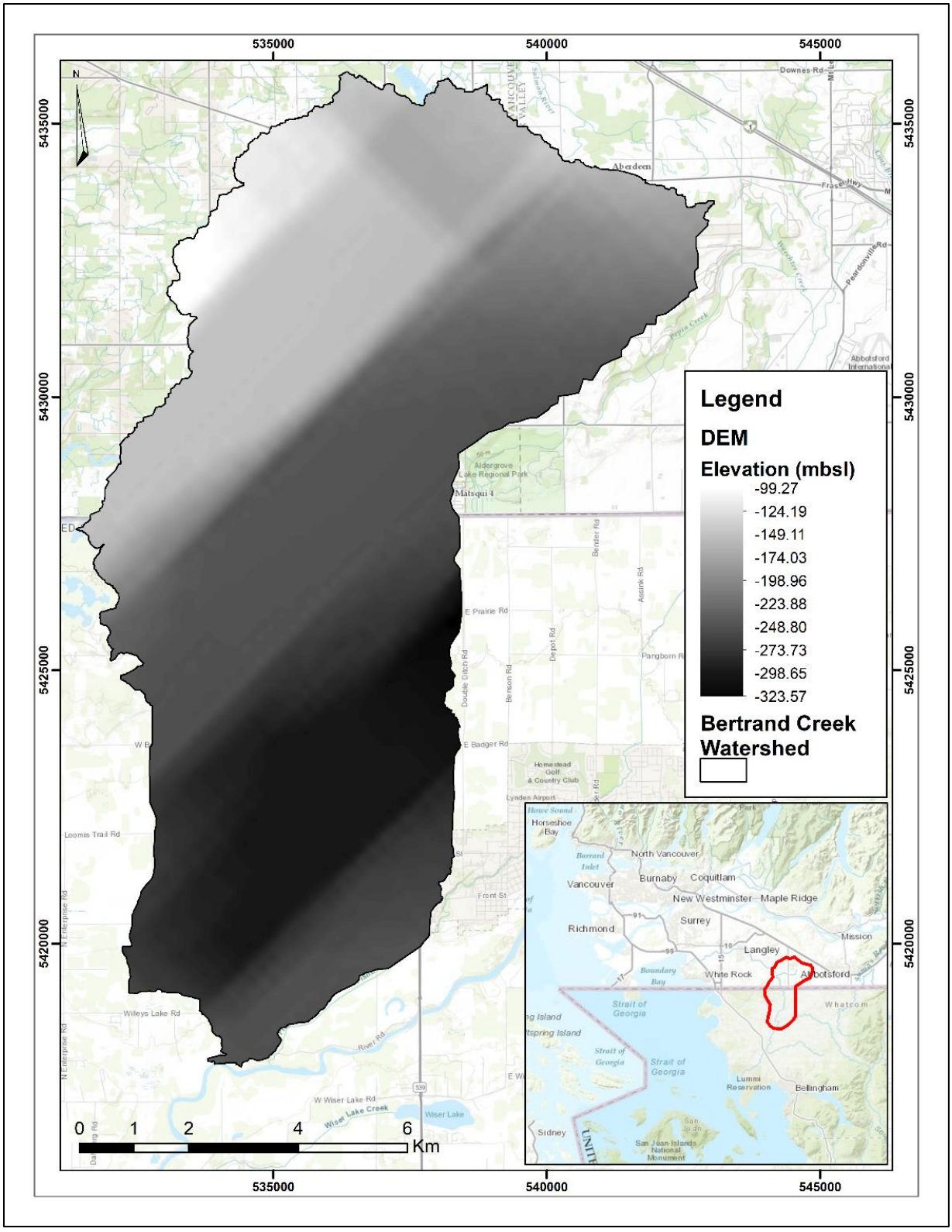

Figure 9: Bedrock DEM with elevation in metres below mean sea level (mbsl). Modified from Scibek and Allen (2005).

3.3 Well Lithology Logs

3.3.1 Lithology Logs and Distribution

The three-dimensional geologic model was developed almost entirely based on lithology logs for drilled wells. An existing lithology log database (Scibek and Allen, 2005) was utilized as baseline dataset for this study. The database includes lithology logs extracted from the B.C. GWELLS database along with a selection of lithology logs for Washington (WA)[1] as of 2005. Within the Bertrand Creek Watershed, 565 well lithology logs were available in the existing database.

Many new wells have been drilled since 2005 and additional lithology logs are available. Therefore, a preliminary step was to gather the new well log entries for B.C. and WA. Figure 10 shows the locations of wells with lithology logs in the new updated database. Below are the sources of well logs used to update the database:

British Columbia

- B.C. GWELLS Database

Washington

- Washington Department of Ecology (WA Ecology, 2020)
- Additional wells from LENS Groundwater Study (Cox and Kahle, 1999) not included in the 2005 model.

3.3.2 Data Quality

Lithology logs are the fundamental source of information needed to construct a geological model; however, raw lithology data are challenging to interpret due to issues of poor data quality. Raw lithology logs in GWELLS were examined and found to contain many entry errors. In some cases, the information is different from what was written on the actual well construction report. Many of the entries are truncated to new empty lines, among many other formatting issues. Positional accuracy of wells may also be inaccurate, especially for wells drilled before the availability of high precision GPS devices. A large majority of lithology logs lack adequate detail with regards to the depth interval lithologic description along with the absence of any formalized standardization scheme. Thus, semantic heterogeneity, the difference in meanings of words, becomes a prevalent issue and weakens overall data quality.

The lack of adherence to standard grain size classification (along with an explicit statement of which system was used) rendered grain size interpretation highly uncertain. This was especially a concern for terminology describing coarse grained sediments such as stones, cobbles, boulders or gravels. Without a classification system, coarse grain size descriptors are ambiguous and hold loose meaning. What one person may refer to as “cobble” could be referred to as “boulder” or “stone” by someone else. Further ambiguity arises from descriptions that combine these terms such as “Cobbles and Stony Sand”, “Some Gravel and Cobbles” or “Till and Cobbles with Some Boulders”. These are not particularly descriptive especially without the explicit use of a classification system[2] because these combinations only demonstrate relative size differences between coarse grained sediments within the described interval.

[1] The selected well logs for Washington for the 2005 study were obtained from both Washington Department of Ecology and the LENS Study.

[2] Example grain size classification systems include American Society for Testing Materials (ASTM) and the Unified Soil Classification System (UCSC)

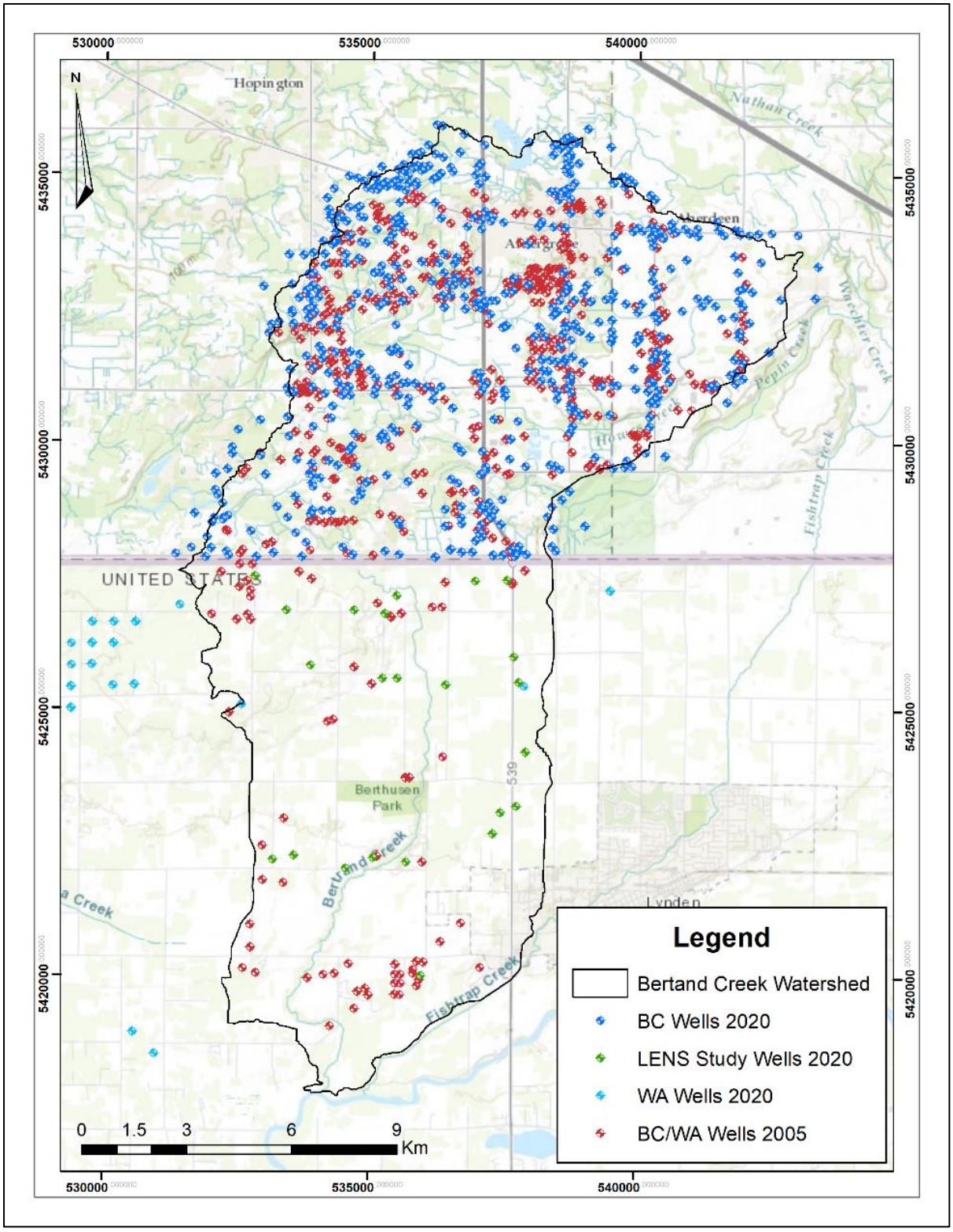

Figure 10: Wells with lithology logs across the study area. Shown in red are the wells in the original 2005 groundwater flow model, and in other colours for wells added for this study (as of June 2020). Only select LENS Study wells were added on the US side.

Notwithstanding the data quality issues, the abundance of well lithology logs in the Bertrand Creek Watershed provided baseline information for constructing the geological model. As described in the following section, these lithology logs were standardized with the aid of detailed Quaternary geology reports to aid in interpretation and eliminate the guess work during well log correlation.

3.3.3 Lithology Log Standardization

Due to the large number of well correlations needed to construct the geologic model, generalizations and simplifications were required to reduce the, sometimes lengthy, interval descriptions down to easily identifiable descriptions consisting of only lithologic material and unique descriptors such as interbedding or presence of organic detritus. This process is standardization. The goal of this standardization process is to ensure broad interpretability of the lithologies and allow for correlation between different wells across the watershed as efficiently as possible. Additionally, terminology and descriptions were standardized such that intervals could be later interpreted with the aid of Armstrong's (1984) comprehensive study on the Quaternary geology of the region, as well as to match the existing hydrostratigraphic units used in the original regional model by Scibek and Allen (2005).

All of the database manipulation was done in Microsoft Excel (2020) utilizing built-in functions and tools, taking advantage of commonality between interval descriptions.

In the original Abbotsford modelling study by Scibek and Allen (2005), the standardization methodology was developed for use in conjunction with a word recognition code. The approach taken in this study involved manual review and aggregate cell editing using terminology similar to that of the original database. Well lithology logs and their interval descriptions were sorted by well tag number (WTN). Wells in Washington also have unique well ID number. Using the high-resolution DEM created for this study, each well was assigned a ground surface elevation using the multi-point to values tool in ArcMap. This was done for both the new and old well databases because the elevation values in the old database had been determined from an older DEM. All measurements in the new database were converted to metres. Next, a new column was created for the standardized lithology interval descriptions. Processing was achieved using Excel's find and replace function as a word recognition tool to aid in editing multiple entries at once that included common terms or descriptors. This tool was used to delete, replace, modify or assign words to entries. In total, 3927 well log interval entries were reviewed and standardized. Many lithology logs were manually reviewed using the original well construction reports.

Few interval descriptions included specific sedimentological observations such as layering characteristics like interbedding or lenses. Many descriptors included very ambiguous terms not easily or readily interpretable such as "fat", "tight", "loose", "clean", "dirty", "gummy", "sticky" or "hardpack". While these terms do carry meaning, they are general and subjective. All of these terms were deleted from the entries, among many others. A very popular descriptor was "Waterbearing", "WB" or "W.B.", which was also all deleted as it pertains to the groundwater, not the lithology.

Some of the interval descriptions lacked proper terminology, and in those cases, words were either replaced or modified. Words that were modified included abbreviations or shorthanded versions of words such as: "sd/sd." for sand or "sdy" for sandy. Words that were replaced ranged from simple terms like "topsoil" to "soil" to more ambiguous terms like "hardpan" to "till". "Dirt" was also a popular descriptor and was replaced with "soil". "With rocks" was replaced with "Stony" as this terminology is used in the Abbotsford modelling report and in Armstrong (1984). "Unknown" was assigned to interval entries that contained blank entries within highly detailed well logs, or if there was a single interval of unknown material.

To conform with naming convention outlined in Scibek and Allen (2005) “cobbles”, “boulder” and “pebbles” were replaced with “gravel”. Another popular descriptor for geologic material containing coarse clasts, including within clays, was the prefix “stony”, which is likely to mean larger sediment fragments dispersed in that interval, or simply, clasts of gravels, pebbles, cobbles or stones. “Stony” was kept as a descriptor as it is used in the old database and in lithologic descriptions in Armstrong (1984).

The connective function word “with”, used to indicate accompaniment, was replaced by using the material that succeeds the connective word and attaching a “-y/-ey” suffix to indicate a subordinate fraction of material. This assumes that the succeeding material that comes after the connective word is of a lesser fraction than that of the preceding material, which is assumed to be the dominant fraction. For example, if a description contains “Sand with Clay”, this then becomes “Clayey Sand”. This further reduces word count and simplifies the descriptions while still preserving the underlying meaning and observation of the logged interval. The connective function word “and” was preserved as this is assumed to signify materials of the same fraction. Unique descriptors such as “organics” or “interbedded” were parenthesized. Table 5 summarizes the most common standardization processing. As a final step, descriptions from the old database were slightly modified by removing slashed (/) descriptions.

Table 5: Summary of standardization for common descriptions encountered throughout the databases.

Process	Original Description	Standardized Description
Replaced	“*With layers of…*” or “*Lenses of…*”	Interbedded
	“*Muck*” or “*Bog*”	Peat
	“*Gravelly Clay*”	Stony Clay
	“*With/some… boulders/cobbles/stones/pebbles/aggregate*”	Stony
	“*Topsoil*” or “*Dirt*”	Soil
	“*Hardpan*”	Till
	“*Sd/Sd./Sdy*”	Sand/Sandy
Modified	“*Material 1 with material 2*”	Material 2(-y/ey) Material 1
Deleted	Adjectives: “*fat*”, “*tight*”, “*loose*”, “*clean*”, “*dirty*”, “*gummy*”, “*sticky*”, “*hardpack*”, “*mostly*”.	N/A
	“*With traces of...*”	
	“*Odd stone*”	N/A
	“*With little…*”	N/A
	“*Grain size*”	N/A
	“*Colour*”	N/A
		N/A
Assigned	“*Pre-existing well*” or “*Dug well*”	Unknown
	“*Organics*” or “*Interbedded*”	(Parenthesized)

3.3.4 Well Database Update

All of the new wells were appended to the old database to produce an updated standardized well database (2020) for the Bertrand Creek Watershed study area. In total, the old database, used in Scibek and Allen (2005), consisted of 565 wells within the study area. Using new wells uploaded to the B.C. GWELLS database, digitized wells from the Washington Department of Ecology well database and wells digitized from the LENS study (Cox and Kahle, 1994), 613 new well lithology logs were added to the existing database. Thus, in total, the Bertrand Creek Watershed study area now has 1178 wells with standardized borehole lithology. Additionally, 161 wells adjacent to the watershed, in Canada and the US, were also standardized for better correlation during geological modelling.

3.3.5 Uncertainty

As well lithologic information provides the foundation for constructing a geological model, certain limitations arise that stem from poor quality of lithologic descriptions, lack of core, lack of deep boreholes across the study area (especially on the US side of the border), and the lack of a digitized well log database for US wells.

Over 100 standardized unique descriptors were identified in the well logs. The subsurface is extremely heterogenous, both laterally and vertically. These factors result in limitations regarding the accuracy of the mapping of the nature of the geologic subsurface. Thus, there exists an infinite number of ways that the distribution of these subsurface materials can be delineated. This means the geological model interpreted from the distribution of these sediments will be highly non-unique.

3.4 Hydrostratigraphy

3.4.1 Approach and Software

One objective of this study was to build a 3D geological model of Bertrand Creek Watershed that could be directly imported into the numerical groundwater modelling software Visual MODFLOW Flex. Ultimately, this was not possible due to limitations of the geologic modelling software Leapfrog Geo v5.1 (Seequent Limited, 2020) in this particular geologic setting. Therefore, the numerical model was constructed using the same approach as Scibek and Allen (2005) – that is, mapping hydrostatigraphic units as discrete hydraulic property zones directly in the numerical modelling software (see Section 4.3).

To aid in this process, the standardized borehole lithology logs as well as the surface DEM and the bedrock DEM were imported into Leapfrog Geo. Visualizing the borehole lithology logs in a 3D context provided valuable insight into the spatial variability of the various lithologic units. The software aided in identifying lithology intervals and grouping lithologies into broad classes corresponding to hydrostratigraphic units identified in previous studies (e.g. Scibek and Allen, 2005).

3.4.2 Lithology Groups

Using the standardized borehole lithology logs in combination with an understanding of the geologic history, intervals were classified into broad lithology groups based on the dominant lithology in the interval. If the interval had one or more dominant lithologies, they were classified into “mix” groups for which three different “mix” groups were created; the coarse mix group for intervals containing sand and gravel or other coarse combination; the fine mix group for silts and clays; and the coarse/fine mix group for intervals containing mixes of coarse sediment with fine sediment such as sand and clay or gravel and silt. These groups are shown in Figure 11, as a function of interval length. The overall goal of this grouping exercise was to first consider what types of materials are present at a given elevation or depth interval and how they are spatially distributed.

Table 6 shows the lithology groupings identified in this study, and which hydrostratigraphic units in the original model by Scibek and Allen (2005) each is associated with.

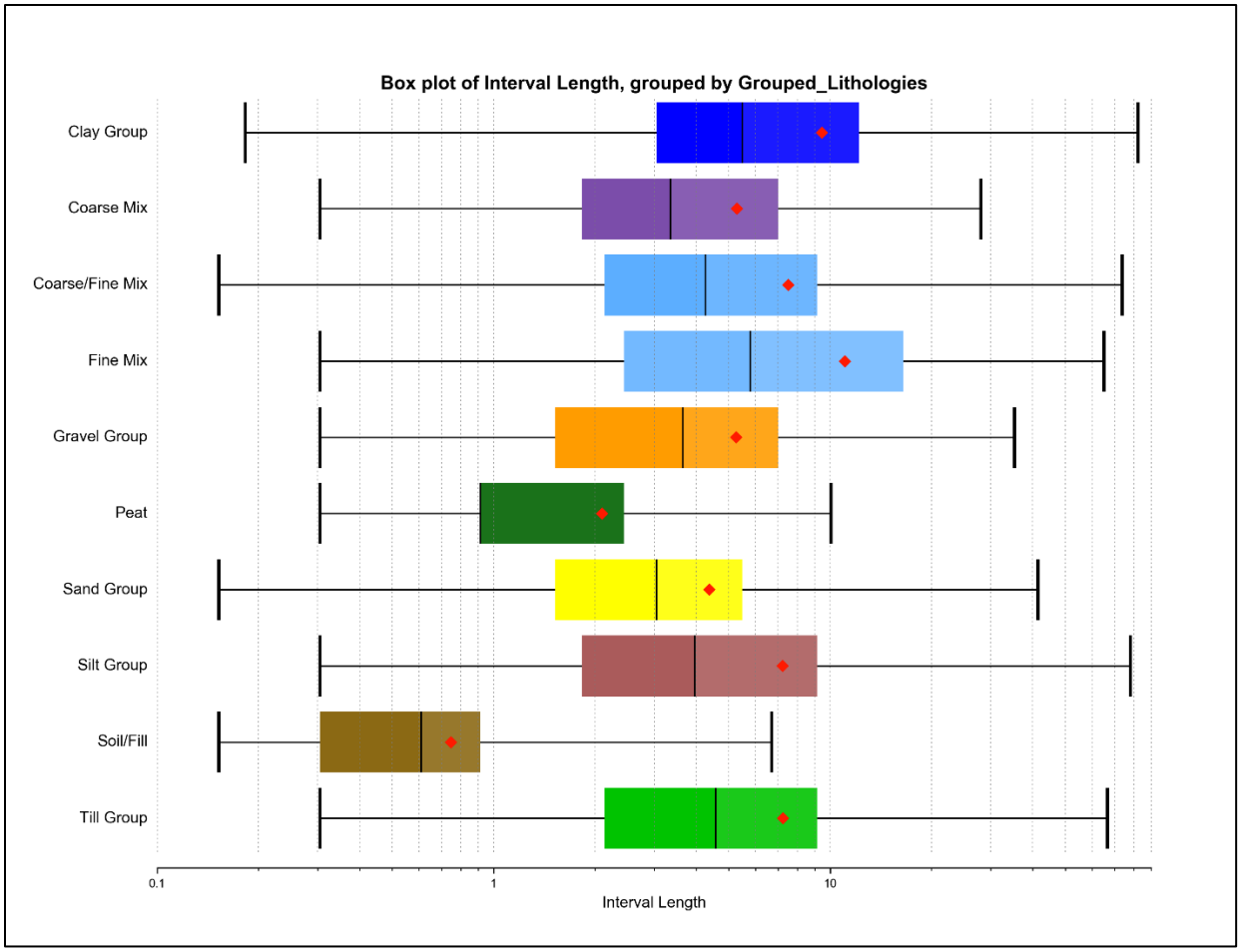

Figure 11: Lithology groupings based on dominant material present in a logged interval. The horizontal axis displays the interval length of a group on a log scale. The red star represents the mean, while the black bar is the median, and the tails are the minimum and maximum interval lengths in a group.

Table 6: Hydrostratigraphic units in Scibek and Allen (2005) and the associated grouped lithology in this study.

Hydrostratigraphic Unit (Scibek and Allen, 2005)	Grouped Lithology
-	Soil Group
Salish Sediments (Peat/Fluvial Channel)	Peat Group
Sumas Drift (Upland Flow Tills)	Till Group
Sumas Drift (Upland Glaciofluvial)	Coarse/Fine Mix
Fort Langley Fm. (Clay/Till)	Clay Group
Sumas Drift (Glaciolacustrine Silt/Fines)	Fine Mix Group, Silt Group
Sumas Drift (Gravel)	Gravel Group, Coarse Mix Group
Sumas Drift (Sand)	Sand Group

3.4.3 Delineating Hydrostratigraphic Units

Delineating hydrostratigraphic units in the context of the regional geologic setting and glacial history of the Fraser Valley is very complicated, as noted in many previous studies that attempted to model aquifers in the Fraser Valley (e.g. Halstead, 1986; Cox and Kahle, 1999; Scibek and Allen, 2005). As reported in Scibek and Allen (2005), fitting surfaces to correlate different lithology intervals is simply not

possible due to the extreme heterogeneity of sediment distribution. In all attempts to regionally characterize these complex aquifer systems, gross simplifications of the hydrostratigraphy of the area were made, albeit justified, considering the extreme heterogeneity of material distribution.

As shown in Figure 12, practically (and conceptually) there are no discernable or obvious correlative relationships between boreholes that can be used to identify laterally continuous layers. While further aggregating intervals into groupings could potentially reveal more distinct relationships, the initial level of detail would be lost, defeating the purpose of higher resolution modelling. Additionally, Leapfrog Geo v5.1 lacks the capability to efficiently model complex stratigraphy, lenses and discontinuous layers using borehole data because it generates surfaces based on age relationships, which as described previously in Section 2.5.2 is problematic in this type of geologic setting.

Therefore, a geological model could not be constructed in Leapfrog. An alternative approach was used for defining the hydrostratigraphic units and their associated hydraulic properties directly in the numerical model, described in detail in Section 4.3.

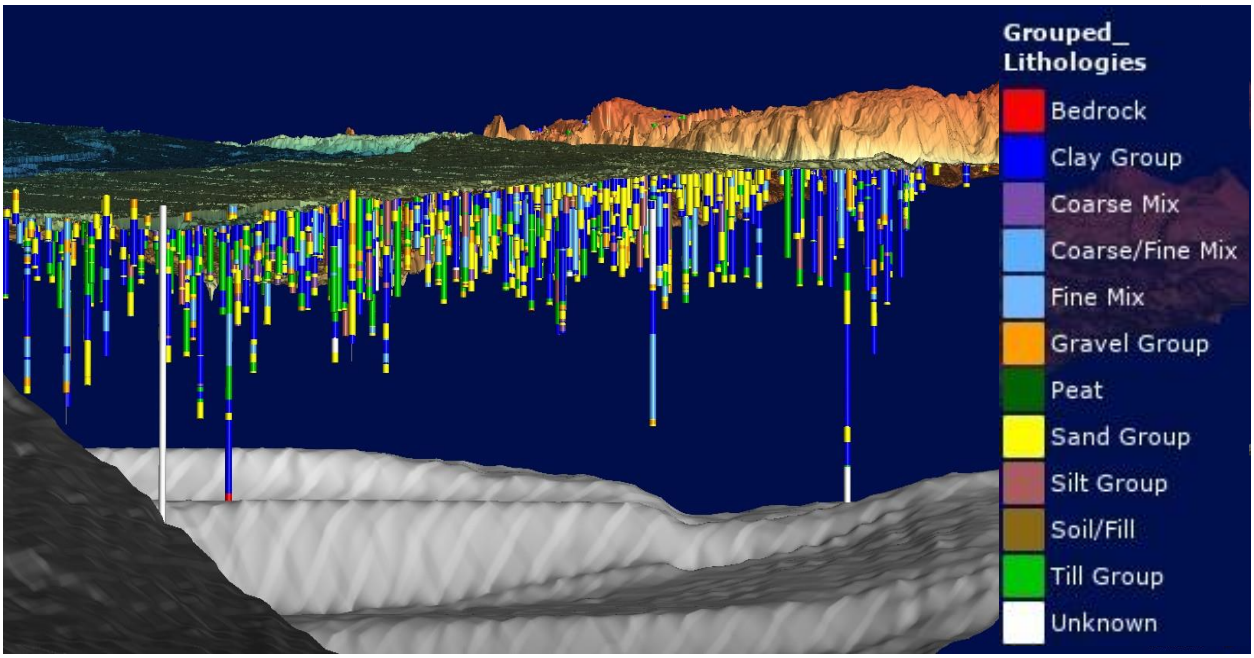

Figure 12: Northwest-looking profile view of boreholes and the resulting groups. Image generated using Leapfrog Geo. The bedrock DEM is shown at the base.

3.5 Surface Water Hydrology

The Bertrand Creek Watershed is approximately 110 km^2 and features several ephemeral tributary streams that feed into the Bertrand Creek. Bertrand Creek is the main and largest stream flowing through the watershed. The headwater source of the Bertrand Creek is located north of Aldergrove, with the creek discharging into the Nooksack River, to the south, in Washington State (Figure 13). Many of the long linear water features are drainage ditches and canals that run through agricultural lands. Nearly all surface water and groundwater flow from the Abbotsford-Sumas aquifer, the main underlying surficial aquifer, discharges into the Nooksack River to the south (Scibek and Allen, 2005).

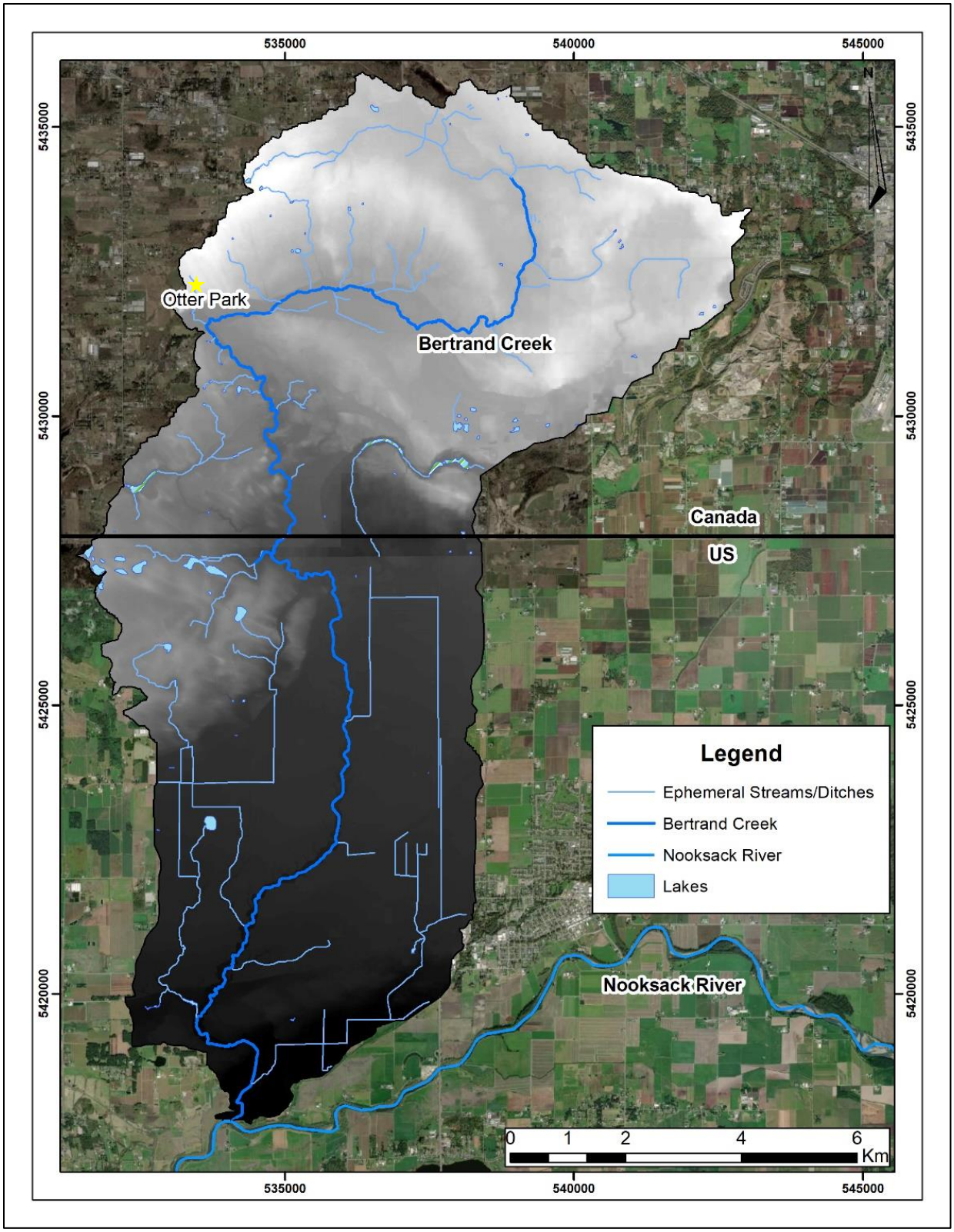

Figure 13: Surficial hydrologic water features within the Bertrand Creek Watershed, with the DEM overlay.

3.6 Recharge and Flow Inputs/Outputs

Recharge to the Bertrand Creek Watershed occurs primarily as precipitation that percolates through the soil column and into the unconfined aquifers as diffuse recharge. Scibek and Allen (2006) undertook a recharge modelling study of the Abbotsford-Sumas aquifer using a series of one-dimensional soil percolation models, with varying vadose zone depths, and ranges of soil and vadose zone hydraulic properties. The recharge model was forced using downscaled climate data from a global climate model (GCM) representing historical climate over the period 1971-2000. The resulting map showed spatially-distributed recharge for the Abbotsford-Sumas aquifer. Scibek and Allen (2005) then applied the recharge to their regional model. Based on the recharge modelling, the annual recharge across the Bertrand Creek Watershed ranges from 974-1041 mm, with an approximate spatially averaged annual recharge of approximately 1016 mm/yr (Figure 14). Of note, is the distinct contrast in recharge values at the Canada-US border as a result of differences in soil mapping and permeability classification between the Ministry of Water, Land and Air Protection (now the Ministry of Environment & Climate Change Strategy) and the US Department of Agriculture.

Additional recharge to the aquifers, in small quantities, include contributions from losing reaches of streams and ditches as well as irrigation of croplands (Cox and Kahle, 1999). Groundwater flow mainly discharges into gaining reaches of streams and lakes, as seepage, as well as into drainage ditches (Scibek and Allen, 2005). The Nooksack River to the south receives baseflow contributions from the Abbotsford-Sumas aquifer (Scibek and Allen, 2005). Additionally, groundwater is also lost through evapotranspiration and pumping wells (Cox and Kahle, 1999).

Because of the heterogenous distribution of surficial glacial and non-glacial sediments, coupled with the fact that Bertrand Creek cross cuts into these sediments, different reaches of the stream can either be segments of groundwater discharge or groundwater recharge. Where there is a hydraulic connection between the surficial aquifers and Bertrand Creek, and depending on the nature of the water table, groundwater may contribute to streamflow as baseflow in gaining reaches, or groundwater may be recharged by the stream in losing reaches. The confluence of Bertrand Creek and the Nooksack River marks the discharge point of Bertrand Creek.

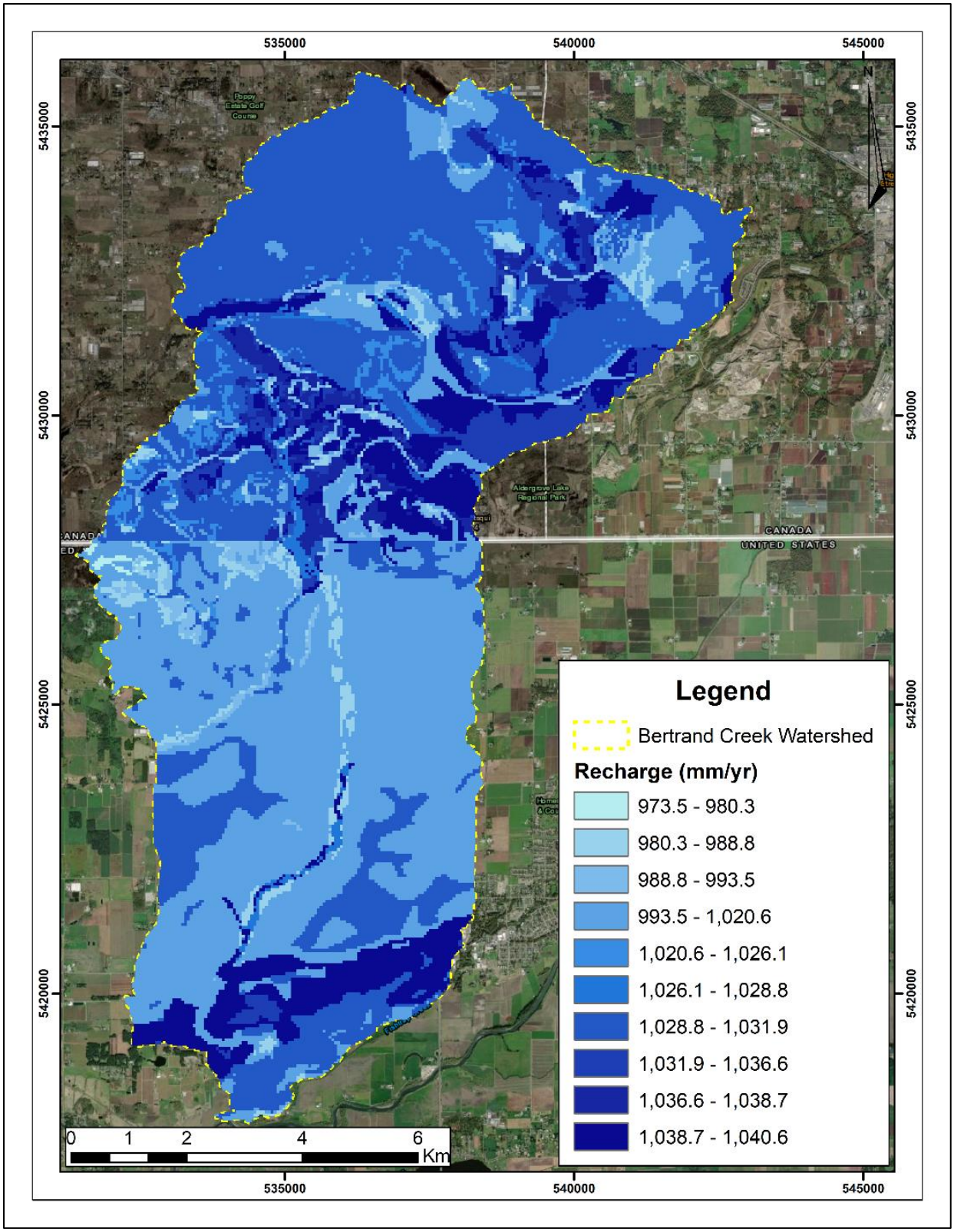

Figure 14: Average annual recharge in the Bertrand Creek Watershed, modified from Scibek and Allen (2006). The distinct contrast in recharge at the Canada-US border is related to differences in the soil mapping and permeability classifications between the two jurisdictions.

3.7 Regional Groundwater Flow

Determination of regional groundwater flow was achieved using the pre-existing Abbotsford-Sumas regional flow model by running it in Visual MODFLOW Flex and observing the regional trends using flow velocity fields and tracking particle movement through the groundwater system. The MODPATH code (Pollock, 2017) in Visual MODFLOW Flex was used for particle tracking. Additionally, a water table map of the Bertrand Creek Watershed was generated using static water level data reported in the well records as contoured by Scibek and Allen (2005).

3.7.1 Flow Velocity Map

Visualizing the flow direction across the Bertrand Creek Watershed (Figure 15) shows an overall regional trend in groundwater flow from north to south. Flow directions seem to suggest that groundwater, in the near surface (represented in the uppermost model layers), flows towards and into the Bertrand Creek, eventually draining into the Nooksack River to the south.

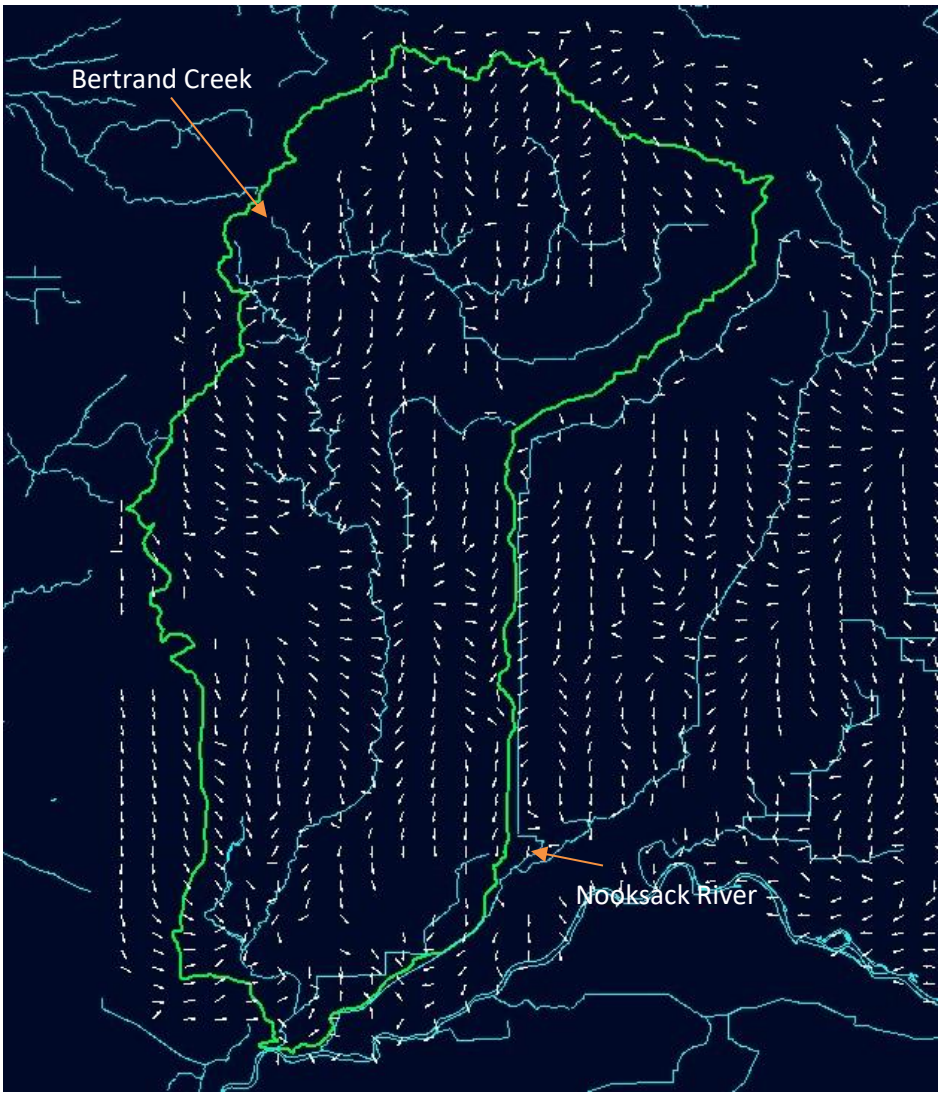

Figure 15: Velocity field map showing the direction of groundwater flow through the Bertrand Creek Watershed in the uppermost layers of the model in the original Abbotsford-Sumas model.

3.7.2 Cross-Catchment Flow

Cross-catchment flow is a particularly important consideration for defining the model domain as well as assigning appropriate boundary conditions in the Bertrand Watershed model. If there are significant contributions and exchanges of groundwater flow through the Bertrand Creek Watershed into the adjacent catchments, then the model domain may need to be adjusted to deviate from the watershed boundary (as it is defined based on surface water divides) or different boundary conditions may need to be considered. Much of the watershed appears to have some component of cross-catchment flow, as shown in Figure 16. Most of that flow enters the watershed along the southwestern boundary. Flow also moves out of the watershed in the northwest and at the south. Note that these velocity arrows are not scaled to magnitude, only direction (scaled velocity vectors are shown in Figure 17).

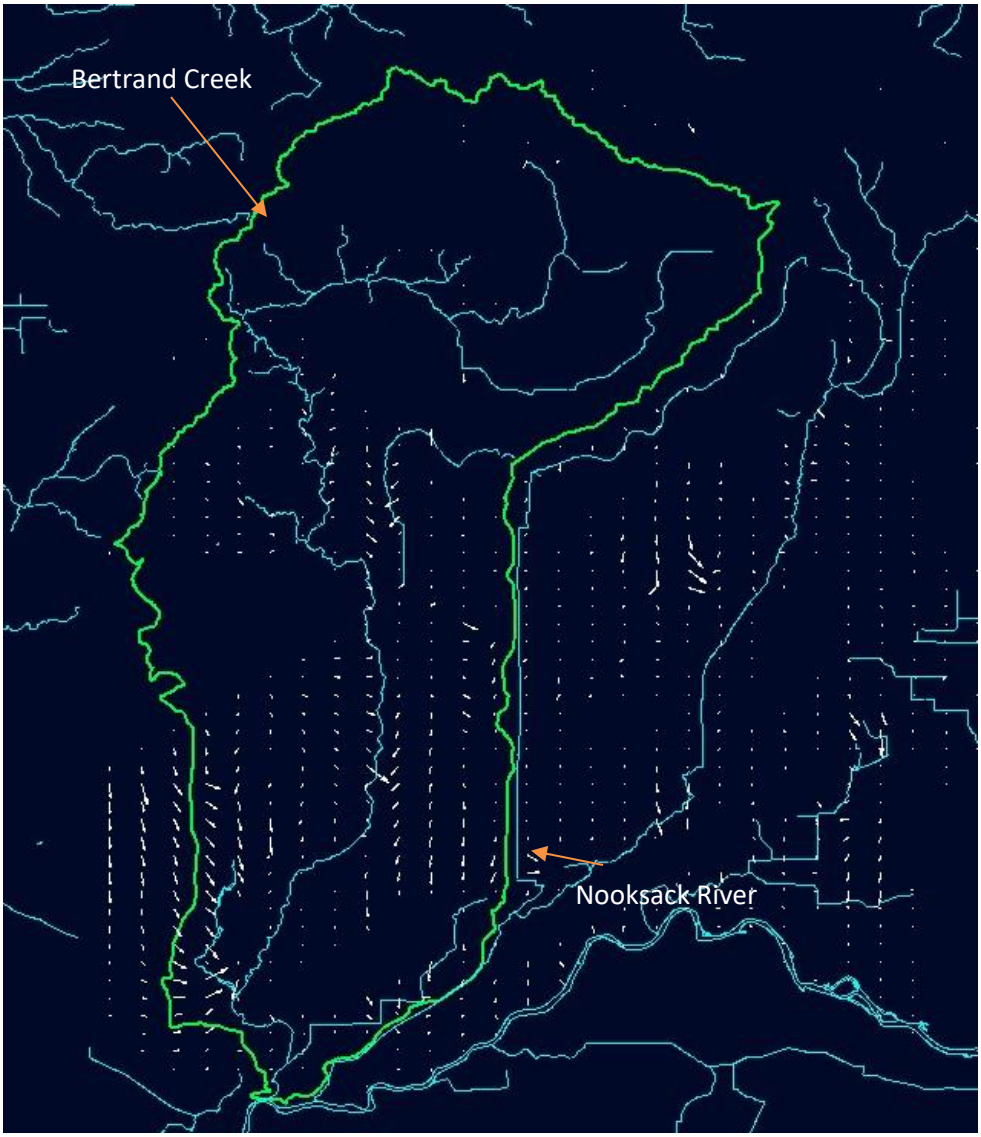

Figure 16: Velocity field map showing the magnitude of groundwater flow through the Bertrand Creek Watershed in the uppermost layers of the model in the original Abbotsford-Sumas model.

Additionally, using the original model, a zone budget for flow mass balance was assigned to the watershed to determine the difference between cross-catchment outflows and inflows. The total inflow to the watershed from the surrounding aquifers is 3061 m^3/yr and the total outflow from the watershed is 1784 m^3/yr. This represents a net positive flow of 1277 m^3/yr into the Bertrand Creek Watershed from the surrounding aquifers. For comparison, annual recharge is 1016 mm over an area of $1.1x10^8$ m^2 for a rate of $1.12x10^8$ m^3/yr. So, cross-catchment flow is a small fraction of recharge and can be considered negligible. This means that the watershed boundary is reasonable to use for a groundwater model.

3.7.3 Particle Tracking

Forward particles were inserted at the northern boundary of the Bertrand Creek Watershed. The particle trajectories seem to agree with the groundwater velocity distribution, showing groundwater flowing from north to south (Figure 17). Interestingly, the groundwater flow paths are quite deep and most terminate at the Nooksack River. Additionally, many of the particles also seem to discharge into some sections of the Bertrand Creek as indicated by the yellow circle in Figure 17. The particle flow paths also reveal the absence of smaller local flow systems which may be an indication of the coarse grid size of the original Abbotsford-Sumas model. This suggests that model refinement and the insertion of additional layering may generate local groundwater flow systems to highlight interactions along Bertrand Creek.

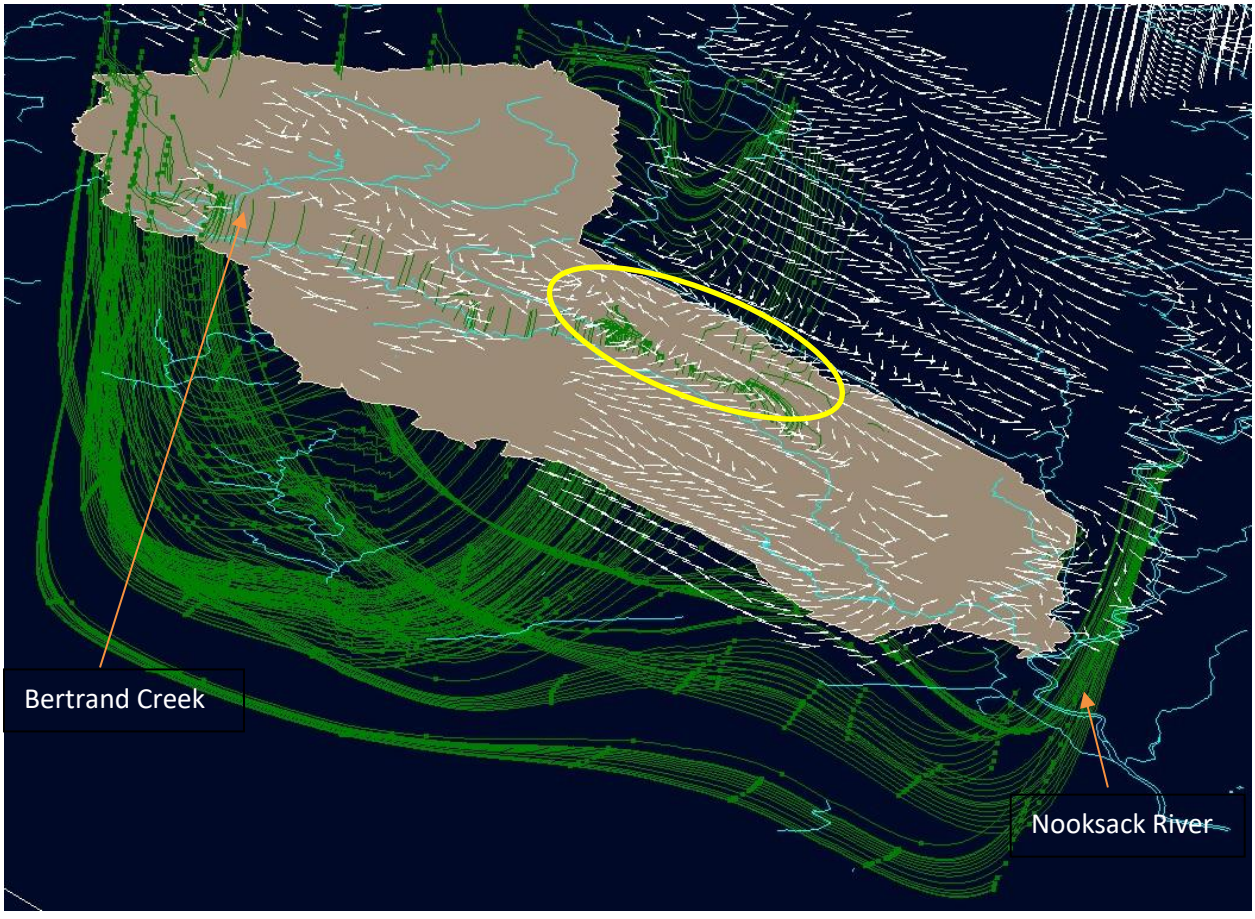

Figure 17: Oblique view of groundwater flow paths represented by particles inserted at the north boundary of Bertrand Creek Watershed in the original Abbotsford-Sumas model.

3.7.4 Static Water Table

Scibek and Allen (2005) used static water levels, recorded upon completion of well drilling (reported in GWELLS and Washington Ecology) along with surface water elevations to construct a water table map for the Abbotsford-Sumas aquifer. The water table map, clipped to the Bertrand Creek Watershed, is shown in Figure 18. Regionally, the hydraulic gradient is low throughout the watershed (~0.003), but slightly increases down-gradient to ~0.016 where groundwater flow discharges into the Nooksack River.

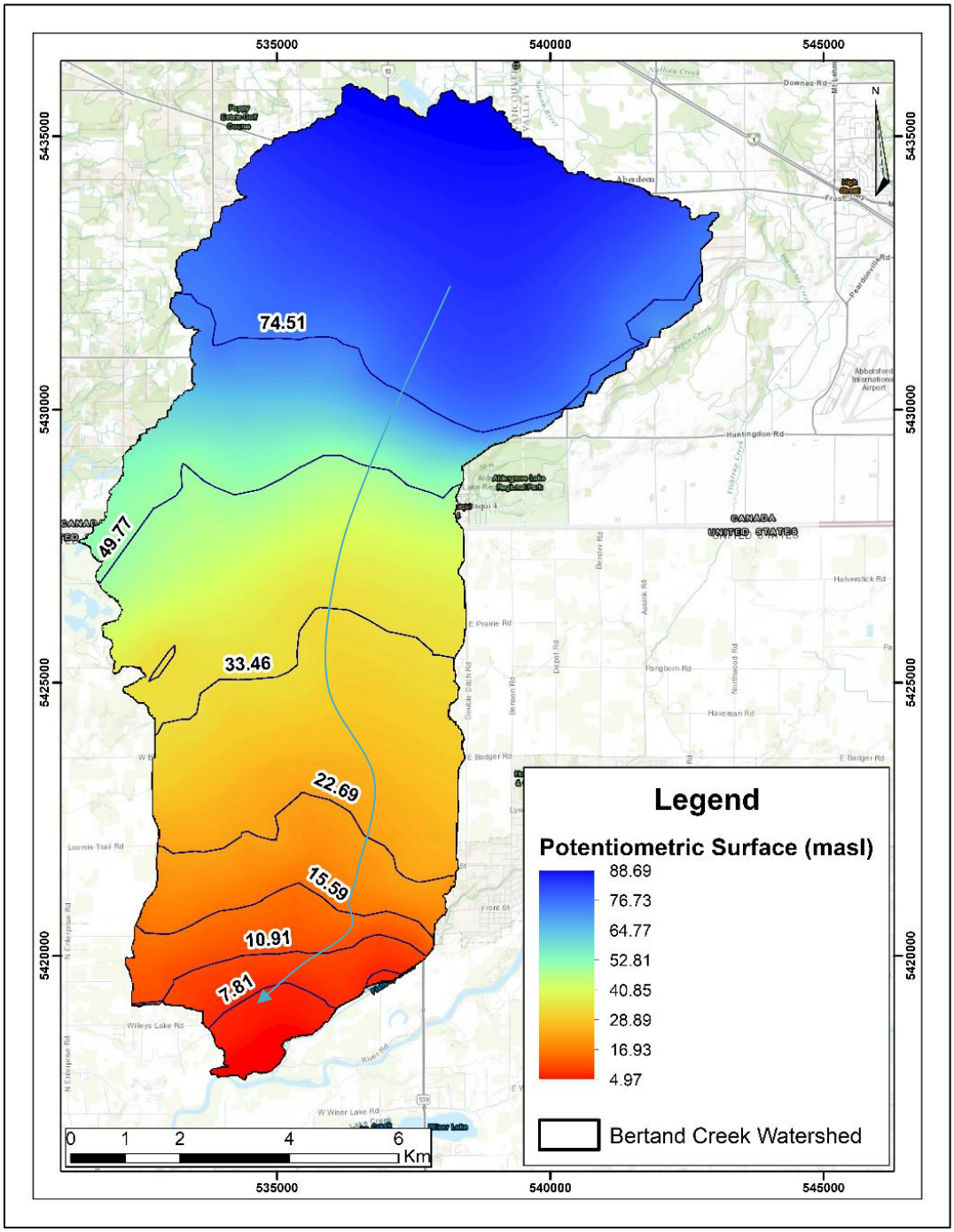

Figure 18: Water table map for the Bertrand Creek Watershed with contour elevations in metres above sea level (masl). Note the general direction of flow is from north to south.

4. NUMERICAL GROUNDWATER FLOW MODEL

4.1 Modelling Software

Visual MODFLOW Flex v6.1 (Waterloo Hydrogeologic Inc., 2019) software was used as the modelling environment for running the MODFLOW 2005 code. The MODFLOW 2005 code is a 3D block-centered finite-difference code (Harbaugh, 2005) that solves the groundwater flow equation at every cell in the model. Additionally, the built-in Zone Budget function is used to determine mass balances in specified cell groups, such as the cells that make up a stream segment or specific aquifer layer.

4.2 Model Domain and Spatial Discretization

4.2.1 Horizontal Extent and Discretization

The model domain encompasses a surface area of approximately 110 km^2 and represents the spatial extent of the Bertrand Creek Watershed extending from Canada to the United States. A uniform finite difference grid, aligned north-south and east-west roughly in line with the regional groundwater flow direction, was constructed. Each grid cell is 25 m x 25 m representing a cell area of 625 m^2. The original model had a variable grid size, ranging from 100 m x 100 m near the edges of the model to 25 m x 25 m in the middle region.

4.2.2 Vertical Extent and Discretization

The surface and bedrock DEMs were imported as ASCII files (Flex allows ASCII, .DEM and .GRD file types for gridded surface data). Unfortunately, Flex could not import the ASCII files for both DEMs at 0.5 m resolution because the files were too large. Because of this, both the surface and bedrock DEMs were upscaled to 7.5 m for import. Visual MODFLOW Flex then automatically upscaled the surface and bedrock DEMs to match the finite difference grid cell size (25 m x 25 m). For any telescopic grid refinements, the grid cell size can be decreased down to 7.5 m while still retaining an accurate surface representation.

The original Abbotsford-Sumas model had 9 computational layers (Table 7), with the uppermost 3-m thick layer representing the surficial geology as mapped in Section 2.4 (Figure 6). Each subsequent computational layer (from layer 2 to 9) represented deeper unconsolidated deposits overlying bedrock (layer 10). Layer 10 was deactivated to represent impermeable bedrock. The computation layer thicknesses were chosen to reflect the dominant lithology in that depth interval, but each layer comprised various lithologies that were added as property zones. Thus, the computational layers really do not reflect true thicknesses of geologic units.

The refined Bertrand Watershed model consists of 16 computational layers representing soils and unconsolidated materials overlying impermeable bedrock (Table 7) A 1-m thick soil zone forms the uppermost computational layer (Table 7) (see Section 4.3.2 for details). The second computational layer represents the surficial geology as mapped in Figure 6. It extends to a depth of 10 m (see Section 4.3.3 for details). Deeper computational layers coincide with those of the original model (Table 7).

Table 7: Comparison of the vertical discretization of the original Abbotsford-Sumas model and the refined Bertrand Creek Watershed model.

Original Abbotsford-Sumas model			Refined Bertrand Creek Watershed model		
Computational Layer	Representing	Thickness	Computational Layer	Representing	Thickness
1	Surficial Geology	3 m	1	Soil	1 m
2 to 9	Combined surficial geology and deeper stratigraphic sequencing	Variable, ranging from 15 m to 30 m	2	Surficial Geology	9 m
10	Bedrock	0 m	3 to 16	Deeper stratigraphic sequences	Variable, ranging from 15 m to 30 m
-	-	-	17	Bedrock	0 m

4.3 Property Zones and Hydraulic Conductivity Values

4.3.1 Hydrostratigraphic Model Refinement and Hydraulic Properties

A main goal of this study was to refine the geological model for the Bertrand Watershed to include the soil zone as well as a more detailed representation of the surficial geology. Including the soil zone in the Bertrand watershed model would enable groundwater fluxes to be better resolved between the aquifers and the streams in areas where the water table is shallow (i.e., in proximity to the streams).

Given that hydrostratigraphic units could not be mapped as continuous layers in Leapfrog Geo and then imported into the numerical modelling software, an alternative approach was used for refining the hydrostratigraphic model. The approach followed that employed by Scibek and Allen (2005), who unsurprisingly experienced the same difficulty in identifying laterally continuous hydrostratigraphic units at the regional scale. The hydrostratigraphic units (i.e., the geological model) were defined directly in the numerical model, with hydraulic property zones defined manually on a computational layer by computational layer basis[3].

The hydrostratigraphic units and computational layering from the pre-existing Abbotsford-Sumas groundwater flow model were utilized as a baseline for constructing and refining the Bertrand Creek Watershed model. The pre-existing Abbotsford-Sumas groundwater model had nine computational layers with seven distinct hydrostratigraphic units represented by unique property zones (Table 8)[4]. Seven existing hydrostratigraphic units were preserved in the refined model, although their spatial distribution was refined in the new model by assigning more detailed zones (see Section 4.3.3). This was accomplished by referencing the grouped lithology logs in Leapfrog Geo (Figure 19).

Four new property zones were defined to represent soils, as described in Section 4.3.2. Finally, because the model would be run under steady-state conditions, storage properties were not required.

[3] Numerical models use computational layers, which are commonly associated with distinct hydrostratigraphic units. However, a single hydrostratigraphic unit can be separated into multiple computational layers. Similarly, a computational layer does not necessarily have to represent a single hydrostratigraphic unit. The computational layer can be heterogeneous and assigned different property zones, each with unique hydraulic properties.

[4] Note, the numbering of these property zones is inconsistent (i.e. missing zone numbers or out of order) because numbering in MODFLOW cannot be altered.

Table 8: Hydrostratigraphic unit association between this study and the original model by Scibek and Allen (2005) and the associated property zones and hydraulic conductivity values. Property zones are colour coded (see Figures 20-22 for the distribution of property zones in the model).

Hydrostratigraphic Unit	MODFLOW Property Zone		Lithology Group	Hydraulic Conductivity (m/day)		
	Original	New		K_x	K_y	K_z
Soil (Low Permeability)	-	10	Soil Group	5	5	0.5
Soil (Moderate Permeability)	-	12		510	510	51
Soil (High Permeability)	-	9		750	750	75
Soil (Very High Permeability)	-	11		1050	1050	105
Salish Sediments (Peat/Fluvial Channel)	7	3	Peat Group	10	10	0.5
Sumas Drift (Upland Flow Tills)	9	4	Till Group	1	1	0.9
Sumas Drift (Upland Glaciofluvial)	14	5	Coarse/Fine Mix	2	2	0.2
Fort Langley Fm. (Clay/Till)	23	2	Clay Group	0.6	0.6	0.06
Sumas Drift (Glaciolacustrine Silt/Fines)	24	6	Fine Mix Group, Silt Group	3	3	0.3
Sumas Drift (Gravel)	26	7	Gravel Group, Coarse Mix Group	6	6	0.6
Sumas Drift (Sand)	28	8	Sand Group	40	40	2

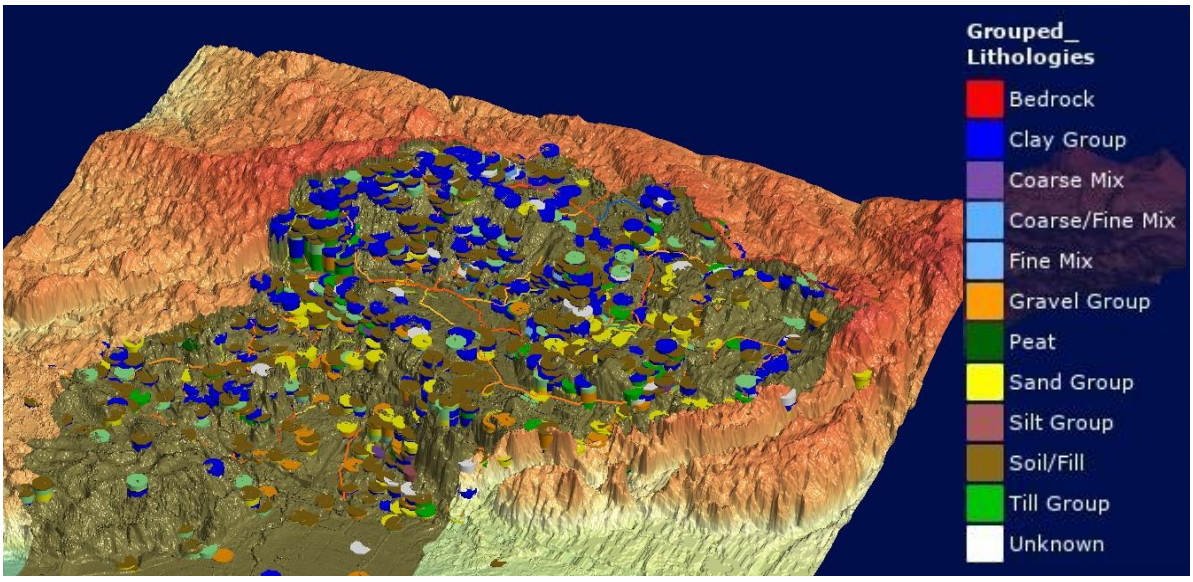

Figure 19: Oblique view of the Leapfrog Geo grouped borehole lithology logs.

4.3.2 Soil Layer

The soil thickness map created by Scibek and Allen (2006) was clipped to the Bertrand Creek Watershed. Within the watershed, the mean soil thickness is approximately 60 cm (0.6 m), with a maximum thickness of 1.8 m and a minimum thickness of 0.16 m. For simplicity, the numerical model includes a uniform one-metre thick soil layer. The soil layer was sub-divided into four distinct hydraulic conductivity zones (Table 8) based on drainage ratings and associated hydraulic conductivity (K) values as outlined in the recharge modelling study by Scibek and Allen (2006). Horizontal components of hydraulic conductivity, K_x and K_y, are assumed to be one order of magnitude higher than the vertical component (Table 8). Figure 20 shows the distribution of the property zones that form the one-metre thick soil layer.

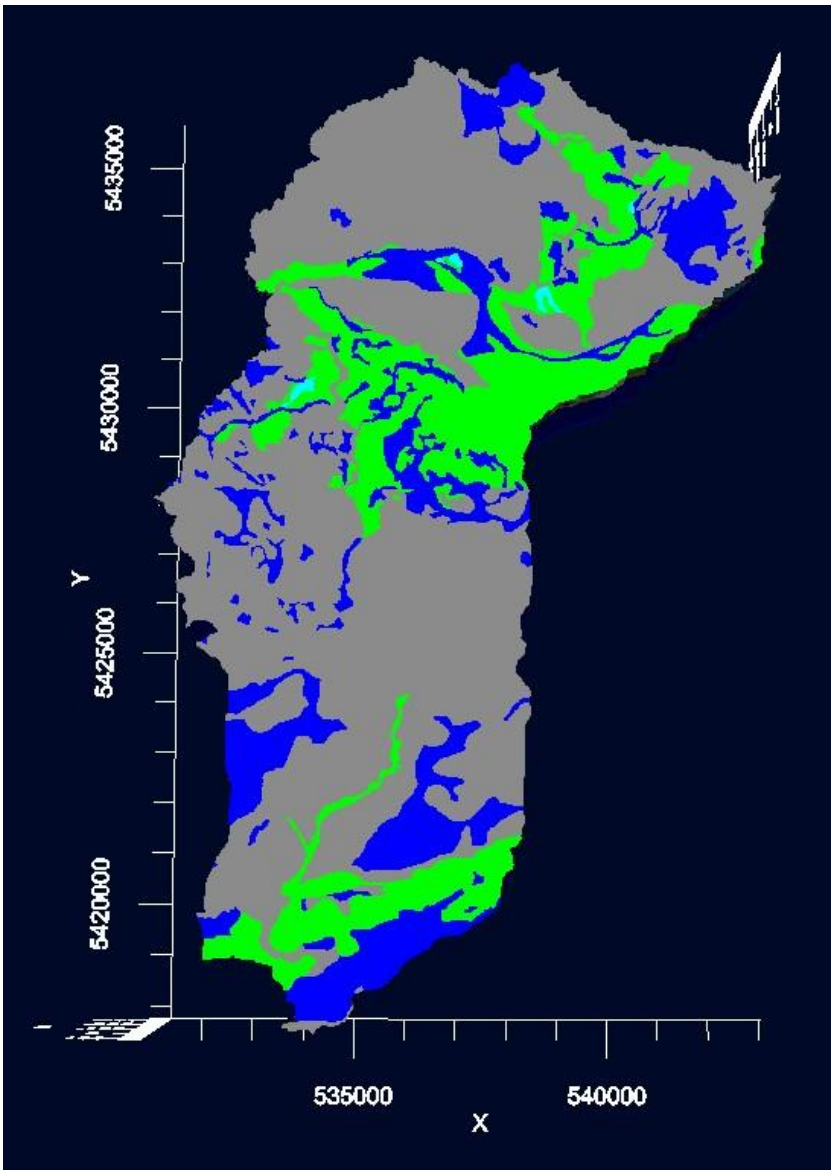

Figure 20: Distribution of hydraulic conductivity zones in the uppermost 1 m layer of soil. Refer to Table 8 for property zone K values.

4.3.3 Surficial Geology

The new 9-m thick surficial geology layer is a modification of the existing 3-m thick top surficial geology layer in the original Abbotsford-Sumas model. The 3-m layer was deepened to 9-m to capture a better representation of the surficial geology. The mean interval thicknesses observed in the grouped borehole lithology logs (red dots in Figure 11) spanned approximately 5 m to 13 m, so a rough estimate of 10 m was used to represent the surficial geology units in the model. The original hydrostratigraphic units were first assigned property zones and, subsequently, further detail was added by assigning more property zones that fit within the surficial geology map bounds and the intervals found within the uppermost 10 m as visualized in Leapfrog Geo 3D. Figure 21 shows the distribution of hydrostratigraphic units in the uppermost 9 m of the surficial geology layer, 1 m below the soil layer.

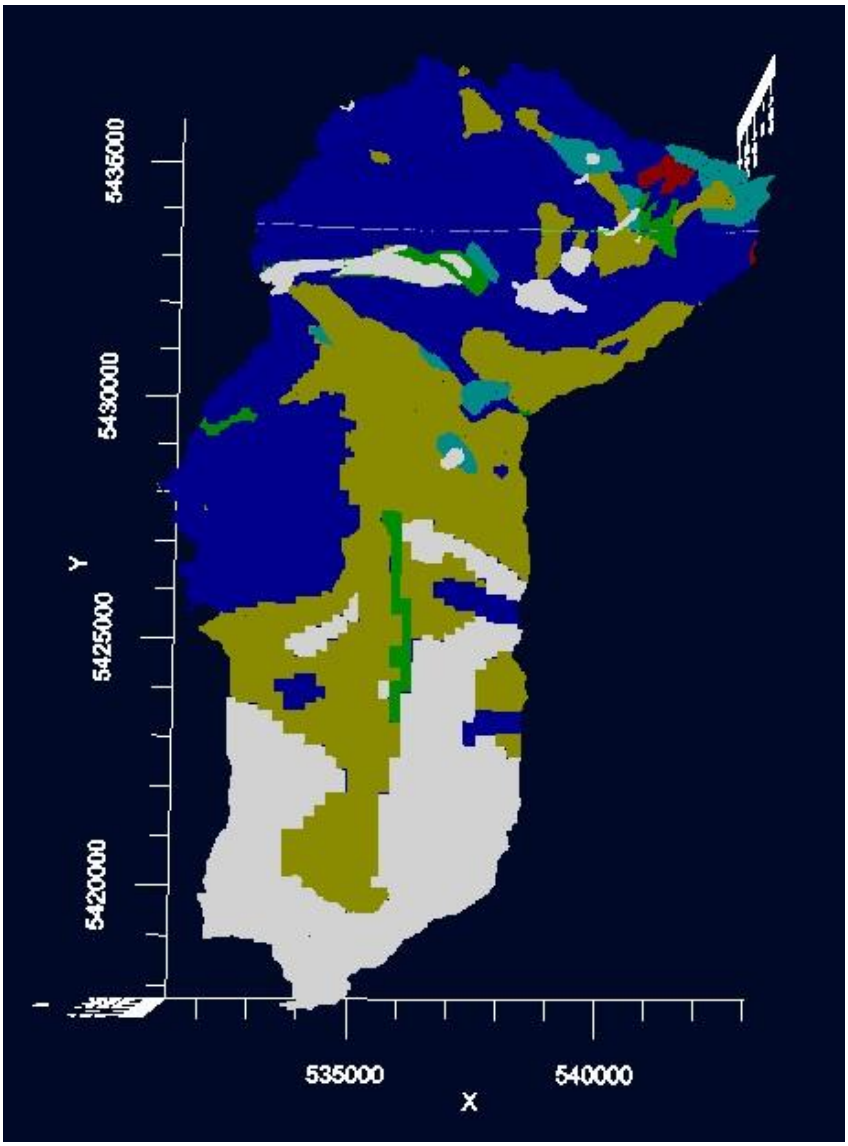

Figure 21: Distribution of hydrostratigraphic units, or property zones, in the uppermost 9 m of the surficial geology layer, 1 m below the soil layer. Refer to Table 8 for property zone K values.

4.3.4 Deeper Stratigraphic Sequences

Deeper stratigraphic sequences, represented by hydrostratigraphic units, are preserved and were not initially refined in the Bertrand Creek Watershed model. However, refinements to deeper layers were made during model calibration (see Section 4.9.3). Figure 22 shows an oblique view of the modelled hydrostratigraphy, as represented by hydraulic conductivity property zones. Similar to the original model, clay (glaciomarine clay – Fort Langley formation / Everson glaciomarine drift) underlies the coarse-grained sediments and is interpreted to extend down to bedrock. Halstead (1986) noted that all drillholes that penetrate to depths of more than 90 m have encountered these materials.

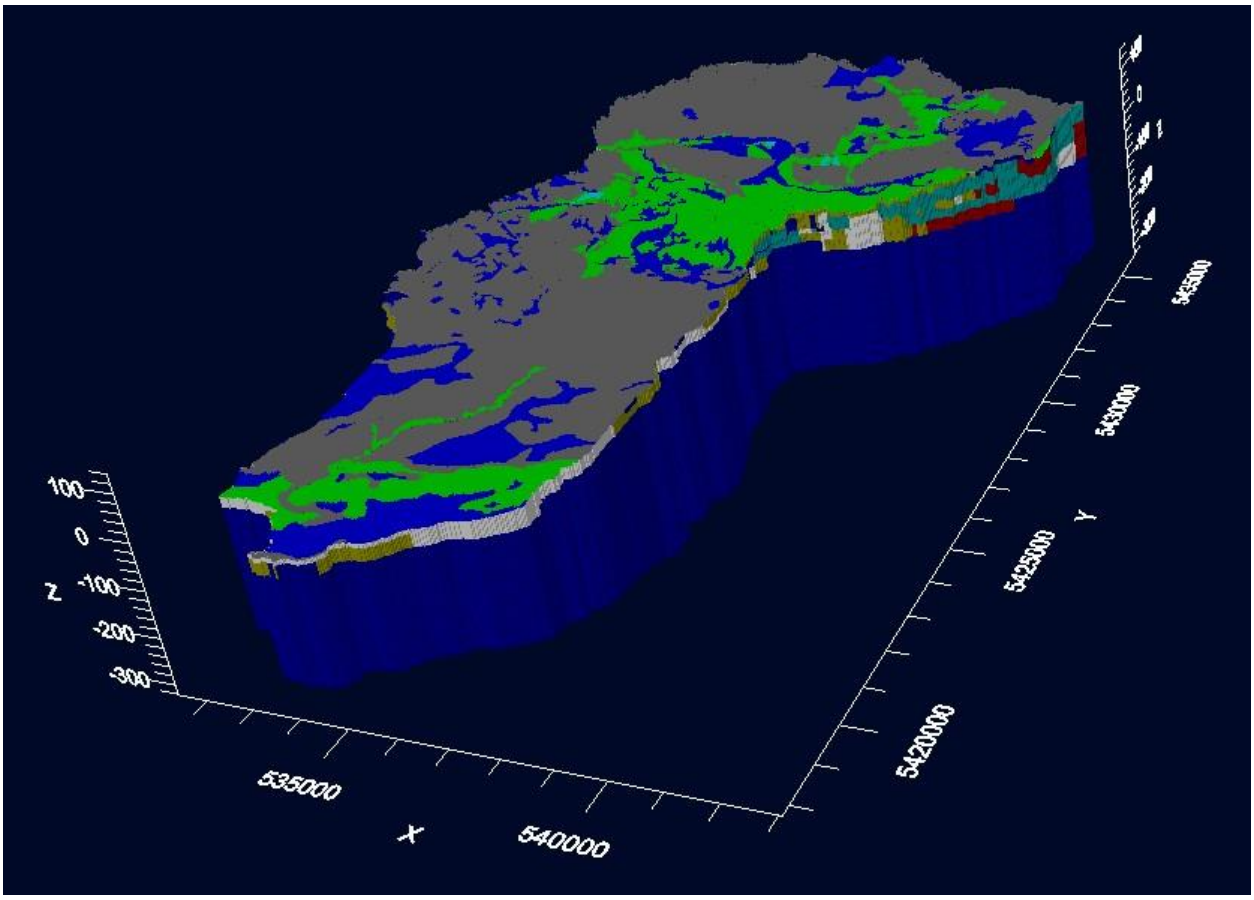

Figure 22: 3D oblique view of the Bertrand Creek Watershed model hydrostratigraphy.

4.4 Boundary Conditions

Between 2005 and 2007, some changes were made to the original model by Scibek and Allen (2005). The model domain was slightly adjusted to more closely represent surface watershed boundaries in some areas (no report), and the boundary conditions were modified by Pruneda (2007). In the following sub-sections, the changes to the boundary conditions of the regional model are summarized before describing how they were implemented in the Bertrand Creek Watershed model. The boundary conditions from Pruneda (2007) were used, along with the addition of inactive cells along the perimeter of the watershed.

4.4.1 Inactive Cells

As the cross-catchment mass balance of inflows and outflows are relatively low (see Section 3.7.2), it was determined that the entire Bertrand Creek Watershed could be bounded by inactive cells, which represent no-flow boundaries. This boundary assignment can be considered as a hydraulic boundary, as opposed to a physical boundary. Thus, no-flow boundaries delineate the watershed boundary in the model. No-flow boundaries were also assigned to the model base as it is assumed that the underlying bedrock is impermeable.

4.4.2 Constant Heads

Constant head boundaries, a type of specified head boundary, occur in two distinct areas within the model domain. This boundary simulates areas of inexhaustible supplies of water to the system. A constant head boundary was assigned to a small area in the middle of the model domain, which represents a swamp or type of wetland that supplies an influx of water into the model. This constant head was assigned a stage value of 85.6 m, identical to the original model.

Similar to the original model, Pruneda (2007) modelled the Nooksack River as a specified-head boundary condition, assuming that the Nooksack River is a large enough body of water that can maintain a fixed stage. However, Pruneda raised the stage by 2.5 m along the river, compared to the original model. The stage values were determined through examination of two USGS gaging stations on the Nooksack River, one upstream at North Cedarville, WA and one downstream at Ferndale, WA. No adjustments were made to the stage values. In the Bertrand Creek Watershed model, the head (stage) at the confluence of Bertrand Creek with the Nooksak River was assigned a stage value of 8.8 m, identical to the modified model by Pruneda (2007).

4.4.3 Rivers

The original model represented all flowing rivers, streams, or creeks as specified-head boundaries or drains. Specified-head boundaries allow for perfect hydraulic connections between the surface water and the underlying aquifer, meaning if the head in the aquifer is below that of the specified-head boundary, a limitless amount of water can be transferred into the groundwater system. These boundary conditions were used by Scibek and Allen (2005) based on the assumption that the coarse-grained nature of the aquifer materials would not limit leakage across the streambed, and also because of the lack of measured streambed conductivity. However, Pruneda (2007) modified the boundary conditions in the model in order to better simulate water exchange between the streams and the aquifer and to make use of new streambed conductivity data collected as part of his research. He changed the boundary conditions for Bertrand, Fishtrap, and Pepin Creeks to River boundary conditions.

Pruneda (2007) divided each creek into sections: seven in Bertrand Creek, six in Fishtrap Creek, and one in Pepin Creek (Figure 23). Each section was assigned a conductance value based on the nearest measurement of streambed hydraulic conductivity (Table 4 in Pruneda, 2007). All river cells north of the first site in both Bertrand and Fishtrap Creeks (i.e., north of the Canada-US border) were given the same conductance value as the first river section in each creek.

In the Bertrand Creek Watershed model, conductance values for river boundary conditions range from 6,566 to 88,750 m^2/day. These conductance values, shown in Table 9, represent a cell size of 25 m x 25 m, a streambed thickness of 0.75 to 1 m, and a hydraulic conductivity range of 7.88-142 m/day (Pruneda, 2007). The conductance value for segment B-1, which extends from Bertrand Creek headwaters to just south of the US border, is based on a field estimate of average hydraulic conductivity of the streambed sediments at Otter Park (Allen et al., 2020). The stage at the headwaters of Bertrand

Creek was set to 87.35 m and linearly interpolated, within Visual MODFLOW Flex, down to 8.74 m where Bertrand Creek enters the Nooksack River. These stage values were obtained directly from Pruneda's model. Riverbed bottom elevations were approximated by subtracting 2.5 m from the surface DEM value in that cell. This assumes that the riverbed is 2.5 m below the adjacent stream banks. This is because the interpolated stream channel surface cannot be reliably used because terrestrial LiDAR has difficulty penetrating water and thus has very low point density.

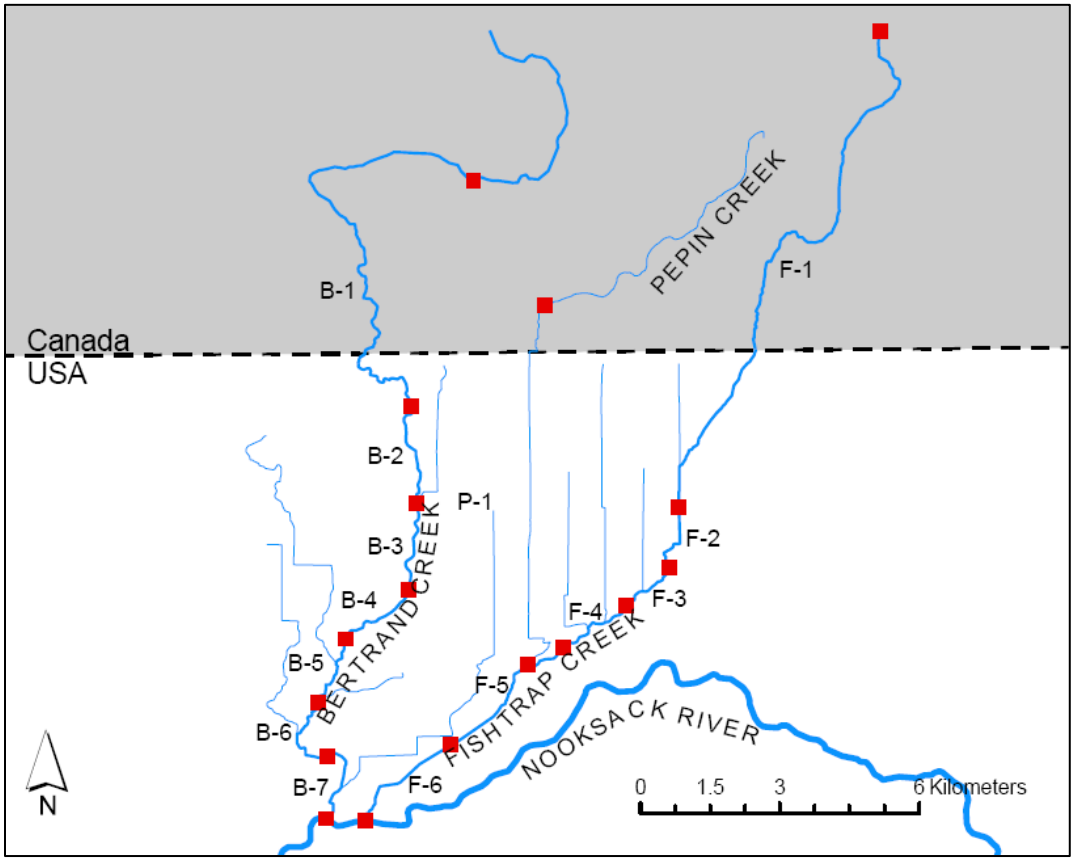

Figure 23. Sub-division of Bertrand Creek into segments (B-1 to B-7) corresponding to different measured conductance values. (From Pruneda, 2007)

Table 9. Corresponding conductance values for each stream segment. (Modified from Pruneda, 2007)

Segment ID	Hydraulic Conductivity (m/day)	Sediment Thickness (m)
B-1*	5.18×10^{1}	1
B-2	1.42×10^{2}	1
B-3	6.08×10^{1}	1
B-4	1.67×10^{1}	1
B-5	5.80×10^{1}	0.75
B-6	5.76×10^{1}	1
B-7	7.88×10^{0}	0.75

* Segment B-1 uses the average streambed sediment hydraulic conductivity and streambed thickness from Allen et al. (2020) for Otter Park in Langley, BC.

4.4.4 Drains

Drain boundaries were assigned to ephemeral reaches of Bertrand Creek, ephemeral streams that flow into Bertrand Creek and agricultural drainage ditches. This boundary simulates ephemeral flow or intermittent flow, where groundwater may enter the drain and leave the system but cannot contribute water back into the model. Pruneda (2007) retained the drain boundary conditions for small creeks and ditches, as in the original model, but modified their original conductance value of 100 m^2/day by assigning values similar to those assigned to the nearest section of Bertrand or Fishtrap creek. Thus, drain conductance values range from 6566 to 88750 m^2/day for a cell size of 25 m x 25 m, a bottom sediment thickness of 0.75 to 1 m, and corresponding range of hydraulic conductivity.

In the Bertrand Creek Watershed model, drain boundaries were assumed to be slightly shallower than the river boundary and were assigned by subtracting 1.5 m from the surface DEM.

4.4.5 Recharge

Recharge, a specified flux boundary, was applied to all active surface cells using the recharge surface developed in Section 3.6 (Figure 14). This boundary simulates recharge to the aquifer by supplying an influx of water to the top cell, providing the model with water.

4.5 Pumping Wells

Existing pumping wells from Scibek and Allen (2005) and Pruneda (2007) were used in addition to new wells (2020) from the groundwater wells point file (B.C. Data Catalogue and GWELLS Database). These new wells include attributes related to intended water use, which are helpful for determining approximate pumping rates. While a well yield attribute exists in many records, this is typically a maximum value that a driller estimates following well construction and is not accurate in indicating the actual pumping rate. Many wells were classified as unknown use and therefore were assumed to be private domestic wells as these are the most common types of wells. For some shallow wells, no screen interval information was given in the attributes. For such cases, the screen bottom was assumed to be 1 m above the well bottom elevation while the screen top was assumed to be 3 m above the well bottom elevation, for a 2 m screened interval for the pumping well. This approach assumes that the lithology near the bottom of the well represents the most productive unit.

New pumping wells for the US (since Pruneda, 2007) were not included due to a lack of a comprehensive database for US well type and water use that include relevant abstraction information. Lindsay and Bandaragoda (2013), in their WRIA 1 groundwater data assessment study for water use in Whatcom County, WA, report significant data gaps in water use source and location information for water type use. In their study, they also cite a comprehensive analysis on irrigation water use (publicly unavailable), called the Bertrand Comprehensive Irrigation District Management Plan (CIDMP), in which it was found that irrigated water accounted for 87% of total water use as opposed to 13% for surface water. However, no volumes or pumping rates are provided. Therefore, only the pumping wells originally included in the Abbotsford-Sumas model will be used in this study for the US portion of the model.

4.5.1 Well Types and Rates

Data regarding accurate pumping rates and abstracted groundwater volumes are very scarce in B.C. as many wells are not licensed and pumping rates are not reported. Therefore, determining accurate pumping rates for input to a model is challenging. Forstner et al. (2018) provide a good discussion on abstracted volume uncertainty in B.C. Additionally, pumping rates vary depending on season and timing for different water uses. This is especially true for irrigation wells. Importantly, for steady-state

groundwater flow models, water is pumped continuously at the same rate for the entire simulation time.

In this model, there are 989 active pumping wells, which is not a complete representation of all active pumping wells within the Bertrand Creek Watershed due to 1) wells not being reported in GWELLS and 2) including only a subset of wells in the US (see Figure 10). Pumping rates were assigned based on the well type, of which four are identified: private domestic, commercial and industrial, irrigation, and water supply systems. Information on pumping rates was obtained from Forstner et al. (2018), who provide the most comprehensive study to date on groundwater use by sector and well type in B.C.

Forstner et al. (2018) broke down the water use, by sector, for the Abbotsford-Sumas aquifer in the following percentages: agriculture (41%), aquaculture (31%), private domestic (13%), municipal (9%) and industrial (6%). While these percentages represent water use in the Abbotsford-Sumas aquifer, of which only a portion is present in the Bertrand Creek Watershed, they nonetheless provide good estimates for aquifers underlying Bertrand Creek watershed.

The following pumping rates are estimated based on values in the municipality of Abbotsford derived from Forstner et al. (2018) and the Abbotsford-Sumas aquifer factsheet (Aquifer 15, GWELLS). See Table B1 (Appendix B) in Forstner et al. (2018) for detailed groundwater abstraction volumes by municipality.

Private Domestic

Nine hundred and ten (910) private domestic pumping wells were defined within the Bertrand Creek Watershed. These include wells that have been classified, under the water use attribute in GWELLS, as domestic wells and wells that are assigned as unknown. Unknown wells were assumed to be private domestic wells because these are the most popular well types and a large majority of wells drilled are for domestic use. Pumping rates were derived from Forstner et al. (2018), using values from Abbotsford, where they reported that private domestic wells accounted for 3.2 million m^3/year of groundwater abstracted for 3070 wells that they classified as private domestic. Dividing the annual volume by the number of wells, results in approximately 2.86 m^3/day per well.

Commercial and Industrial

Twenty-two (22) wells are classified as commercial or industrial use in GWELLS within the Bertrand Creek Watershed. From the Abbotsford-Sumas aquifer factsheet (Aquifer 15, GWELLS) only one single well is registered for industrial and commercial use. The factsheet reports that it is allocated 0.01 million m^3/year of groundwater. Assuming the well pumps near or around this value, this results in 27.4 m^3/day of groundwater abstracted. This value was then used for all wells classified under commercial or industrial use.

Irrigation

Forty-eight (48) wells are classified as irrigation use wells in GWELLS. From the Abbotsford-Sumas aquifer factsheet (Aquifer 15, GWELLS) only four wells are registered as irrigation use. The factsheet reports that these wells are allocated 0.09 million m^3/year of groundwater, or 0.0225 million m^3/year per well. Converting units results in each well pumping 61.64 m^3/day. Therefore, each irrigation classified well was assigned this pumping rate. It is important to note that, in reality, especially for irrigation wells, there is large temporal variations in groundwater volumes abstracted depending on season and annual climate trends. As a steady-state model, seasonal use is not taken into account.

Water Supply Systems

Wells that fall under the water supply system classification include wells used as municipal water distribution systems (MWDS). Nine (9) wells were identified as MWDS wells, all of which belong to the

Township of Langley. Forstner et al. (2018) report that, in the municipality of Abbotsford, MWDS abstract approximately 1.45 million m^3/year of groundwater, split between 26 wells. Dividing the annual volume by the number of wells results in, with units converted to volume per day, approximately 152.79 m^3/day per well. Therefore, this pumping rate is assigned to wells classified as water supply systems. This rate is likely an over-estimate for smaller water supply system wells.

4.6 Model Observation Wells

Model observation wells are used during model calibration for comparing the simulated head to the observed head. Any well that had a reported static water level was included as an observation well. The same observation wells from the original Abbotsford-Sumas model (plus four USGS observation wells added by Pruneda, 2007) were used for model calibration. The observation well top elevation was adjusted using the surface DEM and the depth to water measurement was used to re-calculate the static water level in the wells. There were 603 existing observations wells included in the imported model. These were supplemented by new wells drilled since 2007. Of the 613 new wells with lithology logs that were added to the lithology database for this model, only 422 contained static water level measurements. Thus, in total, there are now 1025 model observation wells with the deepest wells only penetrating down into layer 7 (Figure 24). Deep observation well static water levels are almost non-existent.

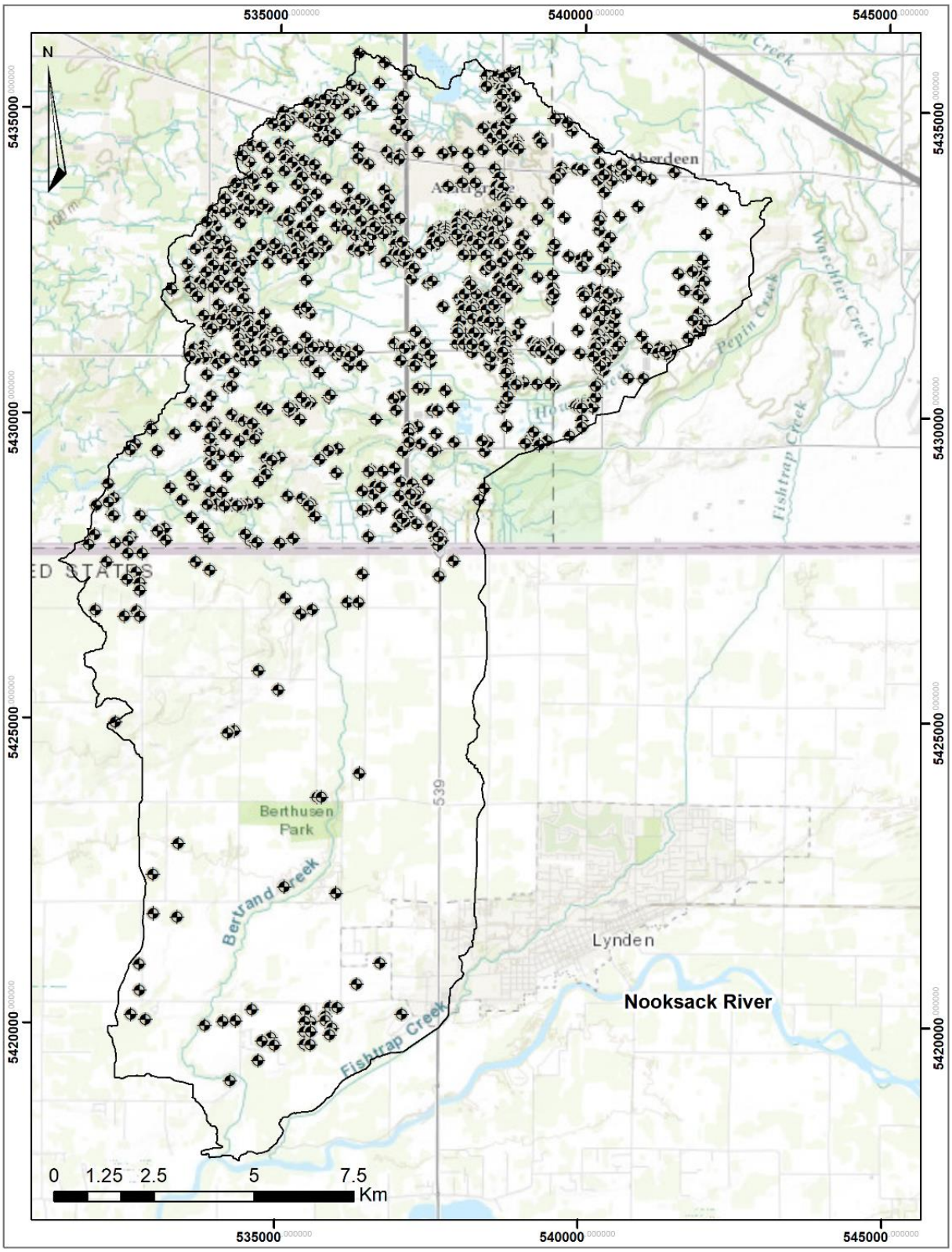

Figure 24. Model observation wells (n=1025) that include the 603 existing wells with the newly added 422 wells.

4.7 Stream Segment Zone Budgets

In order to obtain quantitative results on groundwater exchanges between Bertrand Creek and the surficial sediments, zone budgets were assigned to features so that a detailed water balance could be produced for that specified zone. Zone budgets were assigned to Bertrand Creek using segments of the stream. This segmentation was only performed on the Canadian side of the watershed. These segmentations are based on where distinct changes to the hydrostratigraphy in the uppermost surficial geology layer occur along stretches of Bertrand Creek (Figure 25).

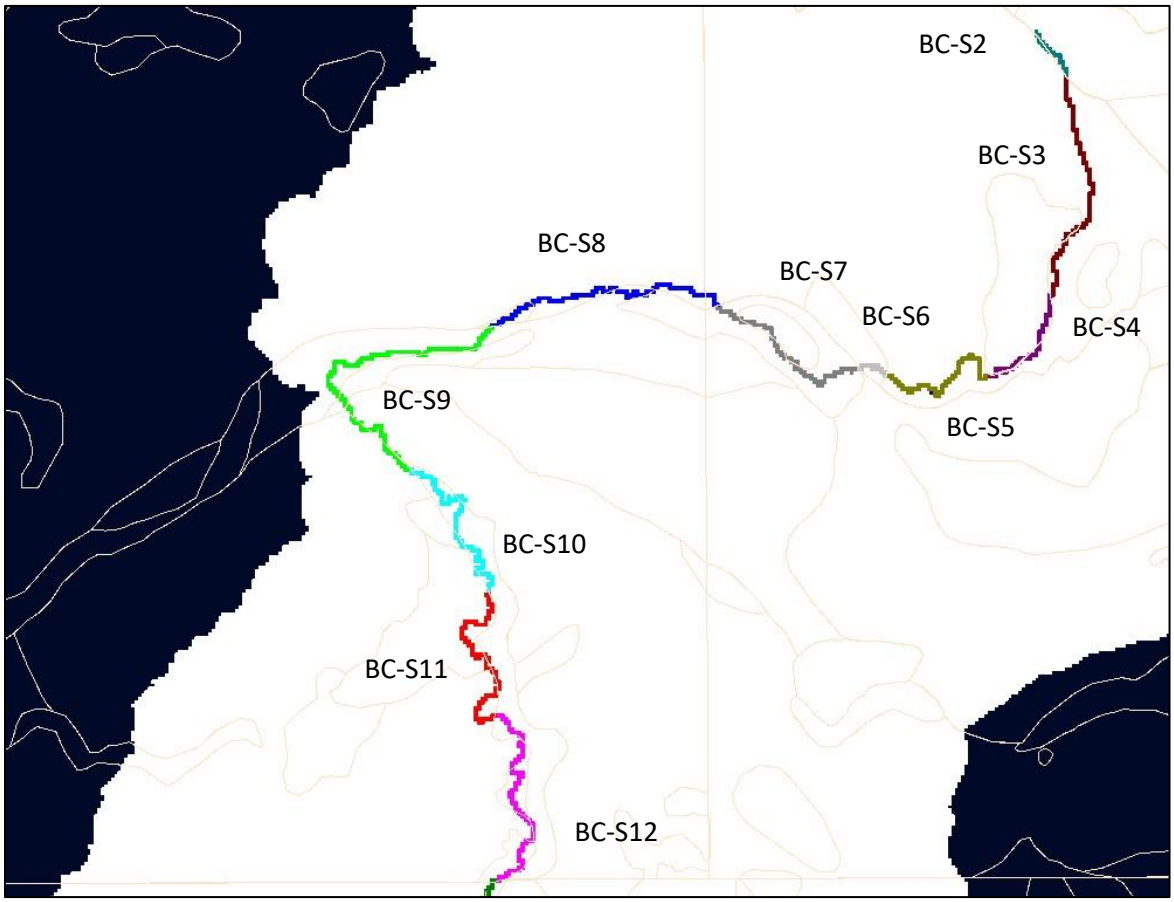

Figure 25: Zone budget segments for Bertrand Creek on the Canadian side of the border. See Table 10 for additional details on zones.

By partitioning Bertrand Creek into discrete segments, losing and gaining stretches of the stream may be more apparent as opposed to simply considering the mass balance for the entire stream. Pruneda (2007) had undertaken a similar zone budget analysis for the US portion of the Abbotsford-Sumas aquifer. Since the same model was used as a basis for the Bertrand Watershed model in this study, this zone budget exercise was not repeated for the US side. Table 10 summarizes the stream segment zones.

Table 10: Zone budget segments for Bertrand Creek. The segment identifier (column two) makes referring to discrete stretches of the stream easier. For example, BC-S4 would refer to segment 4 of the Bertrand Creek within British Columbia.

Zone	Segment ID	Zone Budget Segment	Dominant Hydrostratigraphic Unit
Zone 1	-	Entire Stream	Variable
Zone 2	BC-S1	Entire Stretch within B.C.	Variable
Zone 3	WA-S1	Entire Stretch within WA	Variable
Zone 4	BC-S2	-	Sumas Drift (Upland Flow Tills)
Zone 5	BC-S3	-	Fort Langley Fm. (Clay/Till)
Zone 6	BC-S4	-	Sumas Drift (Gravel)
Zone 7	BC-S5	-	Fort Langley Fm. (Clay/Till)
Zone 8	BC-S6	-	Sumas Drift (Upland Flow Tills)
Zone 9	BC-S7	-	Salish Sediments (Peat/Fluvial Channel)
Zone 10	BC-S8	-	Fort Langley Fm. (Clay/Till)
Zone 11	BC-S9	-	Sumas Drift (Sand)
Zone 12	BC-S10	-	Sumas Drift (Gravel)
Zone 13	BC-S11	-	Sumas Drift (Gravel)
Zone 14	BC-S12	-	Sumas Drift (Gravel)

4.8 Model Settings

The model translation settings are crucial in achieving a solution that can converge. The initial heads distribution is important in being able to kick-start the iterative solving process. Solvers can be very sensitive to the initial condition of the head distribution. The interpolated water table map, in Section 3.7.4, was used as the initial heads for the first run. The ensuing runs used initial heads produced from the immediately preceding successful runs.

The solver settings and cell re-wetting settings are provided in Appendix B.

4.9 Model Calibration

Model calibration seeks to verify the simulated hydraulic heads against the actual measured hydraulic heads in wells. Standard goodness-of-fit statistics are used to evaluate the calibration and the overall performance of the model. The calibration statistics considered were the normalized root mean squared error (NRMSE) and the correlation coefficient. The calibration can also hint towards specific areas or layers where the model is not properly representing the flow system.

Model calibration was carried out in two steps. The first step was to verify the calibration of the model of Bertrand Creek Watershed extracted directly from the regional Abbotsford-Sumas model. This was more a model validation exercise than a calibration exercise because no parameters were adjusted. The goal was to determine how well that raw extracted model performed. The second step involved re-calibrating the new refined version of the Bertrand Creek Watershed model. Both models were calibrated under steady-state conditions against static water levels measured in wells at the end of drilling (as reported in GWELLS).

The calibration strategy involved manually adjusting the hydraulic conductivity (K) values for all hydrostratigraphic units and further subdividing the existing property zones to better represent zonation in particular hydrostratigraphic units. Certain layers were targeted based on the calibration plot that showed clusters of wells with poor calibration. The conductance values for the river and drain boundary conditions were maintained at the field measured values (see Sections 4.4.3 and 4.4.4).

Of note, recharge values were not adjusted during calibration. The spatially distributed recharge had been modelled previously by Scibek and Allen (2006) and the values were considered robust. Thus, it was assumed that areas showing a poor calibration, i.e. where there was a large discrepancy between the simulated heads and the observed heads, were indicative of improperly mapped hydrostratigraphic units and their associated K values rather than errors in the recharge.

4.9.1 Bertrand Creek Watershed Model Extracted from the Regional Model

Figure 26 compares the calculated versus the observed heads and associated goodness-of-fit statistics for the Bertrand Creek Watershed model extracted directly from the original regional Abbotsford-Sumas aquifer. The NRMSE is 17.23% with a correlation coefficient of 0.85 using a total of 1710 observed head values. Scibek and Allen (2005) had achieved a NRMSE of 7.15% and a correlation coefficient of 0.95 using a total of 1695 observed head values. Therefore, the calibration results are surprisingly good considering that the extracted model represents only a portion of a regional model.

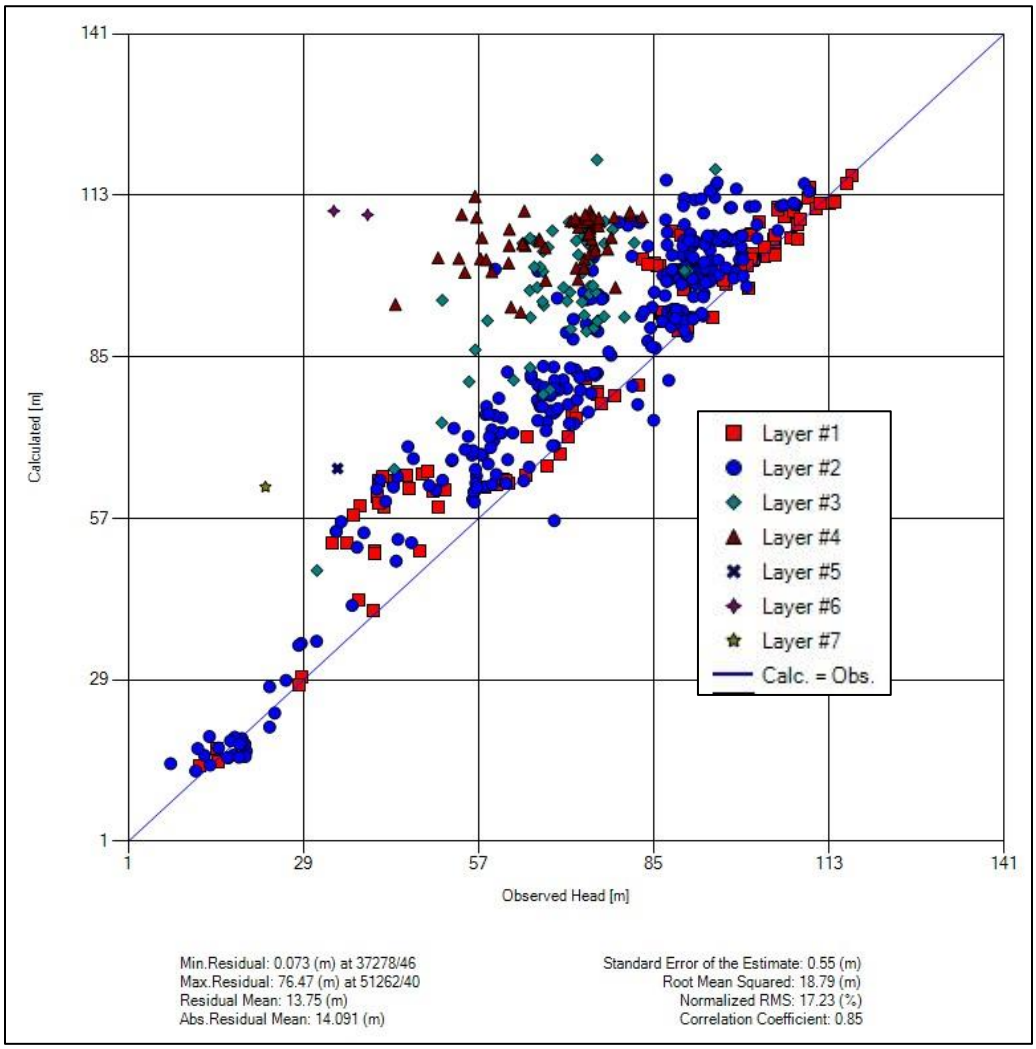

Figure 26: Calibration plot of the Bertrand Creek Watershed model extracted from the original Abbotsford-Sumas regional groundwater flow model developed by Scibek and Allen (2005).

4.9.2 Initial Model Non-Convergence

The initial refined model, with the addition of a 1 m soil layer, did not converge to a solution despite numerous attempts to change solvers and solver settings. Even with cell re-wetting activated, there were too many dry cells at the surface that caused numerical instability, ultimately leading to non-convergence. Therefore, the only option was to remove the 1 m soil layer and replace it with the mapped surficial geology layer (layer 2).

4.9.3 Final Calibration

The final refined model successfully converged to a solution when the soil layer was removed.

To achieve the final calibration, the distribution of property zones and their associated K values were re-considered and slightly modified. Some existing property zones were further subdivided and better resolved for layers 1, 4, 5 and 7 (see Appendix C). This involved targeting areas in which wells showed poor calibration and further subdividing property zones according to the borehole data. Leapfrog was used to visualize the geological materials within different problematic regions of the model. Thus, where wells showed the worst calibration, considerable time was taken in assigning higher resolution property zones based on what the borehole lithology data was suggesting. In terms of changes to hydraulic conductivity values, hydrostratigraphic unit 2, the Fort Langley Fm. clay and tills, was increased by a half order of magnitude (Table 11) as well as the deletion of the soil layer.

Table 11. Summary of changes to hydrostratigraphic units needed to attain final calibration.

Hydrostratigraphic Unit	**Hydraulic Conductivity (m/day)**						**Changes**
	Pre-Calibration			Final Calibration			
	K_x	K_y	K_z	K_x	K_y	K_z	
Soil (Low Permeability)	5	5	0.5	Removed			
Soil (Moderate Permeability)	510	510	51				
Soil (High Permeability)	750	750	75				
Soil (Very High Permeability)	1050	1050	105				
Salish Sediments (Peat/Fluvial Channel)	10	10	0.5	10	10	0.5	n/a
Sumas Drift (Upland Flow Tills)	1	1	0.9	1	1	0.9	n/a
Sumas Drift (Upland Glaciofluvial)	2	2	0.2	2	2	0.2	n/a
Fort Langley Fm. (Clay/Till)	0.6	0.6	0.06	3	3	0.3	+ ½ order of magnitude
Sumas Drift (Glaciolacustrine Silt/Fines)	3	3	0.3	3	3	0.3	n/a
Sumas Drift (Gravel)	6	6	0.6	6	6	0.6	n/a
Sumas Drift (Sand)	40	40	2	40	40	2	n/a

Figure 27 shows the final calibration of the Bertrand Creek Watershed model. An NRMSE of 12.16% with a correlation coefficient of 0.86 were achieved. The three uppermost layers show the best calibration (NRMSE of 8.94% in Figure 28) while layers 4, 5, 6 and 7 show the poorest calibration (NRSME of 26.82% in Figure 29). It is not surprising that the deeper layers have rather poor calibration results because the Bertrand Creek Watershed model uses the watershed boundary as a no flow boundary, except at the southern tip where water can exit through the constant head boundary associated with the Nooksack River. The lateral no flow boundaries do not permit deep regional groundwater flow as shown in the regional model (Scibek and Allen, 2005). However, there are so few observation wells in these deeper layers that their poor calibration does not overwhelm the calibration of the full model. Therefore, it appears that while deep regional flow is affected, the near surface flow system appears to be adequately represented.

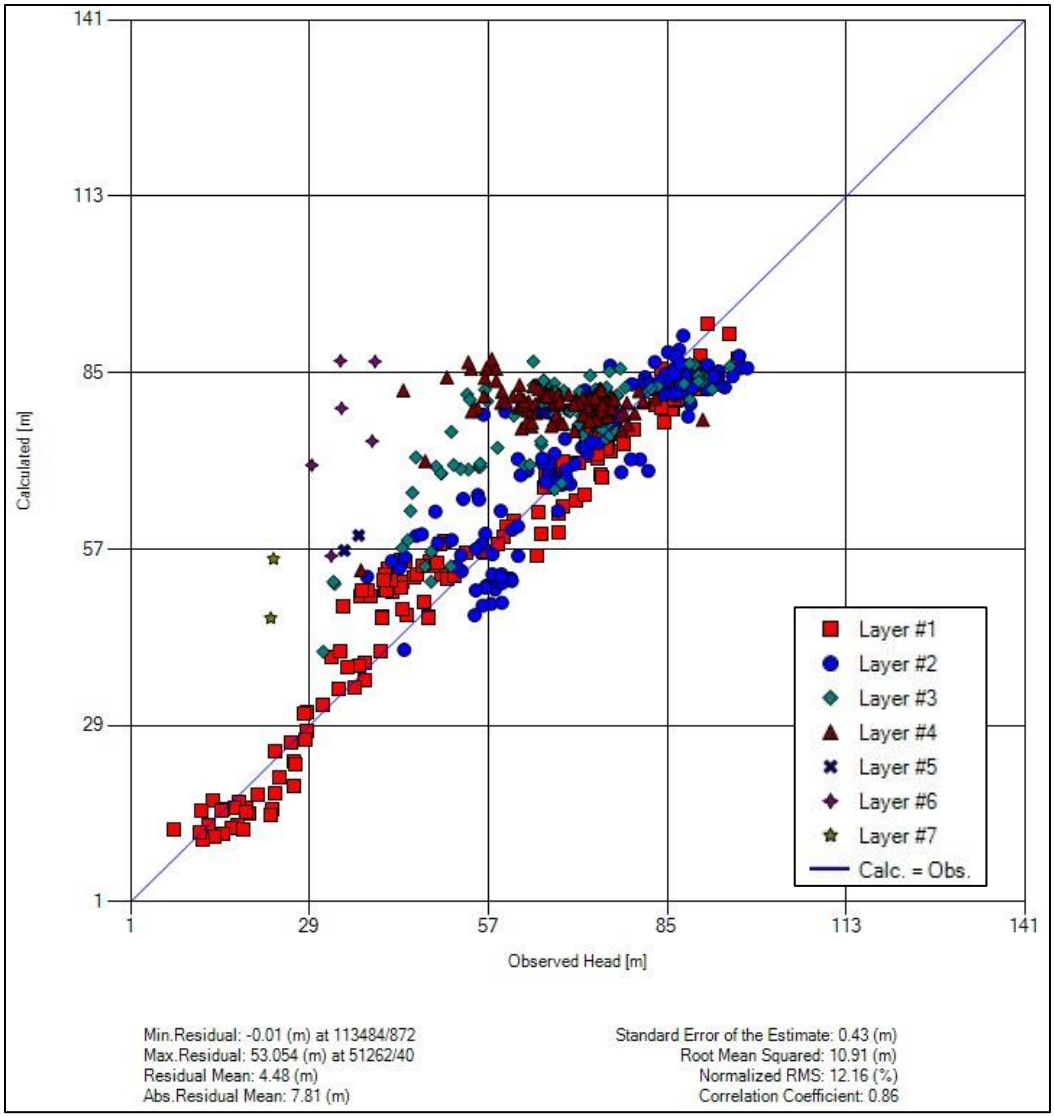

Figure 27: Calibration plot for the final calibrated model including all layers.

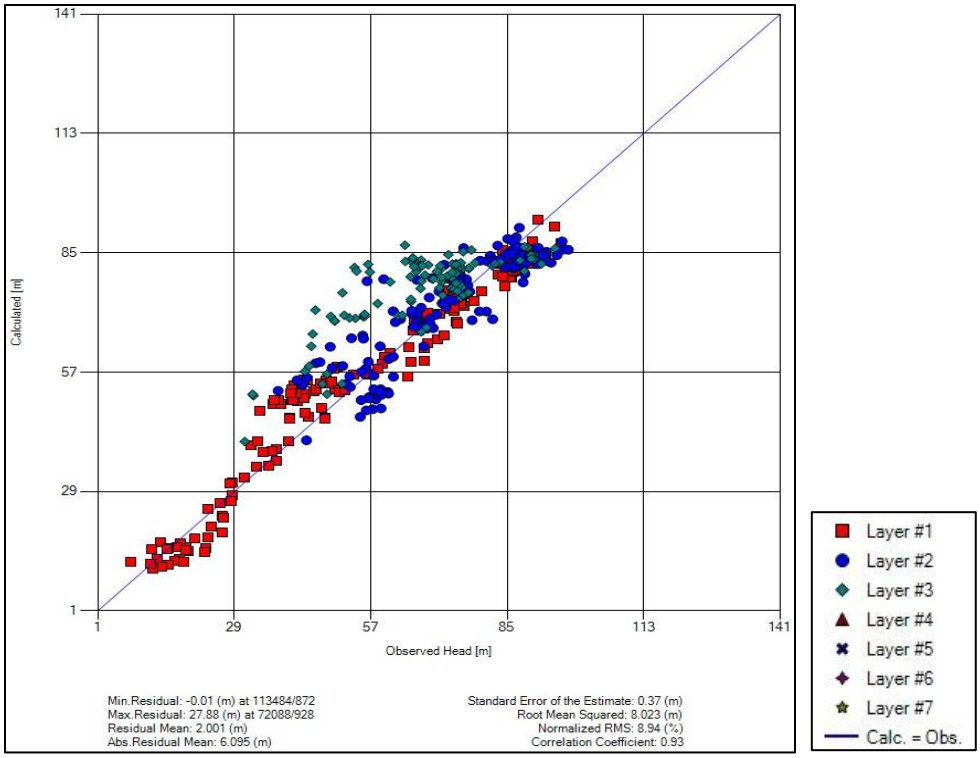

Figure 28: Calibration plot for the final calibrated model for layers 1, 2 and 3.

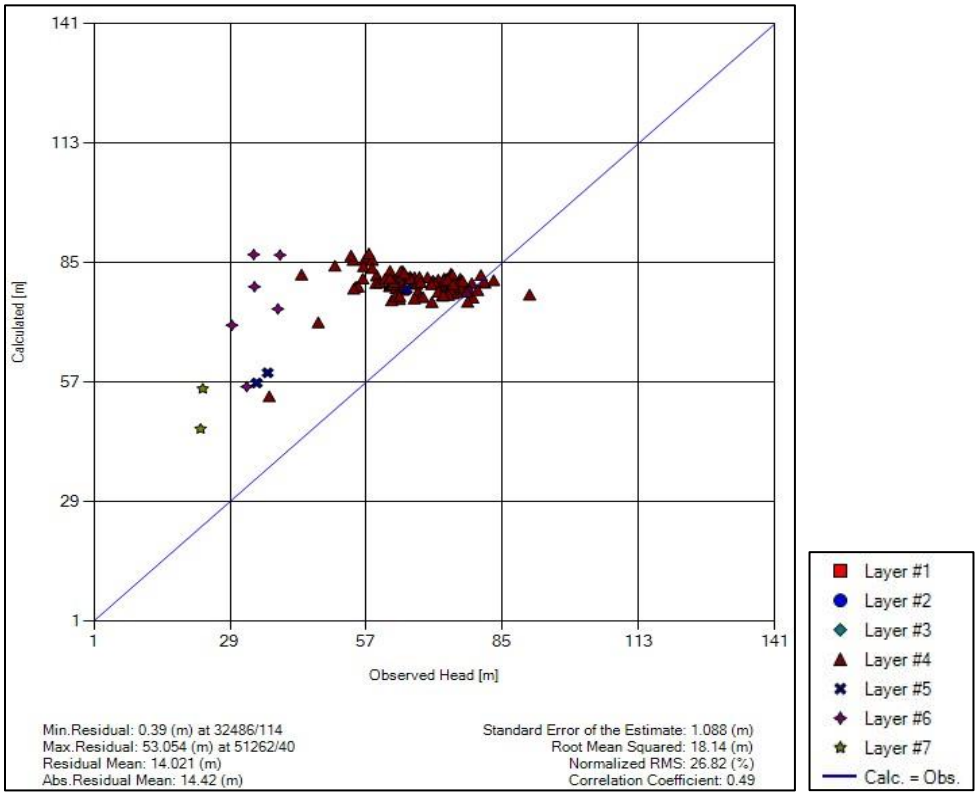

Figure 29: Calibration plot for the final calibrated model for layers 4, 5, 6, and 7.

5. RESULTS

The following results section focuses on the Canadian portion of the Bertrand Creek Watershed as well as the uppermost layers of the models, primarily the surficial geology layer. Additionally, it is important to consider that these results represent the groundwater flow system in a steady state conditions, only offering spatial variability and not temporal variability. Therefore, these results offer a glimpse of the behaviour of groundwater flow under average annual conditions.

Results shown in Sections 5.1 are for non-pumping conditions. Section 5.2 shows results under pumping conditions.

5.1 Non-pumping Conditions

5.1.1 Non-pumping Water Table

The water table represents the unconfined potentiometric surface. Within the model, this surface is irregular and occurs within multiple model layers (Figure 30). Figure 31 shows the water table elevation within the first computational layer of the model, which represents the mapped surficial geology. Because the first layer has a maximum depth of 10 m, this map shows areas where the water table is within 10 m of ground surface. In areas of high topographic relief and higher elevations, particularly in the north and northwest, the water table is deeper than 10 m. The water table is shallower in areas that are topographically flatter and at lower elevations south into the United States. Throughout the watershed, hydraulic gradients are relatively low.

5.1.2 Non-pumping Water Balance

As another indicator of model accuracy, the water mass balance provides information on sources and sinks and where water is being exchanged. The final model, under non-pumping conditions, shows a discrepancy of 0.001 % with a residual of 33.85 m^3/day (Table 12). Inputs to the groundwater system include recharge as well as water entering through constant head and river leakage boundaries. Since constant head and river leakage boundaries allow water to exit and enter the boundary, they can either be a source of water to the groundwater system or a sink to the groundwater system. Drain boundaries only allow water to exit the system.

The rates of recharge and river leakage into the model are the same order of magnitude, while water entering through the constant head boundaries is an order of magnitude lower.

Table 12: Total steady-state mass balance under non-pumping conditions.

Boundary	Inputs (m^3/day)	Outputs (m^3/day)
Constant Head	6.842×10^3	1.256×10^3
Drains	0	1.175×10^6
River Leakage	1.216×10^6	2.047×10^5
Recharge	1.585×10^5	0
Totals	1.381×10^6	1.381×10^6
Residual (Discrepancy)	33.85 (0.001%)	

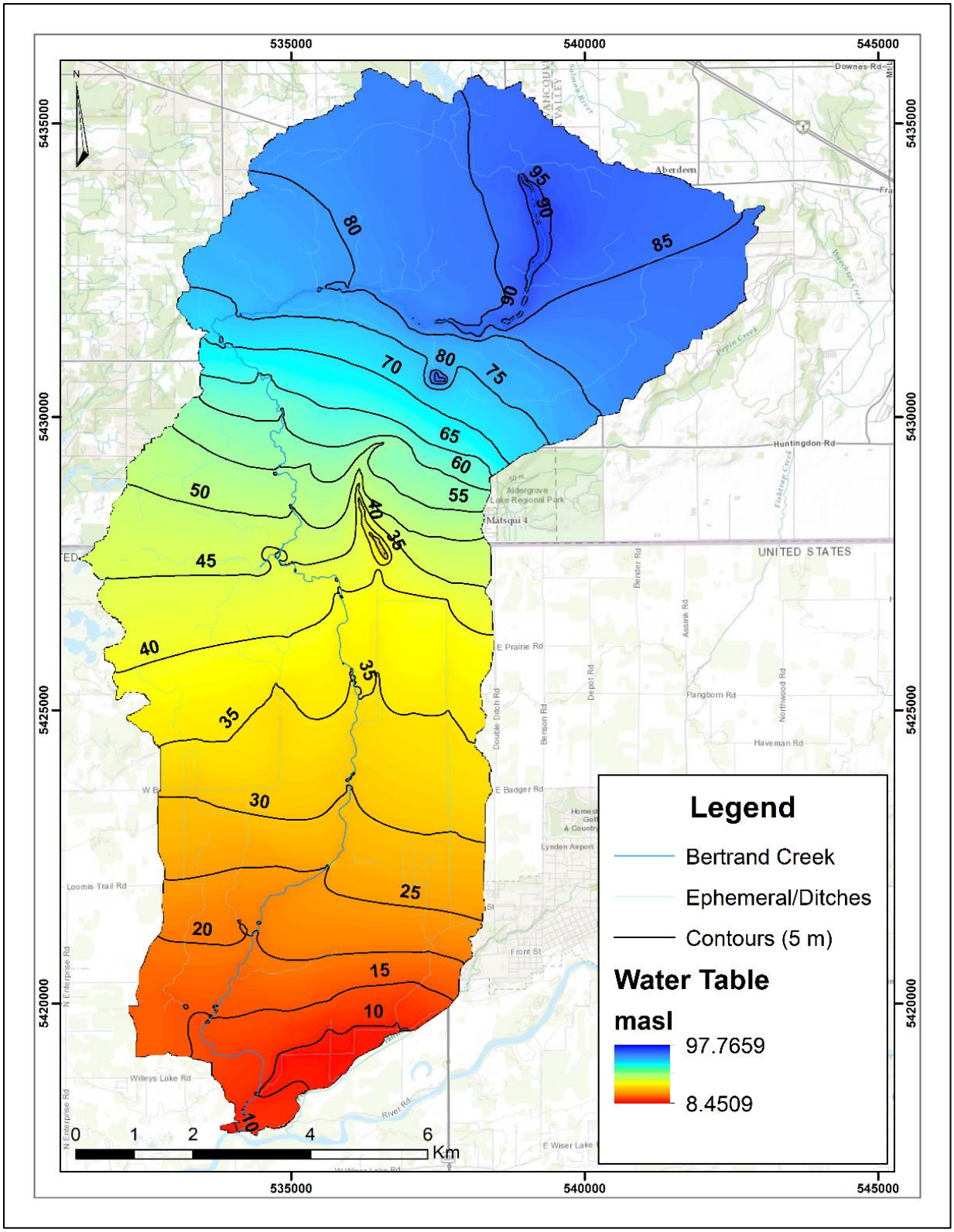

Figure 30: Simulated steady-state water table elevation for the Bertrand Creek Watershed in the absence of pumping. Contour intervals are 5 m increments with elevations in masl.

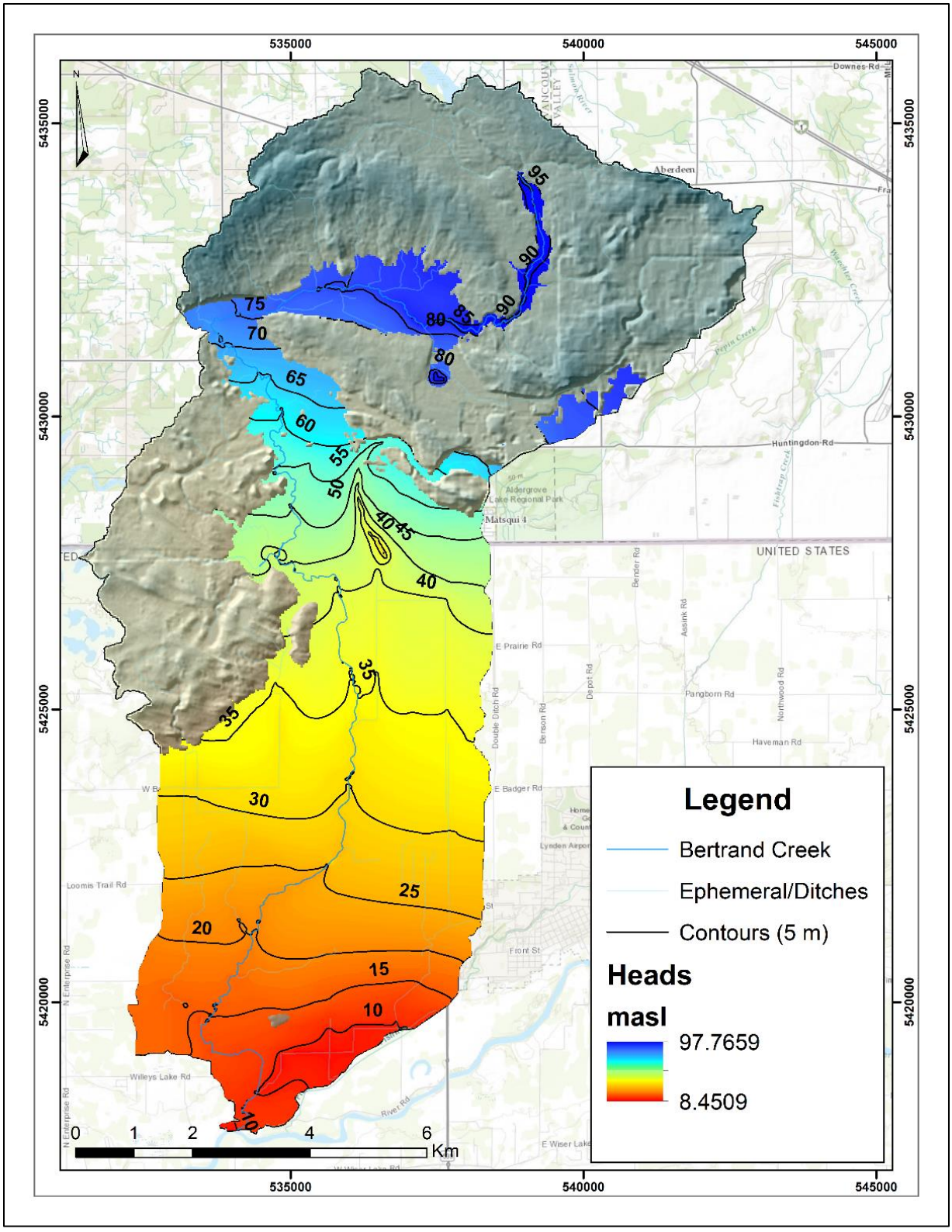

Figure 31: Simulated stead-state water table elevation in the first layer of the model (upper 10 m) in the Bertrand Creek Watershed in the absence of pumping. Contour intervals are 5 m increments with elevations in masl. The water table map is draped onto the surface DEM to show the relation between topography and head distribution.

5.1.3 Non-pumping Groundwater Flow and Vertical Fluxes

Modelling results indicate groundwater flow in the Bertrand Creek Watershed is much more complicated than previously observed on a regional scale. Figure 32 shows velocity vectors in the uppermost layer scaled to direction (not magnitude) to show groundwater flow direction. The velocity vectors are overlaid onto a vertical flux map. Under non-pumping conditions, vertical groundwater fluxes are primarily concentrated in Bertrand Creek as well as in ephemeral streams, ditches and wetlands/lakes. In areas of negative vertical flux (blue areas in Figure 32), the flow in downward (groundwater recharge) and horizontal components of flow are pointing away from Bertrand Creek. This flow is diverted away from the stream seeps down into deeper layers.

At Otter Park, where Bertrand Creek meanders sharply to a North-South oriented direction, the flow vectors also take on this same downward orientation. This sharp bend also represents a transition zone between negative and positive vertical flux (red areas in Figure 32). Downstream of Otter Park, where flow is oriented roughly North-South, vertical fluxes are positive, where groundwater begins to feed Bertrand Creek (groundwater discharge).

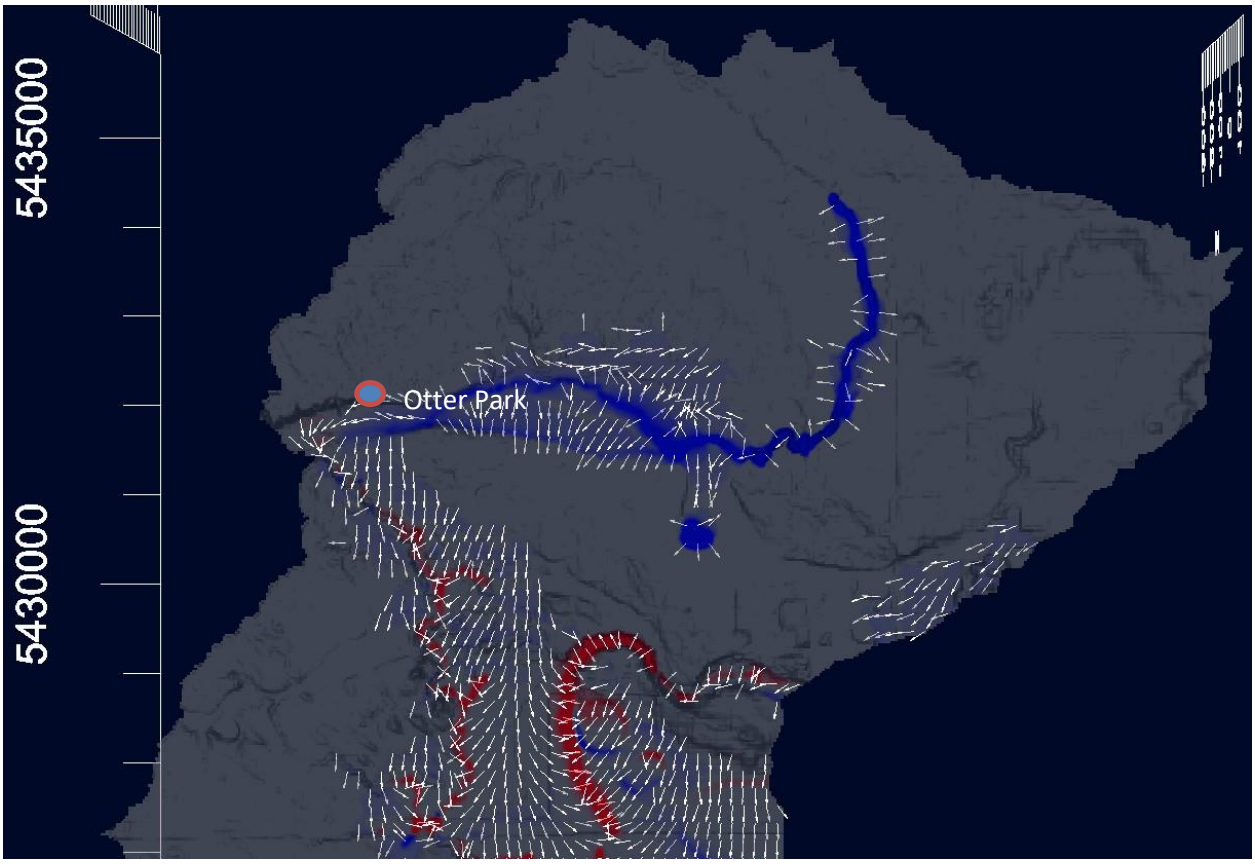

Figure 32: Velocity vectors in the first model layer scaled to direction, not magnitude, for the Canadian side of the watershed. The blue and red areas represent vertical fluxes along Bertrand Creek. Areas in blue indicate a negative flux down into the model (groundwater recharge) while areas in red indicate a positive flux up out of the model (groundwater discharge). The location of Otter Park is shown.

Figure 33 shows the vertical flux as a Darcy flux (m/day). Larger magnitude negative fluxes are seen in the uppermost reaches of Bertrand Creek, upstream of Otter Park. Downstream of Otter Park, the majority of the fluxes remain negative but have a larger component of positive flux indicating that some of the groundwater tends to discharge into Bertrand Creek. Therefore, Otter Park represents a transition zone from a dominantly losing stream to a stream with losing and gaining reaches. Overall, Bertrand Creek is a losing stream (see Section 5.1.4) but varies in its magnitude of exchange with the underlying groundwater system, with respect to the portion of Bertrand Creek within Canada.

Figure 34 shows vertical fluxes overlaid on top of the surficial Abbotsford-Sumas aquifer as well as other smaller portions of aquifers occurring within the watershed. Note that almost all vertical exchanges in the first layer occur in areas dominated by coarse-grained sediments associated with the Abbotsford-Sumas Aquifer #015 (compare with Figure 6).

5.1.4 Non-pumping Zone Budget

Zone budgets were assigned to segments along different reaches of Bertrand Creek. These zones also overlap onto the river boundaries. Thus, it is possible to determine reaches that are losing to the groundwater system or gaining from the groundwater system. Alternatively, from a groundwater perspective, losing reaches of streams correspond to groundwater recharge zones while gaining reaches of streams correspond to groundwater discharge zones. It is important to note that the Zone Budget code refers to inputs and outputs from the perspective of the groundwater system. Therefore, the inputs include all sources to the aquifer system and output terms include all sink components of the aquifer. River leakage as an input refers to surface water discharge zones (groundwater recharge) while river leakage as an output refers to surface water recharge zones (groundwater discharge).

Table 13 summarizes river leakage inputs and outputs to different stream segments (refer to Figure 25 for map of segments) for steady-state conditions. Segments BC-S2 to BC-S12, except BC-S11, are all dominated by losing reaches. Segment BC-S9, which contains Otter Park, marks a transition zone where there are high exchanges, both positive and negative, between Bertrand Creek and the underlying surficial aquifers. The highest volumetric rate of leakage into the stream occurs in segment BC-S8, upstream of Otter Park. Downstream of the Otter Park segment, Bertrand Creek is still dominated by losing reaches, but some reaches gain water. BC-S11 is the only segment that has a net gain of water from the groundwater system. The terminal point of the BC-S12 segment is at the Canada-US border.

Table 13: Summary of mass balance for major groundwater exchange sites in different zone budget segments. Note that river leakage as an input refers to stream water leaking into the aquifers while river leakage as an output refers to groundwater leaking into the stream. Other components (recharge, drains and adjacent segments) that contribute less to the mass balance are not shown.

Segment (Zone)	Inputs (m^3/day)	Outputs (m^3/day)	Steady-State Stream Dynamic
	River to Aquifer Leakage	Aquifer to River Leakage	
BC-S2 (4)	28,042	0	Dominantly Losing
BC-S3 (5)	83,621	1,096	Dominantly Losing
BC-S4 (6)	56,966	1,724	Dominantly Losing
BC-S5 (7)	11,211	4,730	Mostly Losing
BC-S6 (8)	1,561	0	Dominantly Losing
BC-S7 (9)	40,013	4,208	Dominantly Losing
BC-S8 (10)	179,730	555	Dominantly Losing
BC-S9 (11)	151,410	23,726	Dominantly Losing
BC-S10 (12)	75,850	5,477	Dominantly Losing
BC-S11 (13)	3,381	5,261	Mostly Gaining
BC-S12 (14)	52,489	6,796	Dominantly Losing
Total	**684,274**	**53,573**	Dominantly Losing

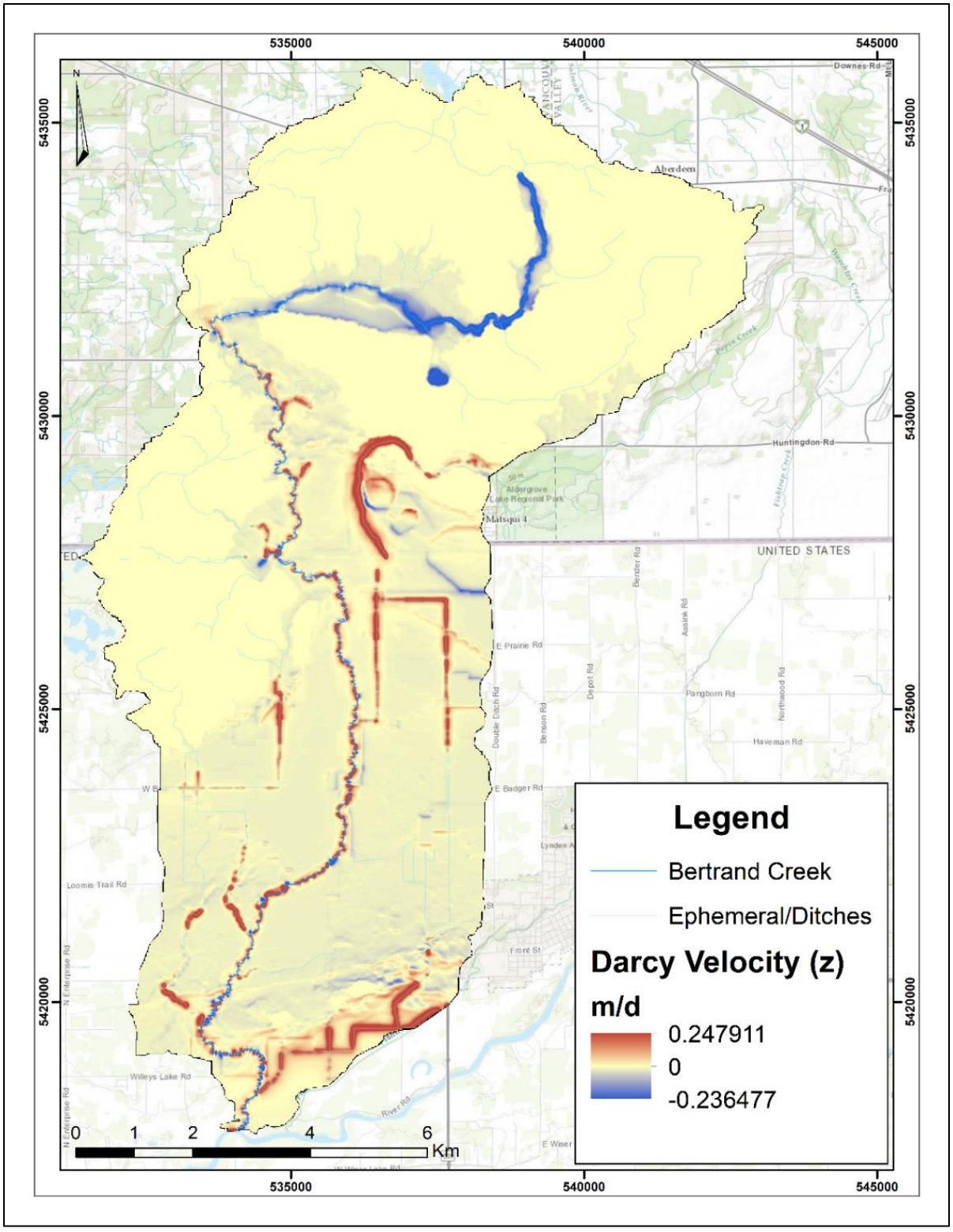

Figure 33: Vertical flux map of the Bertrand Creek Watershed within the first model layer. Areas in blue indicate a negative flux down into the model (groundwater recharge) while areas in red indicate a positive flux up out of the model (groundwater discharge). Areas in yellow, with no component of vertical flux, correspond to dry model cells, where the water table is not present.

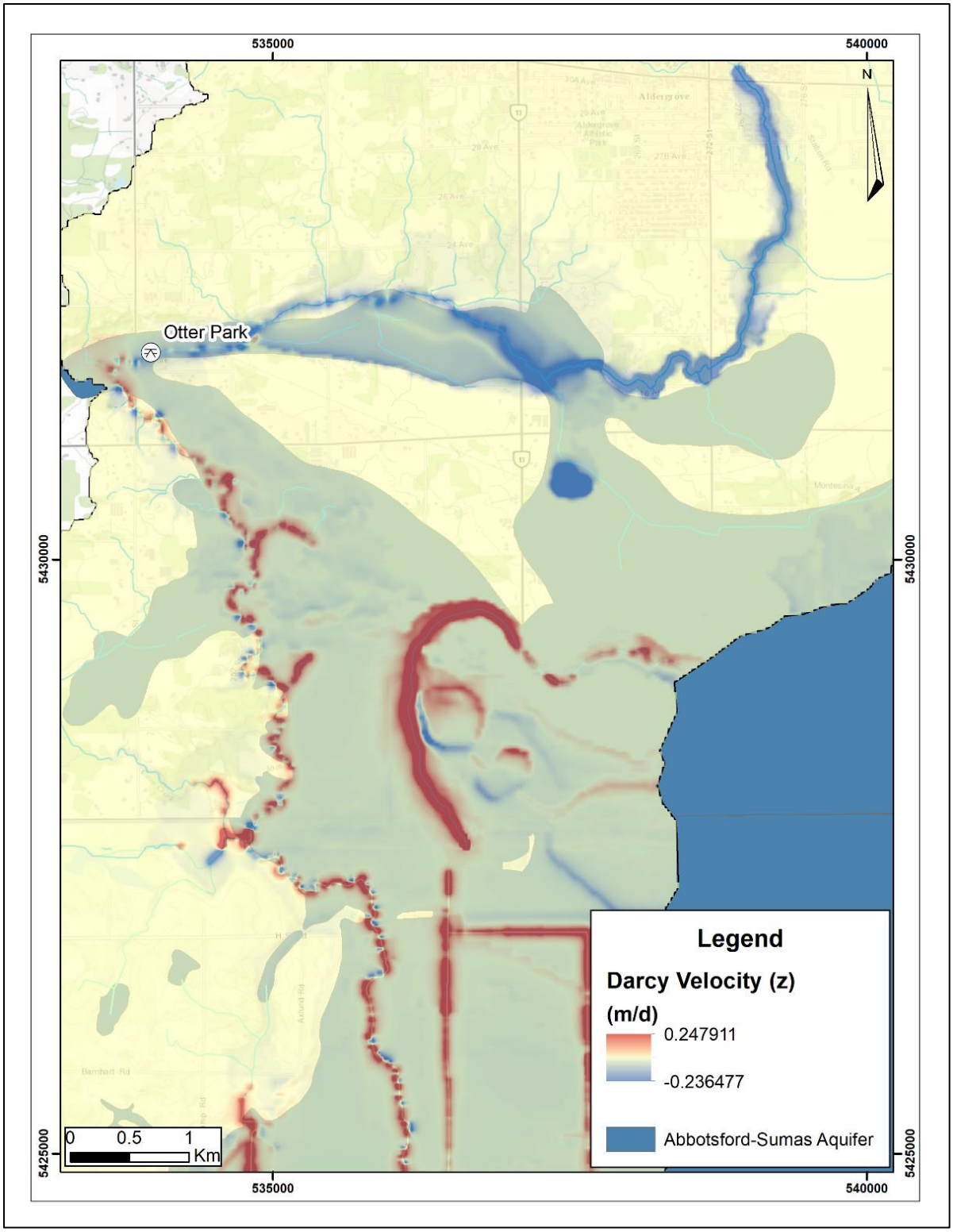

Figure 34: Vertical component of groundwater flux, in the Canadian portion of the watershed, overlaid on top of the underlying surficial aquifers. The dark silhouette is the Abbotsford-Sumas aquifer.

5.2 Pumping Conditions

In total, 1171 active pumping wells were used to simulate pumping conditions. This section compares these results to the results for non-pumping conditions (discussed above), and aquifer-stream connectivity is discussed with respect to Bertrand Creek.

5.2.1 Pumping Water Table

Under pumping conditions, the water table is relatively unchanged, with only small changes to the contours in the northernmost portion of the watershed (Figure 35). These contour changes occur in upland areas of the watershed and show minor changes in contour geometry. Most noticeably, the 85 masl contour encloses a smaller area in comparison to the non-pumping water table (see Figure 30).

5.2.2 Pumping Water Balance

Under pumping conditions, the water balance residual increased resulting in a slightly higher discrepancy (0.01%) than under non-pumping conditions (Table 14), although still significantly lower than 5%. The drain and river leakage boundaries saw the most change. Recalling that river leakage as an input refers to surface waters seeping into the aquifers, under pumping conditions there is more seepage into the aquifers from the streams, approximately a 0.41% change. Likewise, less water seeps into the streams from the aquifers (-1.95% change). Additionally, the drain boundaries throughout the model are receiving less water (-1.02% change). In total, there is a 0.29% increase in the amount of water withdrawn from the groundwater system which can be attributed to the pumping wells.

Table 14: Total steady-state mass balance under average annual pumping conditions. The percent change refers to the relative increase or decrease between non-pumping and pumping model runs. See Table 12 for non-pumping water balance results.

Boundary	Inputs (m^3/day)	Inputs Change (%)	Outputs (m^3/day)	Outputs Change (%)
Constant Head	6.977×10^3	+1.97	1.254×10^3	-0.16
Drains	0	0	1.163×10^6	-1.02
River Leakage	1.221×10^6	+0.41	2.007×10^5	-1.95
Recharge	1.573×10^5	-0.76	0	0
Pumping Wells	0	n/a	2.003×10^4	n/a
Totals	1.385×10^6	+0.29	1.385×10^6	+0.29
Residual (Discrepancy)	118.86 (0.01%)			

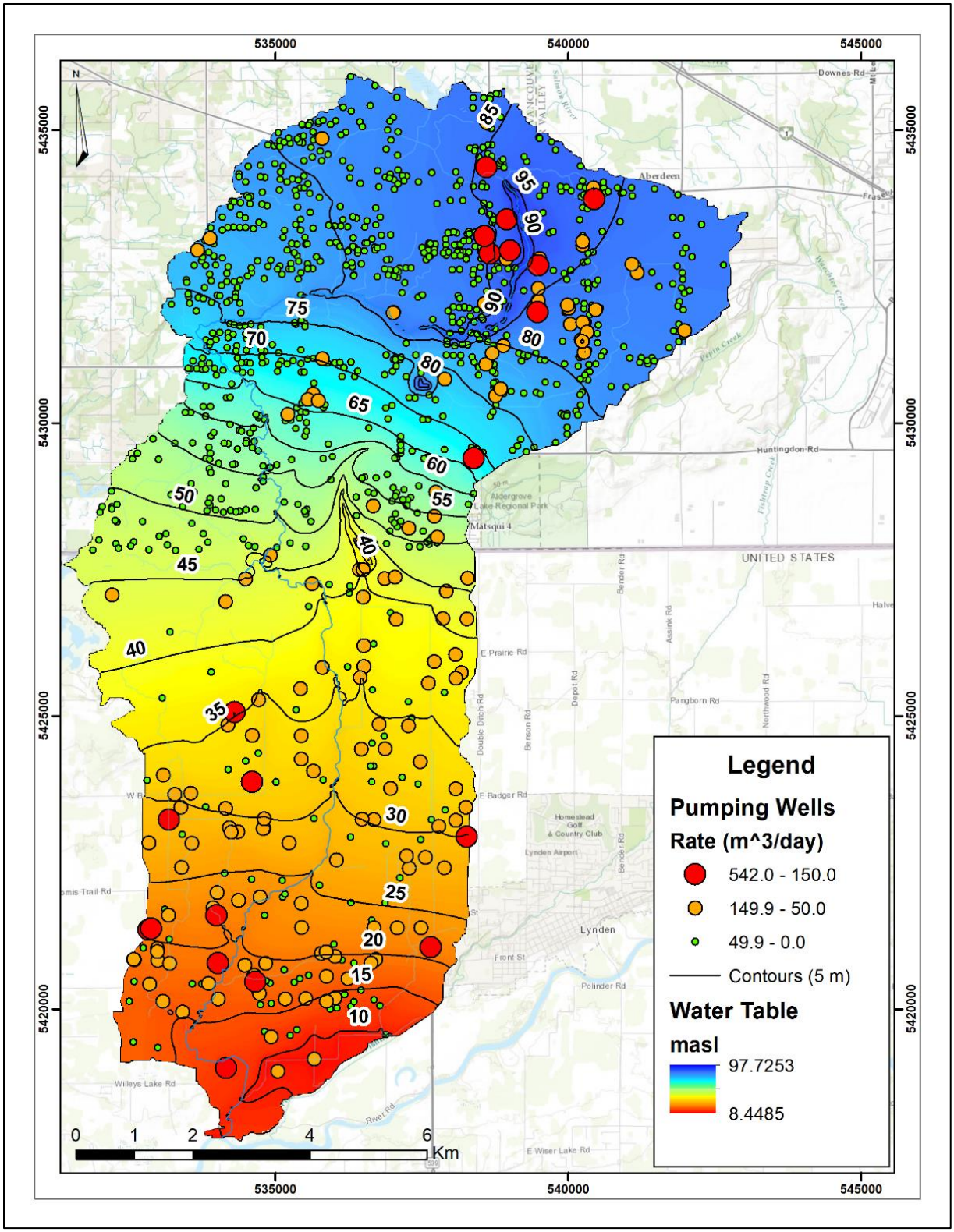

Figure 35: Potentiometric surface map of the water table in the Bertrand Creek Watershed under pumping conditions. Contour intervals are 5 m increments with elevations in masl.

5.2.3 Pumping Flow Patterns and Vertical Fluxes

Figure 36 shows the velocity vectors in the uppermost layer scaled to direction (not magnitude) under pumping conditions. Similar to non-pumping conditions, the vertical flux transition zone at Otter Park is still present, with the flow vectors transitioning from an East-West to North-South direction. As well, downstream of Otter Park, where flow is oriented roughly North-South, vertical fluxes are positive, where groundwater begins to feed Bertrand Creek. Areas of Bertrand Creek upstream of Otter Park still have negative vertical fluxes. In general, flow directions remain unchanged other than slight variations in direction.

Under pumping conditions, the magnitudes of the vertical groundwater fluxes are largely unchanged from non-pumping conditions. Figure 37 shows vertical fluxes in layer 1 of the model. Vertical fluxes of greatest magnitude are along Bertrand Creek, as in the non-pumping model. In the southern part of the watershed, however, shallow wells completed in layer 1 show up as tiny blue dots. These are localized areas of negative flux, where water is being redirected downwards toward the pumping well screens.

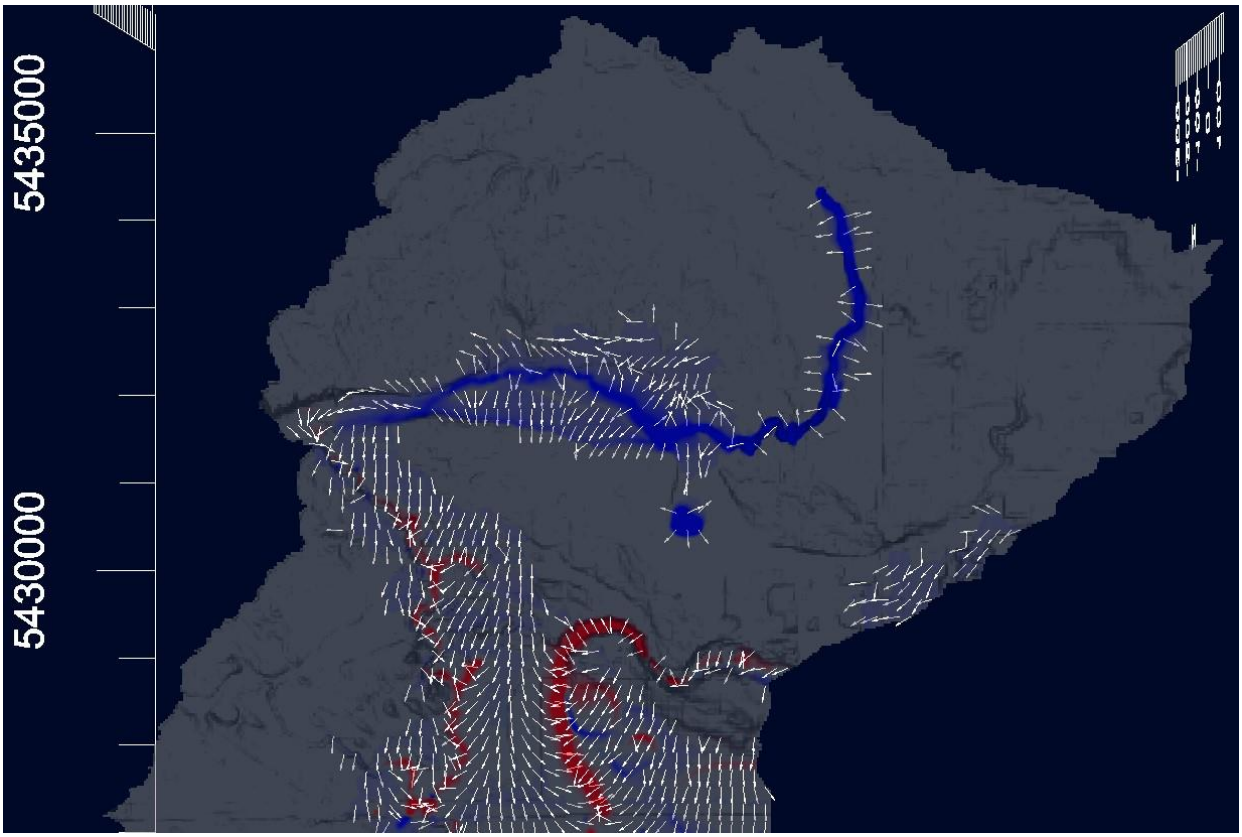

Figure 36: Velocity vectors in the first model layer scaled to direction (not magnitude) for the Canadian side of the watershed under pumping conditions. The blue and red areas represent vertical fluxes along Bertrand Creek. Areas in blue indicate a negative flux down into the model (groundwater recharge) while areas in red indicate a positive flux up out of the model (groundwater discharge).

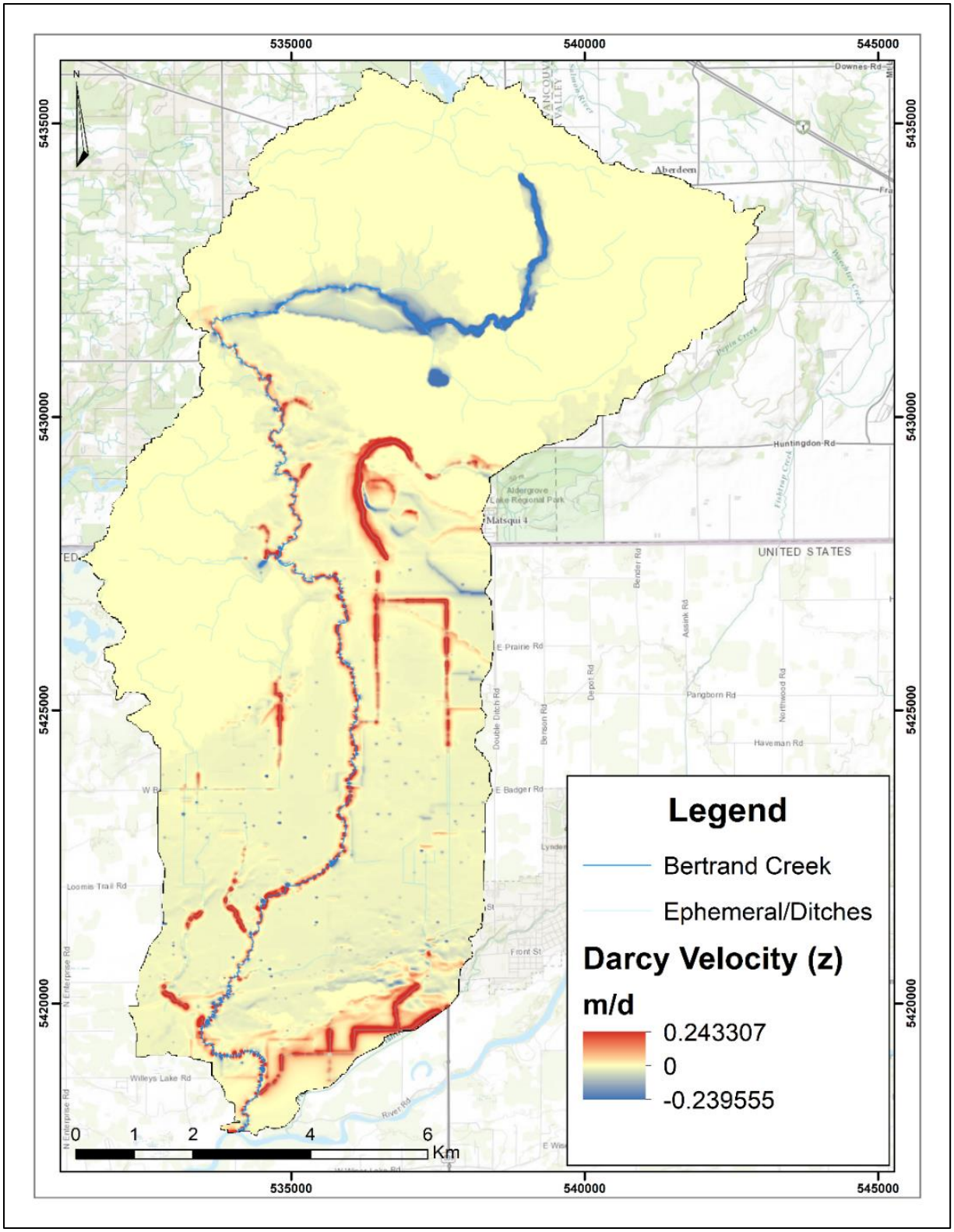

Figure 37: Vertical flux map of the Bertrand Creek Watershed within the first model layer under pumping conditions. Note the small blue dots in the south which represent areas being pumped.

5.2.4 Pumping Zone Budget

The most noticeable results occurred in the zone budget stream segments where quantitative results were acquired. Recall that river leakage as an input refers to surface water discharge zones (groundwater recharge) while river leakage as an output refers to surface water recharge zones (groundwater discharge). Table 15 summarizes river leakage inputs and outputs to different stream segments under pumping conditions.

Table 15: Summary of mass balance for river leakage in different zone budget segments under pumping conditions. The difference columns represent the magnitude of change between non-pumping and pumping conditions. The change column is a percentage representation of the difference.

Segment (Zone)	Inputs (m^3/day)			Outputs (m^3/day)		
	River to Aquifer Leakage			Aquifer to River Leakage		
	Pumping Conditions	Difference from Non-Pumping Conditions	Change (%)	Pumping Conditions	Difference from Non-Pumping Conditions	Change (%)
BC-S2 (4)	28,319	277	+1.0	0	0	0
BC-S3 (5)	84,757	1,136	+1.4	945	-150	-13.7
BC-S4 (6)	57,316	350	+0.6	1,581	-143	-8.3
BC-S5 (7)	11,463	252	+2.2	4,563	-167	-3.5
BC-S6 (8)	1,644	83	+5.3	0	0	n/a
BC-S7 (9)	40,474	461	+1.2	4,036	-172	-4.1
BC-S8 (10)	180,140	410	+0.2	505	-50	-9.0
BC-S9 (11)	151,680	270	+0.2	23,468	-258	-1.1
BC-S10 (12)	75,927	77	+0.1	5,350	-127	-2.3
BC-S11 (13)	3,458	76	+2.3	5,131	-130	-2.5
BC-S12 (14)	52,557	68	+0.1	6,696	-100	-1.5
Total	**687,734**	**3,460**	**+0.5**	**52,274**	**-1,298**	**-2.4**

All segments are once again dominated by losing reaches, where the aquifers are being recharged by the stream (i.e., input to the model). Under pumping conditions, there is an increase in seepage across the river bottom for all segments, which confirms aquifer-stream connectivity. BC-S6 and BC-S11 have the largest positive percentage increase in river leakage, which implies an increased volume of water reaching the aquifers as a consequence of pumping. Along BC-S3, there is a -13.7% decrease in the amount of seepage into the stream (i.e., output from the model) implying less groundwater discharge to the stream, as this water is redirected towards the pumping wells. The transition segment BC-S9, containing Otter Park, where Bertrand Creek changes from a predominantly losing stream to a stream with losing and gaining reaches, experiences a small increase in downward seepage into the aquifer (Inputs to Aquifer). Segment BC-S8 still experiences the largest exchange volumes, both positive and negative, out of all of the other segments. Downstream of Otter Park, in segments BC-S10 to BC-S12, Bertrand Creek is still dominated by losing reaches. However, compared to the upstream segments, there is more water seeping into Bertrand Creek (groundwater discharge). While these segments are still losing, they have an even smaller component of positive flux, or seepage into the stream, under pumping conditions.

In total, in the Canadian portion of the watershed, there is 687,734 m^3/day of seepage into the aquifer from Bertrand Creek and 52,274 m^3/day of seepage into Bertrand Creek from the aquifers. The total volume of pumping is 20,003 m^3/day. In all stream segments, river leakage inputs increase under pumping conditions, meaning that the streamflow is being redirected into the groundwater system by as much as 5.3% more. Moreover, river leakage outputs decrease in all stream segments leading to less water entering the streams, by as much as -13.7% less. In total, there is 1,298 m^3/day less of groundwater leaking into the stream. This represents 6.5% of the total pumping. Overall, pumping in these aquifer systems exacerbates the losing stream dynamic of Bertrand Creek.

5.3 Aquifer-Stream Connectivity and Streamflow Depletion

Under steady-state groundwater flow conditions (i.e. mean annual baseflow conditions), Bertrand Creek is a dominantly losing stream, with the major losing reaches upstream of Otter Park. The meander in Bertrand Creek near Otter Park causes the creek to change flow direction from East-West to North-South. Consequently, the stream transitions from a dominantly losing stream into a stream that has losing and gaining reaches as it becomes aligned with the regional North-South groundwater flow direction. Additionally, at this meander, slightly upstream of Otter Park, the 80 masl water table contour intersects the surface DEM contour marking the point at which Bertrand Creek begins to gain water from the groundwater system (Figure 38). The water table contours also begin to transition from outward pointing v's (loosing) to inward pointing v's (gaining). All stream segments downstream of Otter Park have the water table intersecting the surface contours within the riverbed. In segments upstream of Otter Park, the water table is well below any surface contours. Vertical fluxes representing exchanges between the stream and the groundwater system, along with zone budget results for discrete stream segments quantified the aquifer-stream connectivity by providing exchange volumes in zones of positive or negative vertical flux within the stream.

Because of the nature of the hydraulic connectivity between the surficial aquifers and Bertrand Creek, the stream is sensitive to groundwater abstraction. Under pumping conditions, river seepage across the streambed to the aquifer system increases in all segments, whether those segments had positive or negative vertical fluxes under non-pumping conditions. No stream segments are particularly sensitive to the effects of pumping as all stream segments are affected by pumping.

All segments of Bertrand Creek are therefore potentially at a higher risk of streamflow depletion because of its losing nature and high hydraulic connection with the groundwater system. River seepage, from Bertrand Creek into the surficial aquifer, was exacerbated under the stresses of pumping and resulted in approximately 3,460 m^3/day of additional seepage into the aquifers. This amount of seepage represents 17.3%, of the total pumping rate of 20,003 m^3/day.

An important limitation of using a steady-state groundwater flow model to explore aquifer-stream connectivity and streamflow depletion is that the simulations represent mean annual conditions in both the aquifer and the stream. Streamflow depletion may be more severe during the summer low flow period because the streamflow would be much lower under dry summer conditions. This means that any additional seepage from the stream into the aquifer could potentially result in the stream running dry. Therefore, the results of this steady-state model should be viewed strictly as representing mean annual conditions. A transient groundwater flow model would best be used to examine seasonal variations in exchanges between the aquifer and the stream and to asses the impacts of pumping on these exchanges.

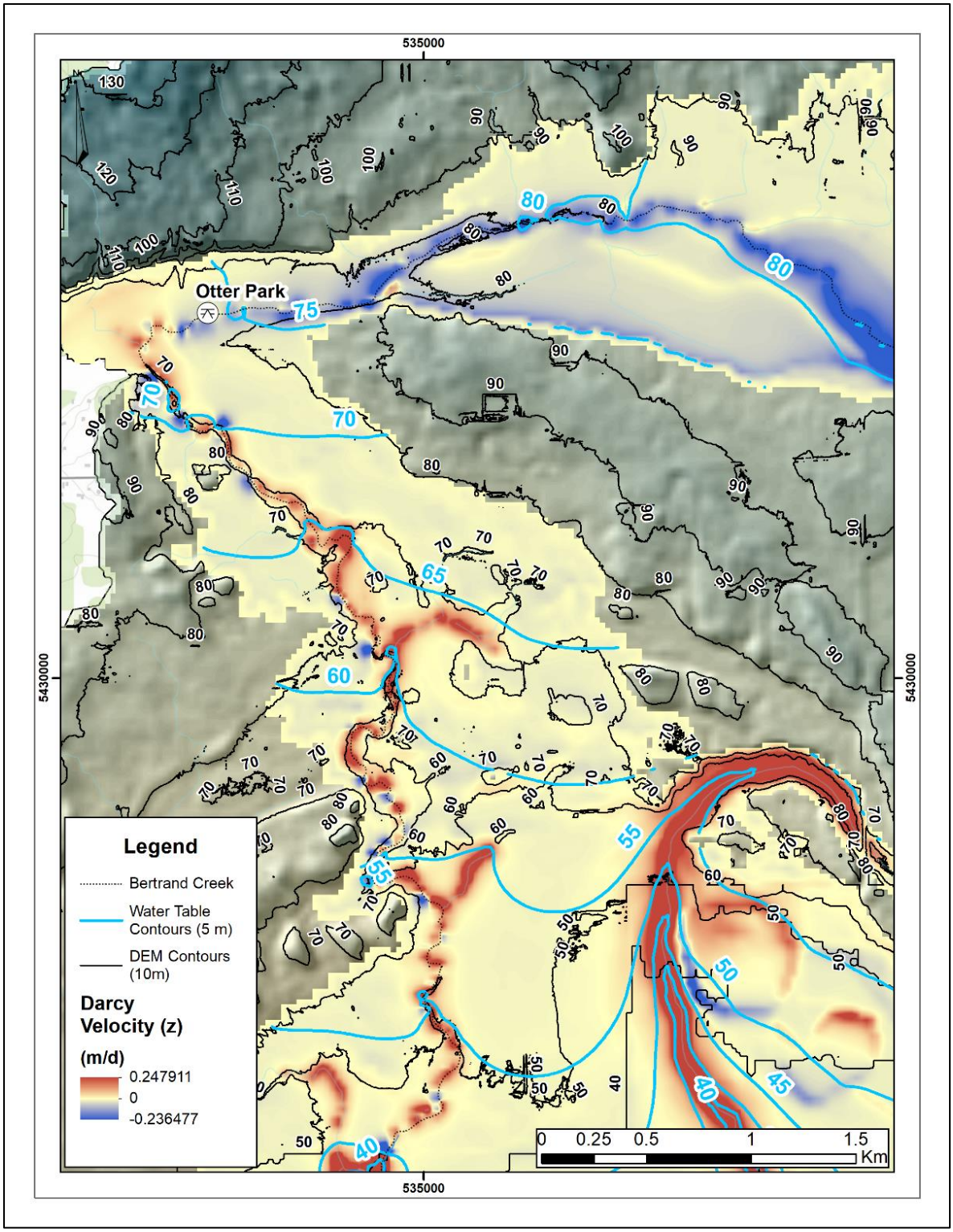

Figure 38: Composite map of water table contours (5 m) under non-pumping conditions and surface DEM contours (10 m) overlaid onto the vertical flux layer. Areas of 0 m/day vertical flux are not displayed. Positive flux (red) represents groundwater flow out of the aquifer system while negative flux (blue) represents flow into the aquifer system. Note the intersection of the 80 masl water table contour and the 80 masl surface DEM contour slightly upstream of Otter Park.

6. CONCLUSIONS AND RECOMMENDATIONS

Recurring instances of observed streamflow degradation within the Bertrand Creek Watershed, with certain stream segments running dry, prompted a hydrogeological investigation into Bertrand Creek. The purpose of this study was to use numerical modelling to assess the nature of the hydraulic connectivity between Bertrand Creek and the groundwater system in order to quantify aquifer-stream exchanges. This was accomplished by constructing a three-dimensional steady-state numerical groundwater flow model of the Bertrand Creek Watershed based on a pre-existing regional groundwater flow model for the Abbotsford-Sumas aquifer (Scibek and Allen, 2005).

Under natural conditions, without the influence of pumping wells, it was found that the segments of Bertrand Creek upstream of Otter Park are dominantly losing reaches. Otter Park represents a transition zone within which the segments of Bertrand Creek transition from dominantly losing reaches upstream of Otter Park into a stream that has both losing and gaining reaches downstream of Otter Park. It is thought that the sharp meander and resulting directional change of Bertrand Creek, aligning it with the regional groundwater flow direction, causes a change in the nature of the stream-aquifer interaction. Additionally, water table contours begin to intersect with surface contours just south of Otter Park in the transition zone.

Under pumping conditions, all stream segments of Bertrand Creek on the Canadian side of the border have greater negative vertical fluxes into the groundwater system. Increases in river leakage into the groundwater system ranged from approximately +0.1 to +5.3% while decreases in river leakage into certain stream segments ranged from approximately -1.1 to -13.7%. River leakage into Bertrand Creek only occurs downstream of Otter Park while river leakage out of Bertrand Creek occurs in all reaches of the stream. In total, under pumping conditions (20,003 m^3/day total volume), approximately 3,460 m^3/day (17.3% of pumping) more water seeps into the groundwater system and approximately 1,298 m^3/day (6.5% of pumping) less water seeps into Bertrand Creek.

Based on the modelling results, streamflow reduction is likely to occur in reaches of Bertrand Creek upstream of Otter Park due to the water table being deeper than ground surface and due to the dominantly losing nature of the stream in these segments. Groundwater abstraction is likely to exacerbate the losing nature of the stream, increasing the likelihood of drought in Bertrand Creek.

Recommendations

The following recommendations could be addressed using the existing groundwater flow model to gain more detailed insight into the dynamics of hydraulic connectivity within the Bertrand Creek Watershed.

I. Extending the Use of the Steady-State Model

Use the current steady-state groundwater flow model to map areas where pumping may lead to greater streamflow depletion. This could be accomplished by strategically placing pumping wells in the model adjacent to Bertrand Creek (e.g. along different segments) at different distances from the stream and observing the effect on exchange fluxes between the stream and the aquifer. This is similar to the approach used by Pruneda (2007), who placed wells in a grid-like fashion across the model domain on the US side of the border and ran the steady-state model for each well position, one well at a time. The streamflow impacts were recorded at the stream outlet for each well position using Zone Budget. Results were then expressed quantitatively as a response ratio, ranging from 0.0 to 1.0. The response ratios were then mapped to identify the relative impacts on streamflow depletion as a function of distance from the stream. This type of modeling exercise for the Canadian portion of the Bertrand Creek

Watershed could help provincial water allocation staff identify areas in the watershed where groundwater license applications might require more or less scrutiny in terms of streamflow depletion.

II. Transient Groundwater Flow Modeling

Develop a transient groundwater flow model or integrated land surface – subsurface model of the watershed. A transient groundwater flow model already exists for the Abbotsford-Sumas Aquifer (Scibek and Allen, 2005). Therefore, it would not be too difficult to convert the steady-state Bertrand Creek Watershed model to a transient groundwater flow model by simply transferring the time varying boundary conditions into the model. However, an integrated land surface – subsurface model of the watershed would be much better suited for a variety of purposes. Integrated models allow for evapotranspiration, overland flow, recharge and streamflow to be modeled explicitly, rather than having to use boundary conditions in a groundwater flow code. This enhanced modeling environment allows for temporal variability in the stream and groundwater dynamics to be examined, particularly the timing of the onset of streamflow drought along different reaches. Additionally, transient modelling would allow for the inclusion of variable pumping rates based on seasonal use. This is particularly important for representing heavy seasonal users of groundwater such as the agricultural industry in the watershed. While the development of a transient model (either groundwater or an integrated model) is more data intensive, the pre-existing transient model will provide an adequate starting point.

III. Integration of Climate Change

Incorporate variations in recharge projected under future climate change. Scibek and Allen (2006) developed an approach for using downscaled climate data from global climate models as input to a recharge model. The recharge results were then used as input to the groundwater flow model. An improved approach would be to use climate data from more recent global climate models as input to an integrated model of the Bertrand Creek Watershed. Incorporating the effects of climate change would provide more insight into how climate change may play a role in future streamflow drought, especially during the drier summer months or during longer periods of drought.

IV. Acquiring Accurate Groundwater Use and Other Hydrologic/Hydrogeologic Data

Acquire accurate groundwater abstraction data. The simulated impacts of pumping on groundwater exchanges with the stream depend on accurate estimates of groundwater abstraction, particularly for large users of groundwater. Large users of groundwater should be required to measure and report actual use so that groundwater abstraction rates can be more accurate in models or water balance calculations. As more wells are licensed in B.C., reported uses could be used to update the model to obtain a more representative picture of actual groundwater use.

Expand hydrologic/hydrogeologic datasets. Hydrologic data, encompassing streamflow and groundwater level data, are vital for constructing and calibrating transient models. At present, the only permanent hydrometric station in Bertrand Creek watershed north of the Canada-US border is right at the border (Station 08MH152). Two temporary hydrometric stations are located at Otter Park, and perhaps one of these should be monitored indefinitely by the province.

As well, there are only two provincial observation wells in the watershed (361, active since 2010, and 458, active since 2014). Notably, neither well existed when the original transient numerical model was developed by Scibek and Allen (2005), and both wells are in the northern part of the watershed, at some distance from the hydrometric station. Adding a third provincial observation well near the hydrometric station would enable a more direct comparison of the seasonal response of the aquifer and stream. It is noted, however, that Bertrand Creek Watershed is well instrumented in comparison to others in the province.

Finally, for investigating exchanges between the aquifer and the stream, accurate streambed hydraulic conductivity (K) measurements are critical. Fortunately, the study by Pruneda (2007) provided estimates of streambed K for several sites in the US, and an average value of streambed K was available for Otter Park; although this single value was used to represent the full length of Bertrand Creek north of the Canada-US border. Acquiring estimates of average streambed K at a series of sites along Bertrand Creek is highly recommended.

REFERENCES

Alexander, M.D., and D. Caissie. 2003. Variability and comparison of hyporheic water temperatures and seepage fluxes in a small Atlantic salmon stream. Groundwater, 41(1): 72–82.

Allen, D.M., B. Johnson, B., A. Garnett, K. Howe, M. Lepitre and M. Simpson. 2020. Assessment of Aquifer-Stream Connectivity Related to Groundwater Abstraction in the Lower Fraser Valley: Phase 2 Field Investigation at Otter Park, Langley. Water Science Series, WSS2020-03. Prov. B.C., Victoria B.C.

Aquifer 15 (Abbotsford-Sumas aquifer) - Groundwater Wells and Aquifers - Province of British Columbia. Available online at: https://apps.nrs.gov.bc.ca/gwells/aquifers/15

Armstrong, J.E. 1981. Post-Vashon Wisconsin Glaciation, Fraser Lowland, British Columbia. Geological Survey Bulletin 322.

Armstrong, J.E. 1984. Environmental and Engineering Applications of the Surflclal Geology of the Fraser Lowland, British Columbia. Geological Survey of Canada, Paper 83-23, 1984, 54 pg. https://doi.org/10.4095/119727.

Bater, C.W., and Coops, N.C. 2009. Evaluating error associated with LiDAR-derived DEM interpolation. Computers & Geosciences, 35: 289–300. doi:10.1016/j.cageo.2008.09.001.

Berg, M.A., and D.M. Allen. 2007. Low flow variability in groundwater-fed streams. Canadian Water Resources Journal, 32(3): 227–246.

Bloomfield, J. P., B.P. Marchant, and A.A. McKenzie. 2019. Changes in groundwater drought associated with anthropogenic warming. Hydrology and Earth System Sciences, 23(3): 1393–1408.

Burri, N.M., R. Weatherl, C. Moeck, and M. Schirmer. 2019. A review of threats to groundwater quality in the anthropocene. Science of The Total Environment, 684: 136–154.

Chesnaux, R. and D.M. Allen. 2006. Particle Tracking Results for Nitrate Hot Spot Study, Abbotsford-Sumas Aquifer, BC, Canada. Final Report to Fraser Health Authority and Environment Canada, December 2006, 30 pp.

Chesnaux, R. and D.M. Allen. 2007. Updated Particle Tracking Results for Nitrate Hot Spot Study, Abbotsford-Sumas Aquifer, BC, Canada: Case for Large-Capacity Production Wells Only Activated in the Model. Final Report to Fraser Health Authority and Environment Canada, February 2007, 17pp.

Clague, J.J. 1986. The Quaternary stratigraphic record of British Columbia—evidence for episodic sedimentation and erosion controlled by glaciation. Canadian Journal of Earth Sciences, 23: 885–894. doi:10.1139/e86-090.

Clague, J.J., 1994. Quaternary stratigraphy and history of south-coastal British Columbia. In: (ed) J.W.H. Monger, Geology and Geological Hazards of the Vancouver Region, Southwestern British Columbia, Geological Survey of Canada, Bulletin 481, p. 181-192.

Clague, J.J. 2000. Recognizing order in chaotic sequences of Quaternary sediments in the Canadian Cordillera. Quaternary International, 68–71: 29–38.

Clague, J.J. and T.S. James. 2002. History and isostatic effects of the last ice sheet in southern British Columbia. Quaternary Science Reviews. 21(1):71–87.

Clague, J.J. and J.L. Luternauer. 1983. Late Quaternary Geology of Southwestern British Columbia. Field Trip Guide.

Clague, J.J. and B. Ward. 2011. Chapter 44 - Pleistocene Glaciation of British Columbia. In: Ehlers, J., P.L. Gibbard, and P.D. Hughes (eds.), Developments in Quaternary Sciences, Quaternary Glaciations - Extent and Chronology. Elsevier, p. 563–573.

Clague, J.J., J.E. Armstrong, and W.H. Mathews. 1980. Advance of the late Wisconsin Cordilleran Ice Sheet in southern British Columbia since 22,000 Yr B.P. Quaternary Research, 13(3): 322–326.

Clague, J.J., R.W. Mathewes, J.-P. Guilbault, I. Hutchinson, and B.D. Ricketts. 1997. Pre-Younger Dryas resurgence of the southwestern margin of the Cordilleran ice sheet, British Columbia, Canada. Boreas, 26(3): 261–278.

Cox, S.E., and S.C. Kahle. 1999. Hydrogeology, Ground-water Quality, and Sources of Nitrate in Lowland Glacial Aquifers of Whatcom County, Washington, and British Columbia, Canada. Water-Resources Investigations Report 98-4195, U. S. Geological Survey. Available online at: http://pubs.er.usgs.gov/publication/wri984195.

de Graaf, I.E.M., T. Gleeson, L.P.H. (Rens) van Beek, E.H. Sutanudjaja, and M.F.P. Bierkens. 2019. Environmental flow limits to global groundwater pumping. Nature, 574(7776): 90–94.

Digital Elevation Model for British Columbia - CDED - 1:250,000 - 0.75 arcsecond - Data Catalogue. 2019, April. Available from https://catalogue.data.gov.bc.ca/dataset/7b4fef7e-7cae-4379-97b8-62b03e9ac83d.

England, T.D.J., and Bustin, R.M. 1998. Architecture of the Georgia Basin southwestern British Columbia. Bulletin of Canadian Petroleum Geology, 46: 288–320. doi:10.35767/gscpgbull.46.2.288.

ESRI, 2018, ArcGIS Desktop: Release 10.6. 3D Analyst Extension. Redlands, CA: Environmental Systems Research Institute.

Fairbanks, R.G. 1989. A 17,000-year glacio-eustatic sea level record: influence of glacial melting rates on the Younger Dryas event and deep-ocean circulation. Nature, 342(6250): 637–642.

Fedje, D., D. McLaren, T.S. James, Q. Mackie, N.F. Smith, J.R. Southon, and A.P. Mackie. 2018. A revised sea level history for the northern Strait of Georgia, British Columbia, Canada. Quaternary Science Reviews, 192: 300–316.

Flood, M. 2004. ASPRS Guidelines - Vertical Accuracy Reporting for Lidar Data. American Society for Photogrammetry and Remote Sensing (ASPRS).

Forstner, T., T.Gleeson, L. Borrett, D.M. Allen, M. Wei, and A. Baye. 2018. Mapping Aquifer Stress, Groundwater Recharge, Groundwater Use, and the Contribution of Groundwater to Environmental Flows for Unconfined Aquifers across British Columbia. Water Science Series, WSS2018-04. Prov. B.C., Victoria B.C.

Green, T.R., M. Taniguchi, H. Kooi, J.J. Gurdak, D.M. Allen, K.M. Hiscock, H. Treidel, and A. Aureli. 2011. Beneath the surface of global change: Impacts of climate change on groundwater. Journal of Hydrology, 405(3): 532–560.

Ground Water Aquifers- B.C. Data Catalogue. 2020. Available online at: https://catalogue.data.gov.bc.ca/dataset/ground-water-aquifers.

Ground Water Wells - Data Catalogue. Available online at: https://catalogue.data.gov.bc.ca/dataset/e4731a85-ffca-4112-8caf-cb0a96905778#edc-pow

Halstead, E.C. 1986. Ground water supply - Fraser Lowland, B.C. National Hydrology Research Institute, Paper 26, Inlands Waters Directorate Scientific Series 145, p 1-52.

Hamilton, T.S., and B.D. Ricketts. 1994. Contour map of the sub-Quaternary bedrock surface, Strait of Georgia and Fraser Lowland. In: Monger, J.W.H. ed., Geology and Geological Hazards of the Vancouver Region, Southwestern British Columbia, Geological Survey of Canada, Bulletin 481, p. 193-196.

Harbaugh, A.W., 2005, MODFLOW-2005. The U.S. Geological Survey modular ground-water model—the Ground Water Flow Process: U.S. Geological Survey Techniques and Methods 6-A16. doi: 10.3133/tm6A16.

Harbaugh, A.W., 1990, A computer program for calculating subregional water budgets using results from the U.S. Geological Survey modular three-dimensional ground-water flow model: U.S. Geological Survey Open-File Report 90-392, 46 p. Available online at: https://www.usgs.gov/software/zonebudget-a-program-computing-subregional-water-budgets-modflow-groundwater-flow-models.

Hayashi, M., and D.O. Rosenberry. 2002. Effects of ground water exchange on the hydrology and ecology of surface water. Groundwater, 40(3): 309–316.

Heidemann, H.K. 2018. LiDAR base specification (ver. 1.3, February 2018): U.S. Geological Survey Techniques and Methods, book 11, chap. B4, 101 p., https://doi.org/10.3133/tm11b4.

Hengl, T. 2006. Finding the right pixel size. Computers & Geosciences, 32: 1283–1298. doi:10.1016/j.cageo.2005.11.008.

LiDAR-derived Digital Elevation Models (1ft) - Nooksack (2013); North Puget (2017); North Puget (2006). Washington State Department of Natural Resources. Available from https://lidarportal.dnr.wa.gov.

Lindsay, C., and C. Bandaragoda. 2013. WRIA 1 Groundwater Data Assessment: Overview. In Bandaragoda, C., C. Lindsay, J. Greenberg, and M. Dumas, editors. WRIA 1 Groundwater Data Assessment, Whatcom County PUD #1, Whatcom County, WA. WRIA 1 Joint Board. Retrieved from http://wria1project.whatcomcounty.org/.

Malcolm, I.A., C. Soulsby, A.F. Youngson, D.M. Hannah, I.S. McLaren, and A. Thorne. 2004. Hydrological influences on hyporheic water quality: implications for salmon egg survival. Hydrological Processes, 18(9): 1543–1560.

Mascot Geodetic Control Monuments High Precision - Data Catalogue. Ministry of FLNRORD, 2019. Available from https://catalogue.data.gov.bc.ca/dataset/mascot-geodetic-control-monuments-high-precision.

Monger, J.W.H. 1990. Regional setting and adjacent Coast Mountains geology, British Columbia. In: Current Research, Part F, Geological Survey of Canada, Paper 90-1 F, p. 95-107.

Mustard, P.S., and G.E. Rouse. 1994. Stratigraphy and evolution of Tertiary Georgia Basin and subjacent Upper Cretaceous sedimentary rocks, southwestern British Columbia and northwestern Washington State. Geological Survey of Canada Bulletin 481, p. 97-140.

Pearson, M.P. 2004. The Ecology, Status and Recovery Prospects of Nooksack Dace (rhinichthys cataractae spp.) and Salish Sucker (catostomus sp.) in Canada. Ph.D. Thesis, University of British Columbia, Vancouver.

Petrasova, A., H. Mitasova, V. Petras, and J. Jeziorska. 2017. Fusion of high-resolution DEMs for water flow modeling. Open Geospatial Data, Software and Standards, 2: 6. doi:10.1186/s40965-017-0019-2.

Pollock, D.W. 2017. MODPATH v7.2.01: A Particle-tracking Model for MODFLOW: U.S. Geological Survey Software Release, 15 December 2017, http://dx.doi.org/10.5066/F70P0X5X.

Pratomo, D.G., Khomsin, and Putranto, B.F.E. 2019. Analysis of the green light penetration from Airborne LiDAR bathymetry in shallow water area. IOP Conference Series: Earth and Environmental Science, 389: 012003. doi:10.1088/1755-1315/389/1/012003.

Pruneda, E.B. 2007. Use of Stream Response Functions and Stella Software to Determine Impacts of Replacing Surface Water Diversions with Groundwater Pumping Withdrawals on Instream Flows within the Bertrand Creek and Fishtrap Creek Watersheds, Washington State, USA. MSc thesis, Washington State University, 70 pp.

Scibek J., and D.M. Allen. 2005. Numerical Groundwater Flow Model of the Abbotsford-Sumas Aquifer, Central Fraser Lowland of BC, Canada, and Washington State, US. Report prepared for Environment Canada, 203 pp. Available at: Model results (sfu.ca)

Scibek J., and D.M. Allen. 2006. Groundwater Sensitivity to Climate Change: Modelling Recharge to Abbotsford-Sumas Aquifer in British Columbia, Canada and Washington State, US. Report prepared for BC Ministry of Water, Land and Air Protection, and Environment Canada, 145 pp. available at: Microsoft Word - AB_Recharge&Climate Change_Report_Final.doc (sfu.ca)

Seequent Limited. 2020. Leapfrog Geo v5.1. Release version 5.1.

Survey Monument Database. 2020. GeoMetrix Geodetic Survey Office. Washington State Department of Transportation. Available from https://www.wsdot.wa.gov/Monument/default.aspx.

Thomas, I.A., P. Jordan, O. Shine, O. Fenton, P.E-. Mellander, P. Dunlop, and P.N.C. Murphy. 2017. Defining optimal DEM resolutions and point densities for modelling hydrologically sensitive areas in agricultural catchments dominated by microtopography. International Journal of Applied Earth Observation and Geoinformation, 54: 38–52. doi:10.1016/j.jag.2016.08.012.

Wang, L., and H. Liu. 2006. An efficient method for identifying and filling surface depressions in digital elevation models for hydrologic analysis and modelling. International Journal of Geographical Information Science, 20: 193–213. doi:10.1080/13658810500433453.

Washington WRIA Watershed Boundaries | Whatcom County, WA - Official Website. 2020. Whatcom County. Available online at: https://www.whatcomcounty.us/716/Data.

Waterloo Hydrogeologic Inc. 2020. Visual MODFLOW Flex v6.1. Release version 6.1.

Yang, P., D.P. Ames, A. Fonseca, D. Anderson, R. Shrestha, N.F. Glenn, and Y. Cao. 2014. What is the effect of LiDAR-derived DEM resolution on large-scale watershed model results? Environmental Modelling & Software, 58: 48–57. doi:10.1016/j.envsoft.2014.04.005.

APPENDIX A GROUND SURFACE DEM FROM LIDAR DATA

A.1 LiDAR Data

A nominal point density of 20 pts/m^2 was employed during airborne data collection for all return points. Vertical accuracy, in the z-direction, is reported up to 8 cm whereas horizontal accuracy, in the x-y directions, is reported up to 15 cm at a 1σ (or one standard deviation) confidence level (68.3%). The provided LiDAR dataset was already post-processed and classified to include only ground return points. Because ground points were filtered, the actual point density of ground returns was lower than the reported nominal point density of all the returns. Average point density and point spacing were determined using the 3D Analyst point file information tool as shown in Table A1. Determining the output resolution of the LiDAR-derived DEM from the point cloud data was a complex task, requiring certain considerations with respect to data accuracy and point return spacing and density. Different approaches were explored in this study.

Table A1: LiDAR dataset characteristics and statistics. Note that this is filtered for ground returns only. The European Petroleum Survey Group (EPSG) codes refer to a registry database of spatial reference systems. The Canadian Geodetic Vertical Datum (CGVD) is reference surface for which vertical elevation can be defined.

	Number of Points	Mean Point Density (pts/m^2)	Average Point Spacing (m)	Horizontal Coordinate System	Vertical Datum	Elevation Range $Z_{min} – Z_{max}$ (m)
Ground Returns	406,250,443	6.77	0.37	Nad83, UTM Zone 10 (EPSG: 26910)	CGVD 1928	40.00 – 139.29

A.2 Determination of LiDAR-Derived DEM Resolution

Because LiDAR laser pulses are differentially affected by the surface characteristics of features, point spacing becomes irregular and somewhat random (ESRI, 2018). According to the LAS data format to raster function tool (3D Analyst 2018) used to create the DEMs from the point cloud, output pixel size should be several times (at least four times) larger than the average point spacing.

Point density (PD) and point spacing (PS) are two important characteristics of a LiDAR point cloud dataset. Point density is the number of return points within a given square metre, whereas the point spacing is the linear distance between each point, measured in metres. ESRI (2018) defines the point density, assuming uniform point spacing as:

$$PD = \frac{1}{(PS)^2} \quad \text{(Eq. A1)}$$

where:

PD is point density; and
PS is point spacing.

Therefore, higher point densities will yield smaller point spacing, thus theoretically allowing for higher resolution (smaller pixel size) DEMs to be produced. This crude method for determining the resolution of a DEM is not widely employed in the literature or in studies conducted on LiDAR-derived DEMs. Using the provided point density from the dataset, Equation A1 yields a point spacing of 0.22 m. The actual average point spacing is 0.37 m (Table A1), as computed by the LAS point statistics function in 3D Analyst using the ground return point density. Assuming a uniform point spacing will underestimate the actual mean spacing between points in an irregular dataset, leading to an output resolution too fine to account for the necessary error. A resolution of approximately 1.5 m is determined using the actual average point spacing from the suggested four times rule.

The Nyquist frequency theory, or simply, the Nyquist criteria, derived from digital signal processing is sometimes used to determine appropriate grid cell sizes, or resolution, based on point spacing (Bilskie and Hagen, 2013). The modified equation is (Hengl, 2006):

$$p \leq \frac{\bar{h}_{ij}}{2} \quad \text{(Eq. A2)}$$

where:

p is the pixel size; and

$\bar{h}_{ij}$ is the mean shortest distance, or more practically, the average point spacing.

This means that given the average point spacing of the dataset, which is 0.37 m, the smallest appropriate resolution, or grid cell size, is half the average point spacing, in this case a resolution of 0.185 m.

A more accurate determination for DEM resolution can be obtained by considering the positional accuracy of each data point. Assuming normally distributed vertical errors across the point dataset, the American Society for Photogrammetry and Remote Sensing (ASPRS, 2004) defines the Root Mean Squared Error (z-direction), a widely accepted standard when defining positional accuracy for LiDAR data.

$$RMSE_z = \frac{Accuracy_z}{1.9600} \quad \text{(Eq. A3)}$$

where:

RMSE is the Root Mean Squared Error; and

Accuracy is the reported vertical value.

Given the reported vertical accuracy of the provided point cloud dataset (8 cm or 0.08 m), the RMSE is 0.0408 m. However, it must be noted that the ASPRS specifies that ground distances be reported at a 2σ confidence level, or 95% confidence level. Because the provided dataset is reported to a 1σ confidence level, or 68.3% confidence level, the RMSE may be higher than calculated. Furthermore, it is recognized that it is highly likely that there is a higher measure of error since a normal distribution is being assumed. Employing the DEM standards set forth by the United State Geological Survey (USGS) in its LiDAR base specification manual (Heidemann, 2018) in the section for bare-earth surface, or raster DEM production, it was determined that a raster resolution of 0.5 m was appropriate given an RMSE of 0.0408 m. This error falls within the quality level 0 (QL0) category, which classifies minimum raster cell sizes for DEMs based on the RMSE of the vertical accuracy of the LiDAR points, which for QL0, is an RMSE $\leq$ 0.0500 m. This approach is interesting as it utilizes the vertical measures of error to determine horizontal properties of dataset, i.e. the pixel size. This is not surprising since the DEM is a geospatial representation of elevation.

Depending on the method chosen, the DEM output resolution could vary between approximately 0.19 m and 1.5 m. Ultimately, an output resolution of 0.5 m was chosen in order to capture microtopography while maintaining a strict gap above the lowest appropriate resolution for the given dataset and satisfying the criteria for vertical accuracy errors.

A.3 Point Coverage Map

A point density map was created using the LAS statistics to raster tool in order to visualize areas of lower point density or areas that may have sparse point coverage. This process revealed that many waterbodies have low point density but nonetheless contain a sufficient number of points for interpolation without creating any voids. Thomas et al. (2017) showed that even with reduced LiDAR bare-earth point densities, from 40 to 5 points/m^2, DEM elevations are largely unchanged. However, this does rely heavily on the vertical accuracy of each return point. For the provided LiDAR point dataset, the mean point density was 6.77 pts/m^2, with point densities ranging from 0 to 83.56 pts/m^2. These high point density areas are likely overlap areas of the swath widths from the aerial flight lines as can be seen in Figure A1, where north to south trending high density (red) widths can be observed. Many surface water features, such as stream beds and lakes, have almost no points associated due to the lack of a return signal from random scattering effects.

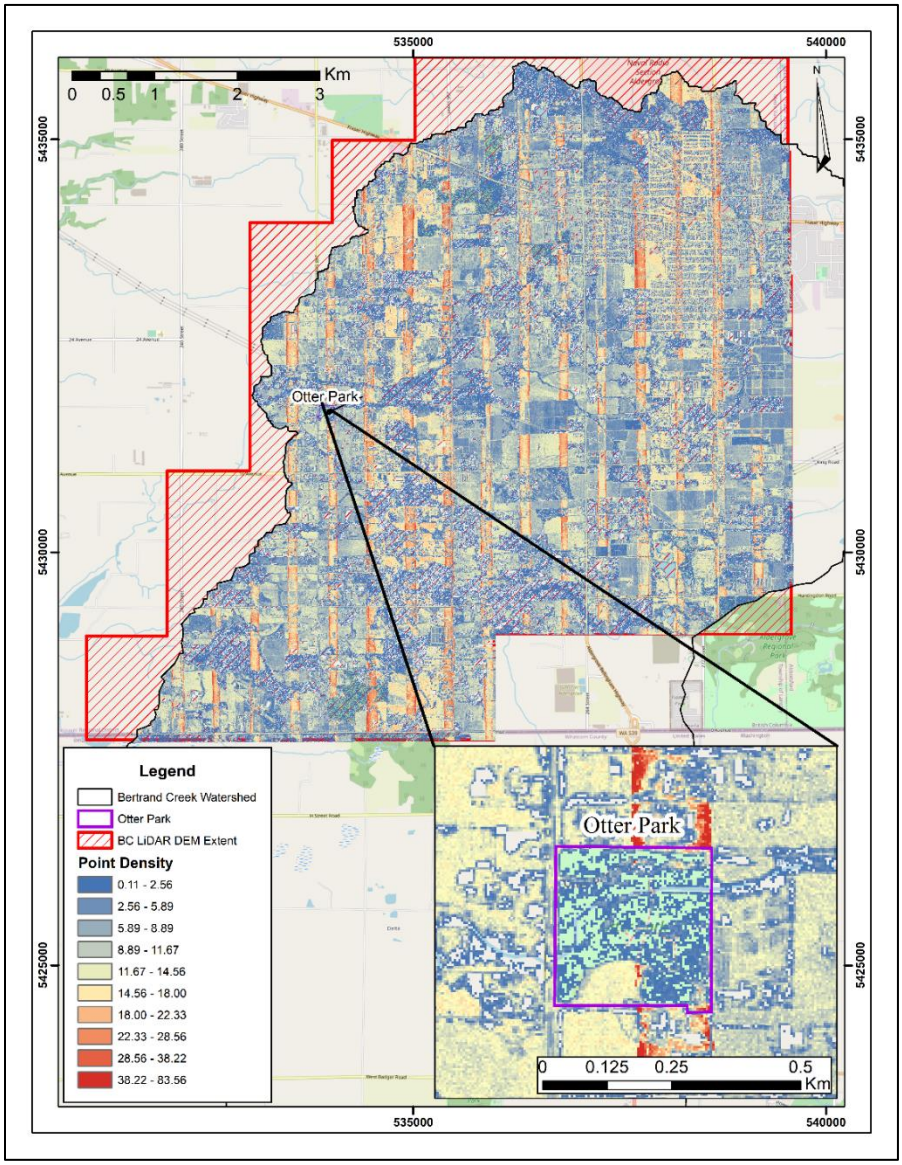

Figure A1: Point density coverage map with a zoom into the Otter Park study site. Note blank patches for absent points.

A.4 Workflow and Interpolation Method

In a meta-analysis of interpolation methods on LiDAR-derived DEMs, Bater and Coops (2009) showed that no interpolation method is universally superior for producing accurate models. Many factors come into effect, such as ground return spacing, complexity of the site morphology, and the mathematical algorithms employed for producing the interpolated raster.

Generally, for LiDAR-derived DEMs, two interpolation techniques can be employed: 1) a triangular irregular network (TIN)-derived method, which uses a linear or natural neighbour technique, and 2) non-TIN-derived interpolations such as binning, which can use different cell aggregation types such as maximum, minimum or mean (ESRI, 2018).

The workflow outline, from 3D point cloud to DEM, is as follows:

- Create a LAS dataset to combine the tiled point cloud sections.
- Using the LAS to raster tool, interpolate the LAS dataset to create a DEM. For this study, a TIN-based interpolation was chosen because it produces a cleaner surface for lower point density areas such as in stream channels (ESRI, 2018). A natural neighbour technique was employed (see Section A.5).
- Use a data area delineation polygon to clip the DEM to erase the unwanted artifacts. This was a necessary step for removing interpolated void spaces around the point cloud perimeter. These artifacts are a by-product of the interpolation process.

A.5 DEM Mosaicking and Resampling

The LiDAR dataset did not cover the full extent of the Bertrand Creek Watershed as shown in Figure A2. Therefore, additional DEM datasets were required to fill the data gaps. Areas not covered by the LiDAR dataset north of the Canada-US border were filled in using the Province of British Columbia (B.C.) openly available 0.75 arcsecond DEM (B.C. DEM 2019) derived from the Canadian DEM national dataset. The resolution of this dataset is latitude-dependant and can vary from 0.75 to 3 arcseconds. At a latitude of 49˚N, 0.75 arcseconds it is approximately 15 m. The actual pixel cell size, or resolution, measured in ArcMap is approximately 18.9 m. South of the Canada-US border, the Washington Department of Natural Resources' (DNR) publicly available high-resolution LiDAR-derived DEM tiles (2017, 2013 and 2006) were used to complete the Bertrand Creek Watershed DEM. The US LiDAR-derived DEM dataset has a resolution of 1 ft or approximately 0.3 m.

Multi-scale fusion of images with mismatched resolutions is possible, but undesirable, and may cause issues during applications of the final product. One method to circumvent this potential issue is to resample the 18.9 m provincial DEM down to 0.5 m in order to match the LiDAR-derived DEM. This can be done using a nearest neighbour assignment algorithm without changing the image dimensions. This process simply increases the number of pixels and does not add any new pixel values. Resampling should not be confused with rescaling or resizing which increases the image size. Each pixel cell is simply sub-divided into smaller pixels of the same value as the parent pixel (Figure A39).

Natural neighbour interpolation is suited for discrete data because it preserves the original nature of the parent dataset, here the provincial DEM tiles. A method better suited for continuous data, such as surfaces, is bilinear interpolation. This method uses a 4x4 pixel sweep of the nearest four pixels and applies a linear interpolation by using weighted averages (ESRI, 2018). This produces a smoother transition rather than sharp pixel contacts with natural neighbour interpolation. This method was used in conjunction with natural neighbour for comparison purposes and overall data quality representation for the final DEM.

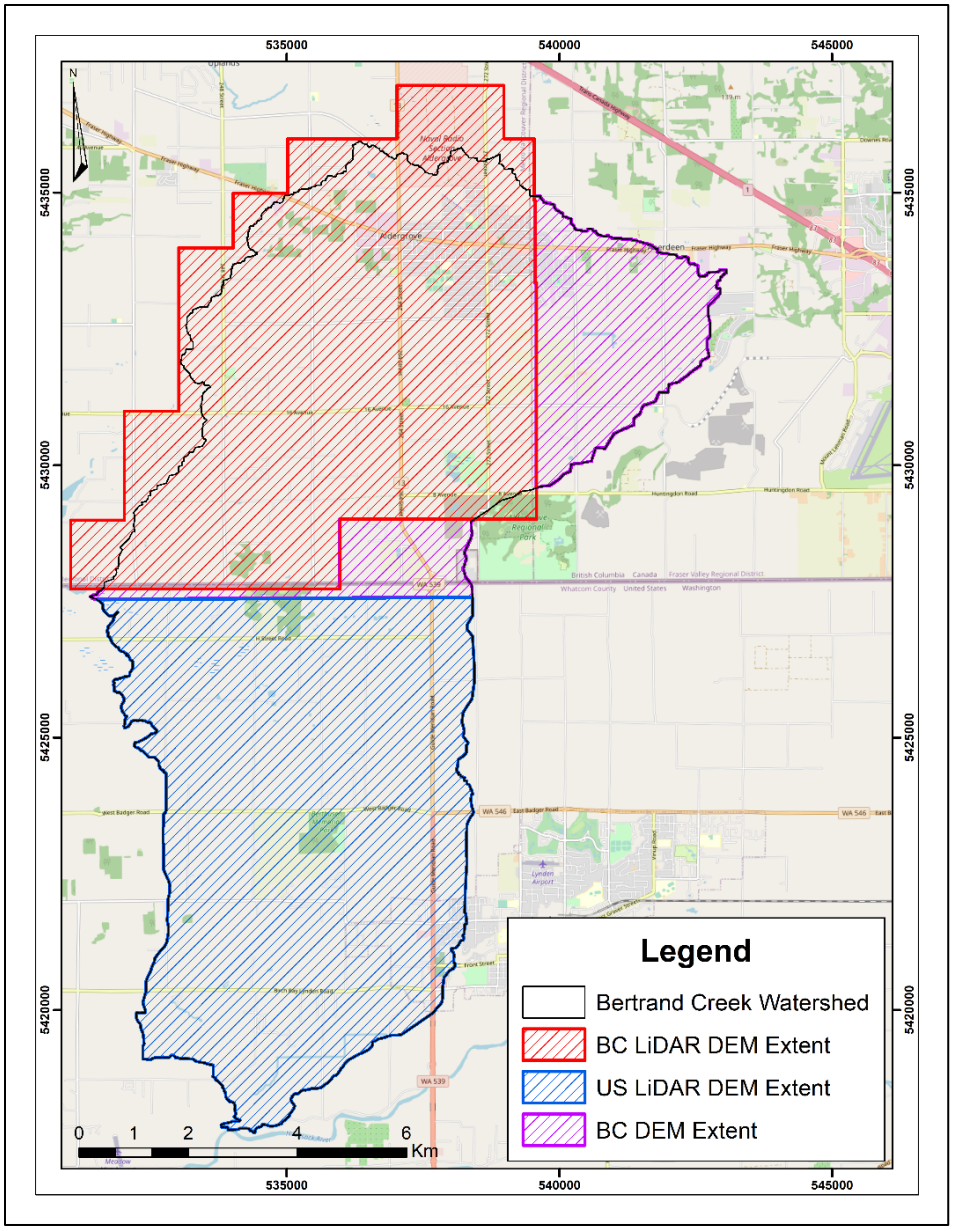

Figure A2: Multiple DEM datasets mosaicked to create the final DEM for the study area.

The 18.9 m provincial DEM was resampled to 0.5 m to match the pixel resolution of the LiDAR-derived DEM. The resampled (natural neighbour) DEM is identical to the original DEM because, as described above, the original pixels were simply replaced by a larger number of pixels of the same value in the same location. The resampled (bilinear) DEM is similar to the original DEM but noticeably smoother. While the result is visually appealing, the data have been altered and the positional accuracy of each pixel is potentially compromised. This will be vetted in the following section for accuracy validation. Additionally, the US DEM was up-sampled from its native resolution of 0.3 m to 0.5 m in order to match the other two datasets.

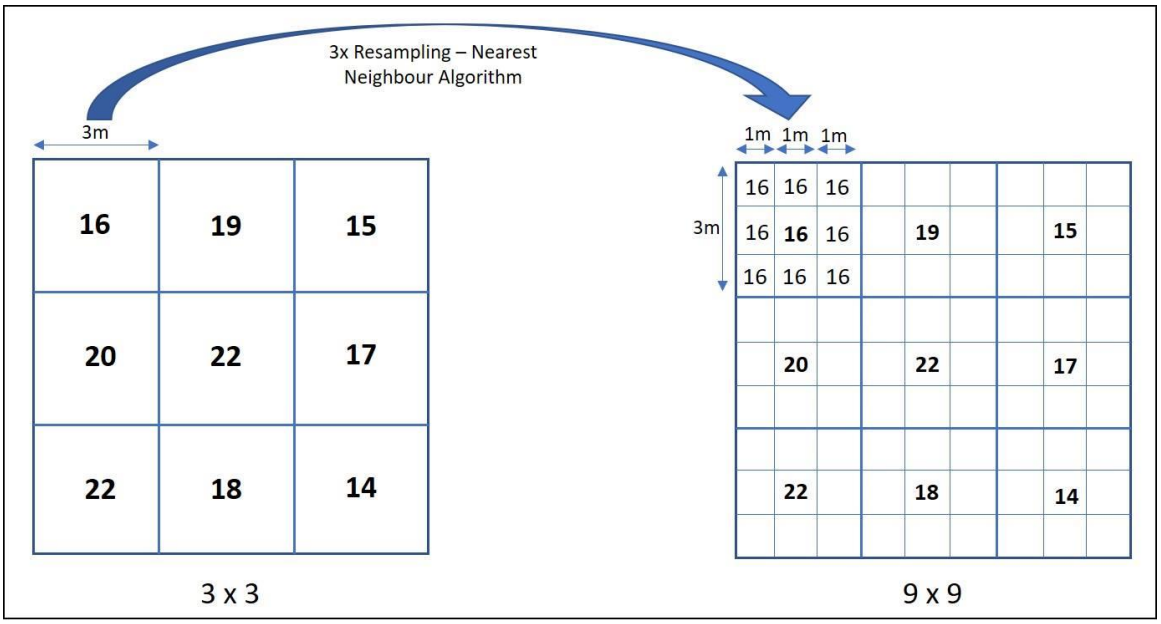

Figure A39: Example of the 2D nearest neighbour resampling technique. Image size is retained but the number of pixels increases. Pixels neighbouring the parent pixel are assigned the same value. Thus, the resulting image should look exactly the same. The example above shows a 3 m pixel that is resampled to 1m. Note that there are 3 times as many pixels, yet the image will retain its original appearance.

The three DEM datasets (LiDAR, provincial, US LiDAR) were merged together using the mosaic to new raster tool in ArcMap. This process results in irregular and disjointed boundaries where the provincial DEMs meets both the LiDAR-derived DEMs due to vertical accuracy differences in the datasets. These positional accuracy differences cause difficulties in image processing and create large steeply sloping banks at the merge interface. Specifically, along the merge interface, the provincial DEM has a higher elevation compared to the LiDAR-derived DEM.

The approach taken was to determine the elevation error of every pixel in the transition zone of the provincial DEM (global DEM error) and express that error as a single constant for the entire DEM. Then, the global error was subtracted from each pixel in the entire provincial DEM. The RMSE was used in this process as described in the following sections.

A.6 Positional Accuracy Validation

The B.C. provincial mascot geodetic control monuments (B.C. Ministry of FLNRORD 2019) were used as the ground control points to validate DEM accuracy on the Canadian side of the border. The Washington Department of Transport geodetic monuments (Washington DOT 2019) were used as ground control points on the US side of the border. This accuracy check was done several times for the different DEM outputs at each step. Accuracy validation was conducted for the following data:

- **i.** LiDAR-derived DEM (0.5 m)
- **ii.** US LiDAR-derived DEM (0.3 m)
- **iii.** Provincial DEM tiles (18.9 m)
- **iv.** Resampled (Natural Neighbour) provincial DEM tiles (0.5 m)
- **v.** Resampled (Natural Neighbour) provincial DEM clipped to the watershed (0.5 m)
- **vi.** Resampled (Bilinear) provincial DEM clipped to the watershed (0.5 m)
- **vii.** Corrected provincial DEM (0.5 m)
- **viii.** Final merged DEM (0.5 m)

The validation process effectively allows for the comparison of the surveyed elevation to the elevation represented by the pixel at any specific point location. The process was carried out using the extract multi values to points tool, with the extracted raster pixel value (elevation) appended to the point file attribute table. These values were then exported to Microsoft Excel for calculation of statistical parameters used to validate the positional accuracy of the vertical measurements.

The main statistical parameters calculated included the RMSE (z-direction), average error and median error. The RMSE was used as the bias correction factor. The error, which is simply the difference between elevation measurements is effectively the residuals. Table A2 shows the results of the calculations. The equations are as follows:

$$Error\ (Residuals) = Z_n - Z_n{}' \quad \text{(Eq. A4)}$$

where:

Z_n is the LiDAR DEM elevation value; and
Z_n' is the surveyed geodetic elevation value

$$RMSE_z = \sqrt{\sum \frac{(Z_n - Z_n')^2}{N}} \quad \text{(Eq. A5)}$$

where:

Z_n-Z_n' is the error or residual; and
N is the number of points.

Table A2: Vertical accuracy statistics calculated with respect to geodetic elevation markers.

Datasets		Number of Geodetic Markers	Residual Range (R_{min} – R_{max}) (m)	Average Error/ Residual (m)	Median Error/ Residual (m)	RMSE (z-direction) (m)
i.	LiDAR-derived DEM	183	-1.379 – 1.421	0.133	0.139	0.237
ii.	US LiDAR-derived DEM	11	-0.355 – 0.324	0.097	0.164	0.224
iii.	Provincial DEM Tiles	1538	-11.668 – 13.064	2.999	3.102	4.080
iv.	Resampled provincial DEM Tiles	1538	-11.668 – 13.064	2.999	3.102	4.080
v.	Resampled (natural neighbour) provincial DEM Clipped to Watershed	46	-4.467 – 9.647	3.031	3.781	4.327
vi.	Resampled (bilinear) provincial DEM Clipped to Watershed	46	-4.467 – 9.163	3.055	3.659	4.323

The results indicate that the resampled (natural neighbour) provincial DEM statistics do not change, and that the resampling method results in insignificant error. Interestingly, the bilinear resampled provincial DEM statistics are nearly unchanged with a 0.08% change in RMSE compared to the natural neighbour resampled provincial DEM.

The LiDAR-derived DEM had a very small RMSE of approximately 0.237 m, which is slightly larger than the computed RMSE assuming a normal distribution of error during the resolution determination step. This indicates that the error is likely not normally distributed or that the vertical accuracy is slightly larger than 8 cm; however, the latter is likely not the case. Figure A3 shows the histogram plots for the residuals (errors) for the LiDAR-derived DEM, created in this study.

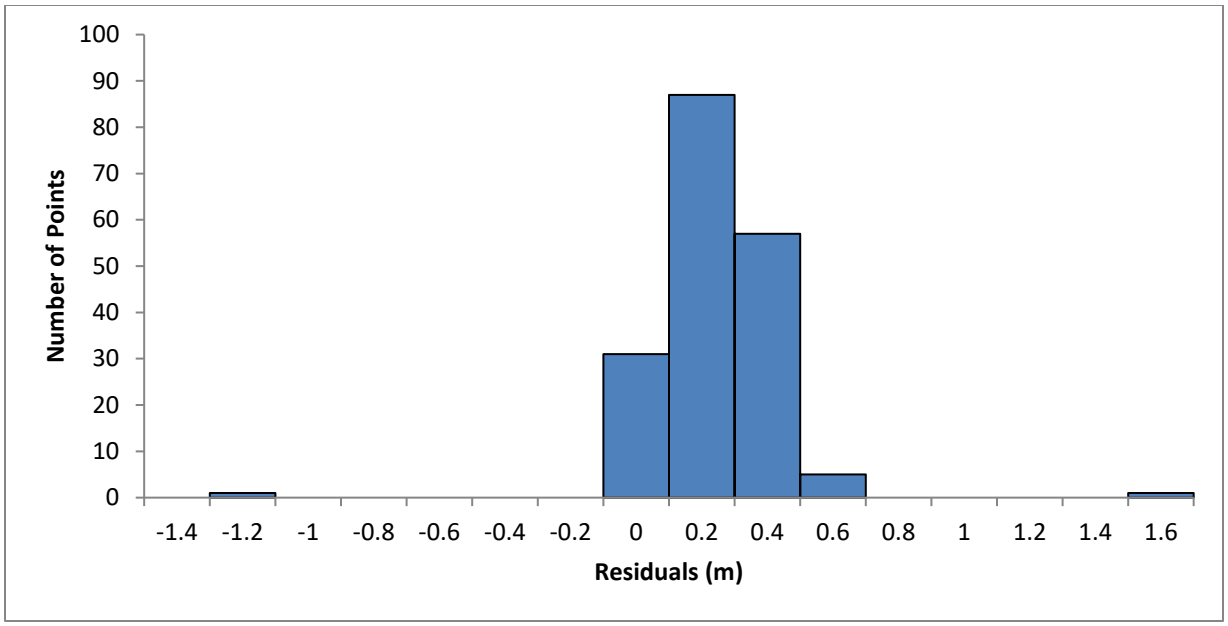

Figure A3: LiDAR-derived DEM residuals histogram.

The US LiDAR-derived DEM also had a very similar RMSE of only 0.224 m. However, the resampled provincial DEM has a higher RMSE of 4.327 m and 4.323 m for the natural neighbour and bilinear interpolation methods, respectively, which are significantly higher than those of their LiDAR-derived counterparts. Because of the low positional accuracy of the provincial DEM and high RMSEs, it was determined that corrective measures were needed in order to attempt to rectify the discrepancy in the merge interfaces. Because the bilinearly interpolated provincial DEM is essentially unchanged from that of the natural neighbour interpolated provincial DEM, the former is used for the final DEM.

A.7 Bias Correction

The RMSE was used as a bias correction factor in order to rectify the elevation change discrepancy at the merge interface. In order to try and match the RMSE of the LiDAR-derived DEM, this value was subtracted from the RMSE of the provincial DEM. Thus, the amount needed to subtract the RMSE from the provincial DEM is the correction factor.

$$Correction\ Factor = RMSE_{provincial} - RMSE_{LiDAR} \quad \text{(Eq. A6)}$$

Using raster algebra, the correction factor of 4.086 m was subtracted from each pixel within the provincial DEM in order to try and match its RMSE with the LiDAR-derived DEM. Table A3 summarizes the final statistics of the process.

Table A3: Vertical accuracy statistics calculated with respect to geodetic elevation markers.

	Number of Geodetic Markers	**Residual Range (R_{min} – R_{max}) (m)**	**Average Error/ Residual (m)**	**Median Error/ Residual (m)**	**RMSE (z-direction) (m)**
Corrected provincial DEM	67	-8.5729 – 5.541	-0.99700	-0.538002	3.19147
Final Merged DEM	209	-8.5729 – 5.541	-0.15001	0.108398	1.54715

The bias correction successfully lowered the RMSE by almost a metre, which effectively lowered the overall error in vertical accuracy and alleviated the merge boundary by smoothing it out, but not perfectly. There still exist zones that are steeper than in reality. This is simply a function of data limitation with regards to the resolution coarseness of the provincial DEM. The bias correction method lowered the minimum residual significantly and perhaps a more effective algorithm can be developed to narrow the residual range. Figure A shows the effects of a successful bias correction on a section of the merge boundary. However, not all merged boundaries were smoothed out perfectly.

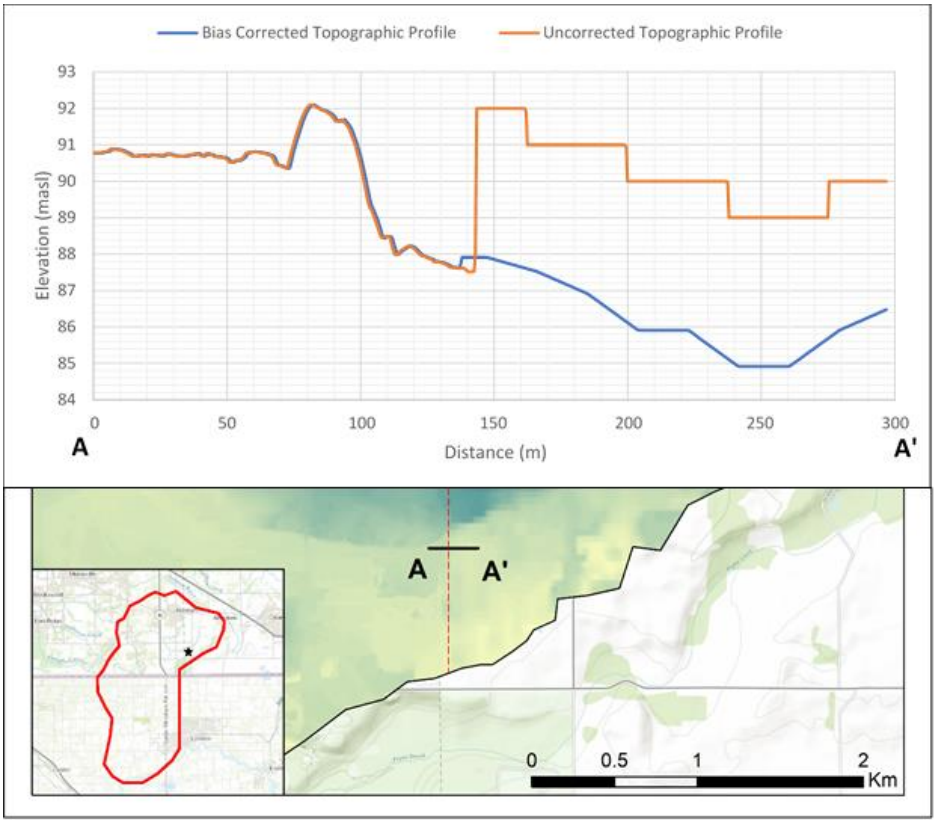

Figure A4: Changes in elevation values for the bias corrected and uncorrected provincial DEM at the merge interface between the LiDAR-derived DEM and the provincial DEM.

A.8 Final Surface DEM

The aggregate RSME of the final merged DEM is 1.547 m, which is quite reasonable considering the input data of the less accurate provincial DEM. But as this DEM is a product of multiple data sources, it has a variable RMSE depending on the location. Areas that have been infilled using the provincial DEM will necessarily have a higher RMSE, unlike its LiDAR-derived counterparts that have much lower RMSEs at a centimeter scale.

APPENDIX B VISUAL MODFLOW FLEX FLOW SIMULATION SETTINGS

B.1 Solver Settings

The PCG solver was used to obtain the steady-state solution. The parameters for the solver are as follows:

Max outer iterations (MXITER)	= 65
Max inner iterations (ITER)	= 95
Pre-conditioning method (NPCOND)	= Modified Incomplete Cholesky
Head change criterion (HCLOSE)	= 0.01 m
Residual criterion (RCLOSE)	= 0.001 m
Relaxation Parameter (RELAX)	= 1
Estimate of upper bound (NPBOL)	= 1 (calculate estimate)
Damping factor (DAMP)	= 1.0

B.2 Cell Rewetting Settings

The rewetting settings allow for a cell to become re-saturated if the head drops below the bottom elevation of that cell, in an unconfined aquifer layer. This is especially important for uppermost surficial geology layer and the soil layer. The parameters for the rewetting setting are as follows:

Wetting method (WETDRY)	= From sides and below
Wetting threshold (WETDRY)	= 0.5
Wetting Iteration interval (IWETIT)	= 8
Wetting head (IHDWET)	= Calculated from neighbours
Wetting factor (WETFCT)	= 1
Head value in dry cells	= -1E30
Saturated thickness bottom layer	= False

APPENDIX C MODIFICATIONS OF HYDRAULIC CONDUCTIVITY ZONES DURING CALIBRATION

This appendix compares the distribution of hydraulic conductivity zones from the conceptual model (left figure) and the calibrated model (right figure) for different layers in the model. Only minor adjustments were made.

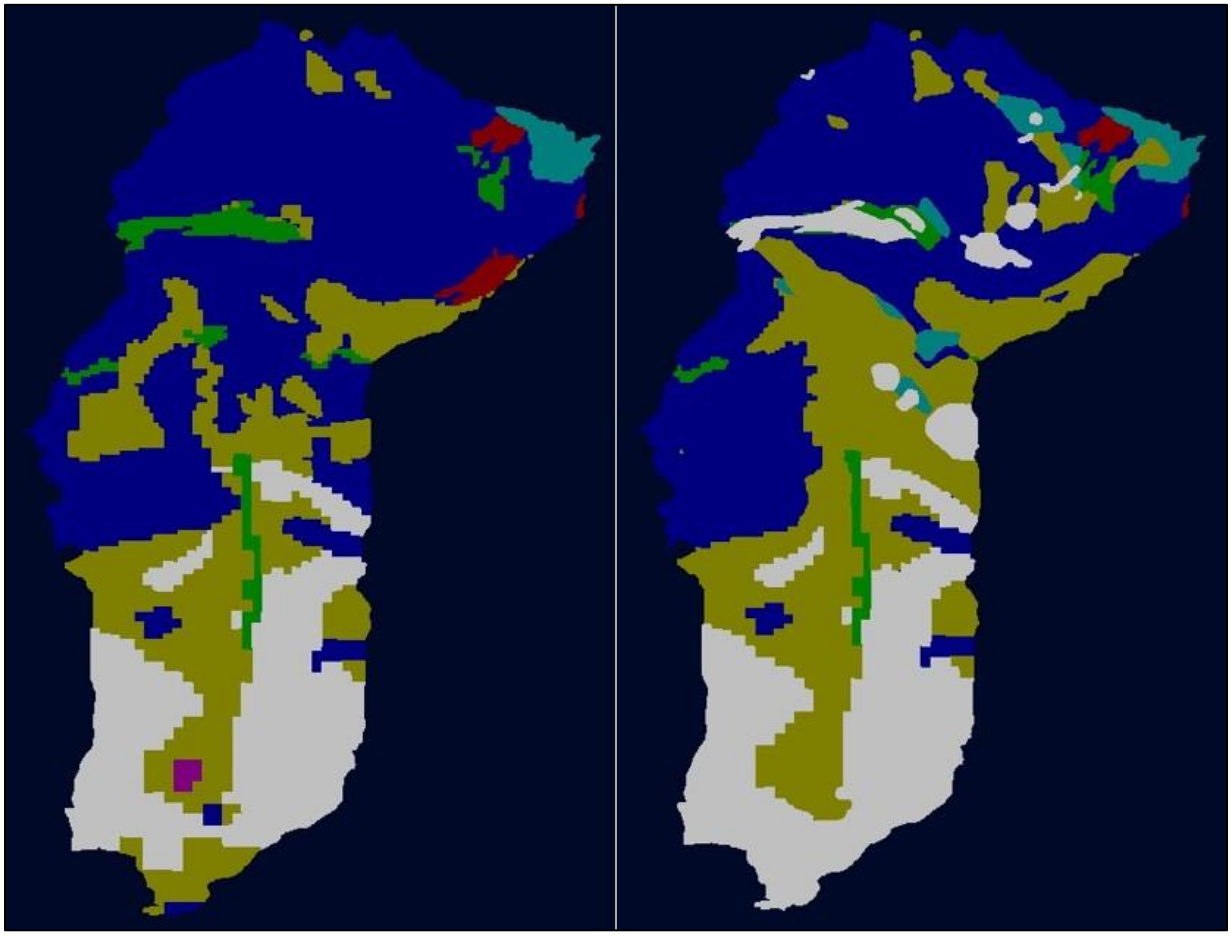

Figure C1. The results of the hydrostratigraphic unit refinement performed to achieve final calibration in layer 1 of the model. Units were redistributed while additional subdivisions of existing units were added to better represent and resolve smaller scale changes to the subsurface. The left portion is the pre-calibration version and the right portion is the final calibrated version.

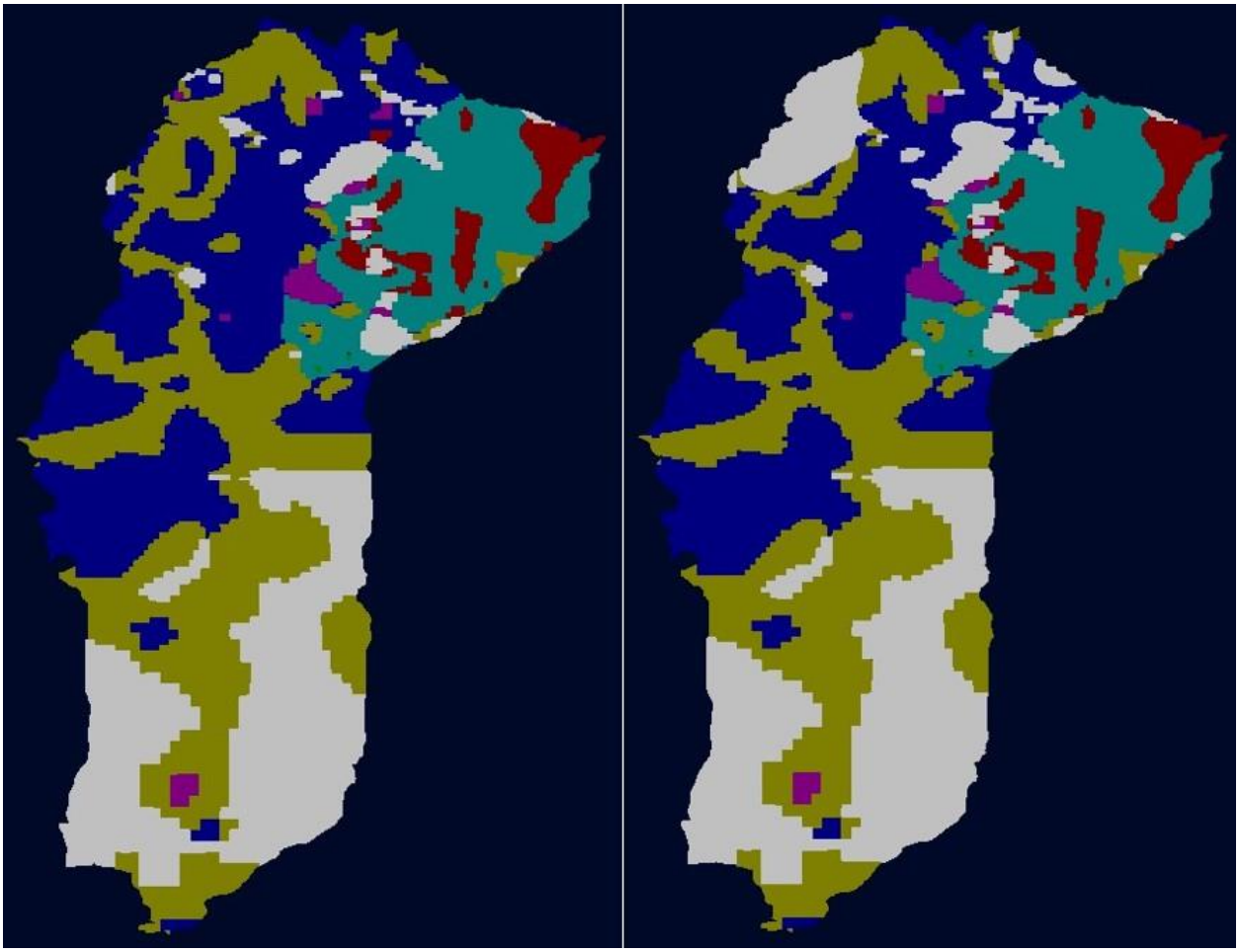

Figure C2. The results of the hydrostratigraphic unit refinement performed to achieve final calibration in layer 4 of the model. The left portion is the pre-calibration version and the right portion is the final calibrated version.

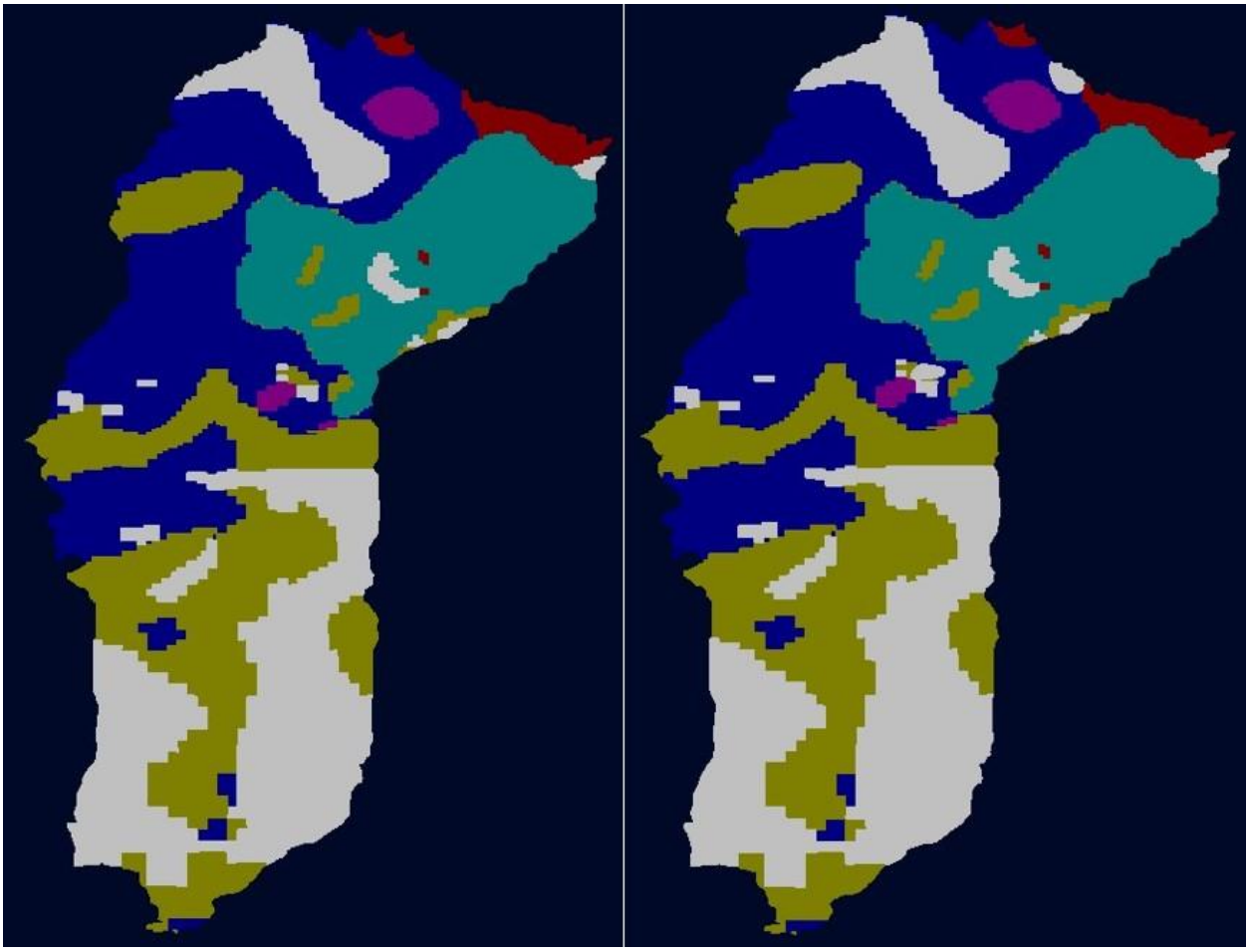

Figure C3. The results of the hydrostratigraphic unit refinement performed to achieve final calibration in layer 5 of the model. The left portion is the pre-calibration version and the right portion is the final calibrated version.

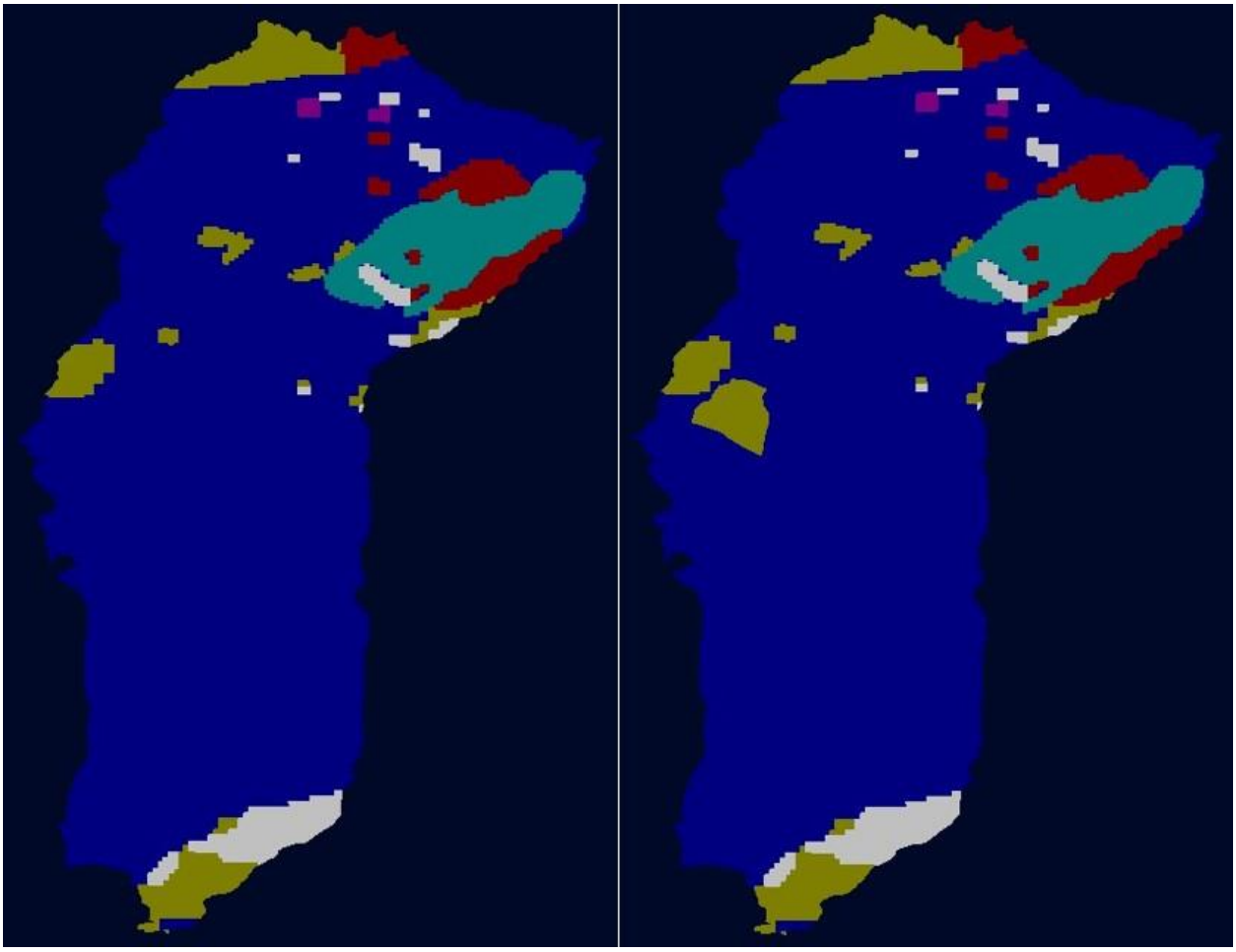

Figure C4. The results of the hydrostratigraphic unit refinement performed to achieve final calibration in layer 7 of the model. The left portion is the pre-calibration version and the right portion is the final calibrated version.